Water Solutions Pvt. Ltd.

Effluent Dispersion Modelling at Thilafushi Island, Maldives

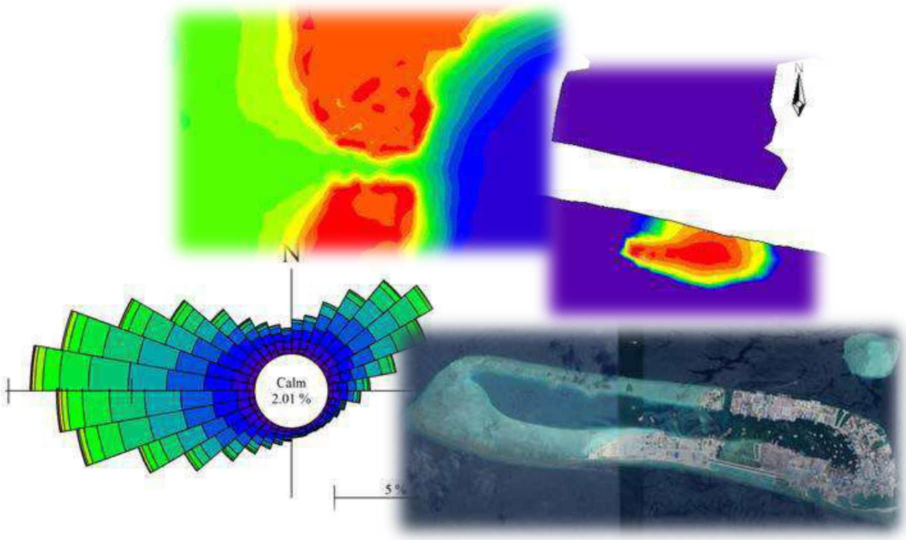

Final Report

October 2018

Lanka Hydraulic Institute Ltd

Client	Client's Representative
Water Solutions Pvt. Ltd	Mr. Ahmed Jameel
Project	**Project No.**
Effluent Dispersion Modelling at Thilafushi Island, Maldives	1808
Authors	**Date**
Eng. M.S.L. Fernando Eng. (Ms) B.M.V. Basnayake	October 2018
	Approved by
	Eng. J.K.P. Kurukulasuriya Eng. Dr. K. Raveenthiran

Revision		By	Checked	Approved	Date

Key words	Classification
Wind - Wave Transformation Hydrodynamic Thermal Dispersion	☐ Open ☐ Internal ☒ Proprietary

Distribution	No. of Copies:	
	Soft	**Hard**
Water Solutions Pvt. Ltd 1st Floor, Ma.Fas Eri, Ameenee Magu, Malé, Maldives,.	01	02

Lanka Hydraulic Institute Ltd

Coast and Water

177, John Rodrigo Mawatha, Katubedda, Moratuwa, Sri Lanka.
Tel. Nos. 2650409 / 2650471 / 2650472-3, Fax No. 2650470 - Email: lhi@lhi.lk

TABLE OF CONTENTS

LIST OF FIGURES

LIST OF TABLES

1 INTRODUCTION

Water Solutions Pvt Ltd (WS) is currently assisting Ministry of Environment and Energy (MEE) to undertake an Environmental Impact Assessment (EIA) for Waste Management Project at Thilafushi Island, Maldives. As part of the project, an incinerator is proposed to burn waste material and seawater through an intake will be used to cool condenser. After cooling process, the hot seawater will be re-discharged through an outfall into the sea. As part of the EIA work, the dispersion behaviour of the discharged hot water need to assessed.

Water Solutions Pvt Ltd requested Lanka Hydraulic Institute Ltd (LHI) to submit a proposal for Effluent Dispersion Model study for the proposed cooling system of incinerator, and we, Lanka Hydraulic Institute Ltd (LHI), submitted the proposal in response to the requirements. After reviewing the proposal, LHI was awarded the contract to conduct the Effluent Dispersion Model study for the proposed cooling system of incinerator.

This report includes six chapters. Background of the project and basic methodology used in the study are given in Chapter 1. The details of collected wind data and analysis of it are given in Chapter 2. Wave transformation method and model usage for wave generation are discussed in detail in Chapter 3. In order to assess the water circulation, a set of hydrodynamic models was performed; those methods and results are discussed under Chapter 4. As the main part of study, thermal dispersion modelling system and discussion of its results are presented in Chapter 5. Finally the conclusions are given in Chapter 6.

1.1 Background

The Thilafushi island is located in North Male Atoll, Maldives, and around 7km westwards to Male City (Figure 1.1). Presently, the island is used as the main waste dumping site in the country capital Male and its adjacent inhabited islands and the airport at Hulhule. The Government of the Maldives has identified solid waste disposal as a priority problem and decided to implement a solid waste management plan to minimize the environmental problem.

As a part of the project, an incinerator has been proposed to burn the waste. The cooling system of incinerator will run using sea water as coolant. The dispersion of hot water in marine environment is required to assess with respect to the coastal process of region.

This island is subjected to two monsoon period namely South-West and Nort-East; South West monsoon is considered as from May to November while North East as from December to April. Energy of swell waves approach from southern Indian ocean may reduce due to diffraction and other interaction of other atoll reefs, and mainly sea waves are affected to the island. Sea currents are developed around the island reef mainly wind, wave and tidal effect.

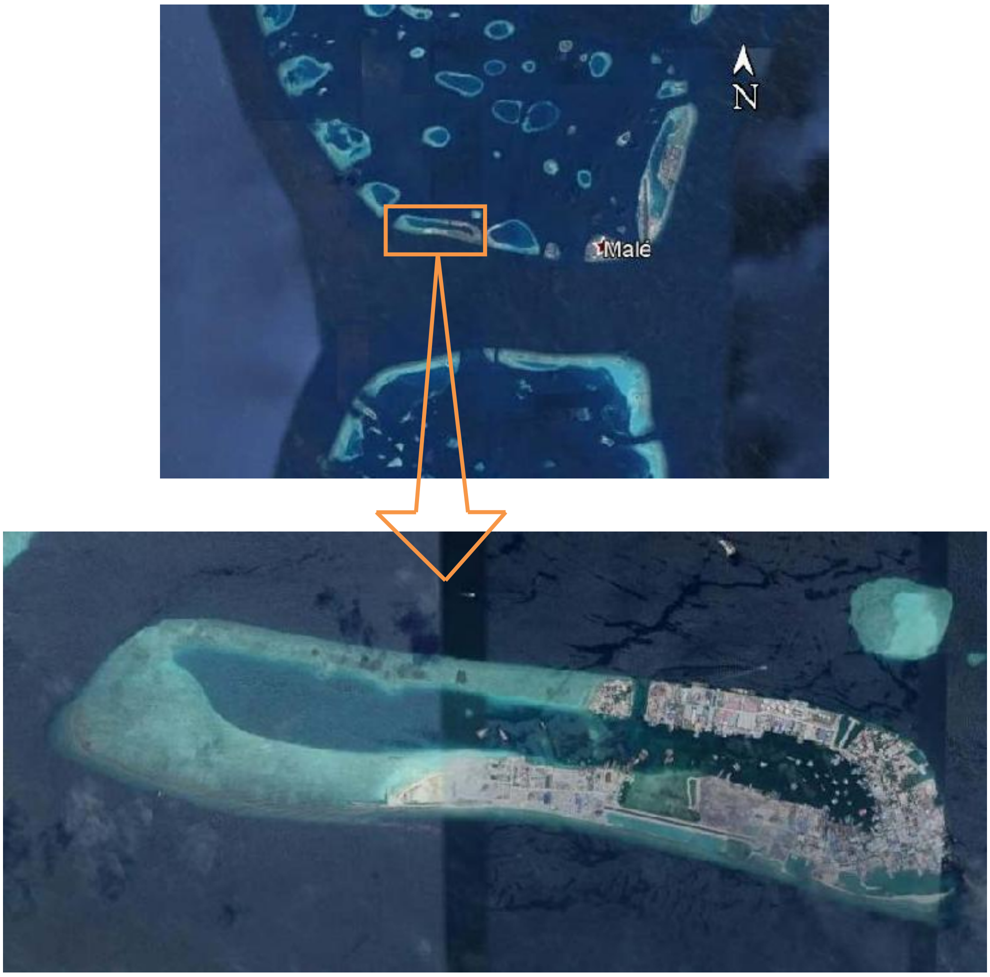

Figure 1.1: Location of Thilafushi Island

1.2 Objective of the Study

The discharge of effluent in the coastal area is a sensitive issue in the context of environmental conservation and therefore dispersion of the effluent requires proper assessment to ensure that nearshore coastal environment will not be subjected to pollution and health risk due to discharged effluent. For this purpose it is extremely essential to ensure that effluent constituent is diluted to acceptable levels within the receiving water in the immediate vicinity of discharge point. Secondly, the advection dispersion of the effluent should be favourable to the environment for every monsoon period.

The objective of this modelling task is to simulate the dynamic behaviour of hot water discharged through the outfall, and to assess the impacts on the surrounding areas of the outfalls, near-shore areas and beaches.

1.3 Basic Methodology of Study

Since the hot water dispersion is to be assessed for different monsoons and tidal conditions, at the first stage, wave conditions and tidal conditions require to be developed at site location. In order to develop wave conditions for different monsoon periods at site location, long period wind data was used in a Wind-Wave Transformation Model (MIKE 21 SW). In order to find out current conditions, a Hydrodynamic Model (MIKE 21 HD) was utilised with giving wind/wave condition and tidal variation as input parameters. After that thermal dispersion model, CORMIX was used to find out initial dilution in near field and its results were further applied to the Hydrodynamic Model couple with thermal dispersion tool to assess the dilution in 2D plain.

Main activities of study are given below.

1. Obtain and analyze of UK Met Office (UKMO) wind data at site location.
2. Develop model bathymetries using Admiralty Chart Maps and measured data
3. Find out wave condition near the site using Wind-Wave Transformation Model (MIKE 21 SW)
4. Simulate a regional Hydrodynamic Model using known tidal boundaries in order to find out hydrodynamic conditions at local model boundaries.
5. Simulate local Hydrodynamic Model with applying wind, wave and tidal condition and find out current condition at site for different monsoons.
6. Apply current conditions obtained from Hydrodynamic Model in CORMIX model and find out initial dilution in near field.
7. Simulate again Hydrodynamic Model couple with thermal dispersion tool and applying CORMIX model results to assess the dilution in 2D plain.

2 WIND DATA AND WAVE GENERATION

The wind data was obtained based on the hind-cast data from Numerical Weather Prediction Atmospheric Global model of the UK Met Office (UKMO). The available nearest suitable data point (3.984 N, 73.477 E) which located in the South Male Atoll was selected with considering fetch length and open sea area which would be adopted in the wind wave model (Figure 2.1). Real time observational data from satellite wind radar, ship and buoy data were (and are) assimilated into the atmospheric model. This process strives to give the best possible rendition of the 'surface' wind field at analysis or run time, in order to give an optimum forecast. In effect, the atmospheric wind fields represent a hybrid of numerical and real data. It is the analysis time steps of these models of whatever resolution which go to make up the archive on which hind-casts are based.

Wind speed and wind direction for 30 years during January 1986 to June 2016 were utilized for the study. The data set contents 89,112 no of records with the interval of 3 hours. Analyses were carried out to assess the distribution of wind parameters and given in the Figure 2.2 and the Table 2.1.

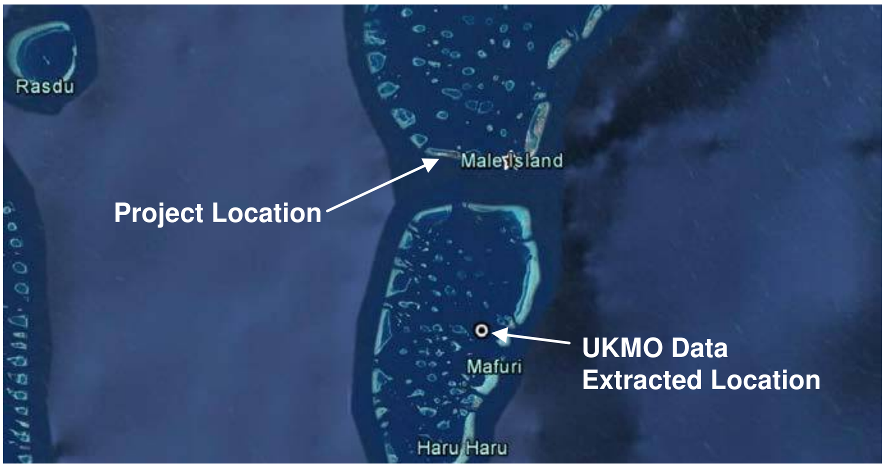

Figure 2.1: Wind Data Extracted Location

2.1 Analysis of UKMO Wind Data

Analysis of raw data before apply it in the model is an essential part in wind - wave transformation numerical modelling process to gain an idea about the wind climates of the region. Therefore analyses for UKMO data were carried out based on wind speed and direction.

Figure 2.2 illustrates clearly wind distribution pattern in 360^o angle. The length of slices represents the percentage of occurrence while the colour code for the wind speeds. Furthermore, Table 2.1 shows the occurrence of wind by values in different directions and various speeds. According to the analysis, two dominant wind directions can be observed; i.e. West and North-East. The wind reached from South- East quadrant is negligible.

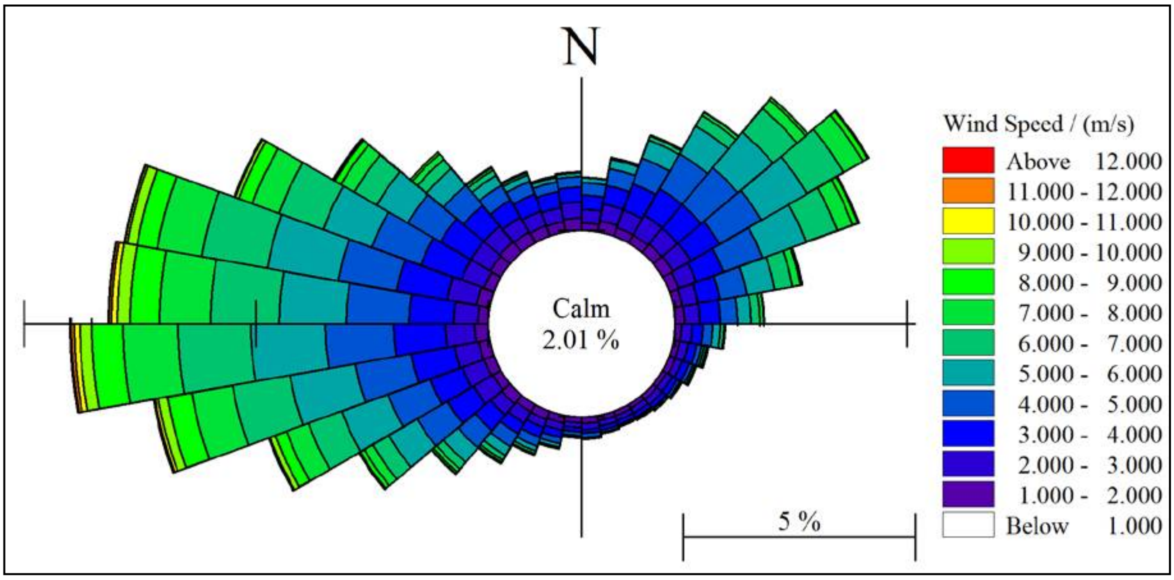

Figure 2.2: Annual Distribution of Wind

Table 2.1: Directional Distribution of Wind Statistics (Percentage Occurrence for Wind Speed vs Wind Direction)

Dir (Deg.N) / Speed (m/s)	0 -- 10	10 -- 20	20 -- 30	30 -- 40	40 -- 50	50 -- 60	60 -- 70	70 -- 80	80 -- 90	90 -- 100	100 -- 110	110 -- 120	120 -- 130	130 -- 140	140 -- 150	150 -- 160	160 -- 170	170 -- 180	180 -- 190	190 -- 200	200 -- 210	210 -- 220	220 -- 230	230 -- 240	240 -- 250	250 -- 260	260 -- 270	270 -- 280	280 -- 290	290 -- 300	300 -- 310	310 -- 320	320 -- 330	330 -- 340	340 -- 350	350 -- 360	Total
0 – 1	0.03	0.06	0.06	0.05	0.06	0.07	0.06	0.04	0.09	0.03	0.03	0.05	0.04	0.06	0.05	0.04	0.05	0.08	0.03	0.06	0.07	0.06	0.06	0.06	0.07	0.06	0.11	0.03	0.08	0.07	0.08	0.06	0.07	0.06	0.06	0.03	2.07
1 – 2	0.17	0.24	0.20	0.21	0.24	0.26	0.21	0.19	0.20	0.14	0.14	0.14	0.10	0.12	0.10	0.10	0.11	0.12	0.11	0.16	0.19	0.18	0.24	0.21	0.23	0.24	0.30	0.23	0.30	0.23	0.27	0.29	0.27	0.24	0.23	0.18	7.07
2 – 3	0.29	0.38	0.43	0.48	0.44	0.45	0.43	0.35	0.34	0.23	0.19	0.16	0.15	0.14	0.13	0.11	0.11	0.13	0.12	0.17	0.19	0.28	0.32	0.49	0.51	0.53	0.64	0.53	0.64	0.54	0.48	0.45	0.39	0.34	0.31	0.29	12.16
3 – 4	0.31	0.40	0.57	0.67	0.67	0.72	0.60	0.49	0.42	0.24	0.19	0.16	0.13	0.10	0.09	0.09	0.09	0.08	0.08	0.16	0.22	0.27	0.44	0.65	0.73	0.96	1.10	0.95	1.13	0.92	0.77	0.58	0.41	0.38	0.35	0.26	16.39
4 – 5	0.26	0.38	0.58	0.86	1.03	1.05	0.90	0.61	0.37	0.20	0.10	0.08	0.07	0.03	0.04	0.04	0.05	0.09	0.08	0.13	0.20	0.31	0.48	0.75	0.97	1.26	1.48	1.36	1.31	1.11	0.82	0.55	0.38	0.29	0.21	0.19	18.62
5 – 6	0.10	0.19	0.42	0.68	0.99	1.13	1.00	0.59	0.30	0.16	0.06	0.05	0.03	0.03	0.03	0.01	0.04	0.05	0.04	0.07	0.11	0.21	0.41	0.70	1.07	1.40	1.63	1.45	1.51	1.15	0.75	0.48	0.23	0.14	0.09	0.08	17.39
6 – 7	0.02	0.04	0.09	0.26	0.69	0.90	0.72	0.39	0.19	0.08	0.05	0.03	0.02	0.01	0.00	0.01	0.02	0.01	0.03	0.04	0.06	0.11	0.20	0.40	0.76	1.24	1.56	1.49	1.43	0.98	0.57	0.25	0.12	0.07	0.03	0.02	12.89
7 – 8	0.00	0.01	0.03	0.08	0.23	0.47	0.35	0.18	0.08	0.03	0.03	0.02	0.01	0.01				0.01	0.02	0.02	0.02	0.06	0.09	0.21	0.50	0.90	1.16	1.07	0.98	0.62	0.33	0.15	0.05	0.03	0.00	0.01	7.78
8 – 9		0.00	0.03	0.02	0.05	0.12	0.11	0.04	0.01	0.01	0.02	0.00							0.01	0.00	0.01	0.02	0.04	0.09	0.25	0.52	0.65	0.62	0.43	0.30	0.14	0.04	0.03	0.02			3.60
9 – 10				0.02	0.04	0.05	0.03	0.00	0.00	0.00	0.00										0.00	0.01	0.01	0.02	0.12	0.21	0.24	0.28	0.21	0.08	0.04	0.01	0.00				1.39
10 – 11						0.00	0.01															0.01	0.00	0.01	0.03	0.06	0.13	0.12	0.06	0.02	0.02	0.00					0.47
11 – 12																									0.01	0.02	0.06	0.04	0.02	0.01	0.00	0.01					0.18
12 – 13																									0.01	0.01	0.04	0.01	0.01	0.01	0.00						0.09
13 – 14																								0.00			0.01	0.01									0.02
14 – 15																											0.00										0.00
15 – 16																												0.00									0.00
Total	1.18	1.70	2.42	3.33	4.44	5.22	4.42	2.86	2.00	1.12	0.81	0.69	0.54	0.51	0.44	0.41	0.47	0.58	0.51	0.81	1.08	1.53	2.28	3.60	5.26	7.42	9.13	8.22	8.09	6.03	4.27	2.89	1.95	1.56	1.28	1.06	100

3 WAVE CLIMATE MODELLING

3.1 Introduction

Wave climate condition is one of main input parameter for the hydrodynamic model. Therefore it is required to develop wave climate conditions for different monsoons in order to set up the hydrodynamic model. The wave data is not available for the desired location on the sea fit for usage. Most of the time wave data measured point is far away from the project location and it has to be transformed to a desired location by a model. In this case, MIKE 21 numerical wave model was used for wind wave generation and transformation process. The objectives of the wave climate modelling of this scheme is establishing nearshore wave climate at the site.

3.2 Model Used – MIKE 21 SW Model System

MIKE 21 SW includes a new generation spectral wind-wave model based on unstructured mesh. The model simulates the growth, decay and transformation of wind-generated waves and swells in offshore and coastal areas. It includes two different formulations, namely, directional decoupled parametric formulation and fully spectral formulation. The directional decoupled parametric formulation is based on a parameterization of the wave action conservation equation. The parameterization is made in the frequency domain by introducing the zeroth and first moment of the wave action spectrum as dependent variables. The fully spectral formulation is based on the wave action conservation equation, where the directional-frequency wave action spectrum is the dependent variable.

The basic conservation equations are formulated in either Cartesian co-ordinates for small-scale applications or Polar Spherical co-ordinates for large-scale applications.

MIKE 21 SW includes the following physical phenomena:

- Wave growth by action of wind
- Non-linear wave-wave interaction
- Dissipation due to white capping
- Dissipation due to bottom friction
- Dissipation due to depth induced wave breaking
- Refraction and shoaling due to depth variation
- Wave-current interaction
- Effect of time varying water depth and flooding and drying

The discretization of the governing equation in geographical and spectral space is performed using cell-centered finite volume method. In the geographical domain, an unstructured mesh technique is used. The time integration is performed using a fractional step approach where a multi-sequence explicit method is applied for the propagation of wave action.

3.3 Model Setup

MIKE 21 SW model was used to generate waves and transfer them to the proposed site location base on UKMO wind data. All data set obtained from UKMO; i.e. 3 hour interval data from 1986 to 2016 were transferred to the site location.

The model was established by digitizing from the Admiralty charts No. 1013 & 3323, and near shore bathymetry data which were provided by WS. The preparation of model bathymetry was completed using flexible mesh as a requirement of SW model with reference to the Mean Sea Level. Figure 3.1 shows the regional model bathymetry of MIKE 21 SW model.

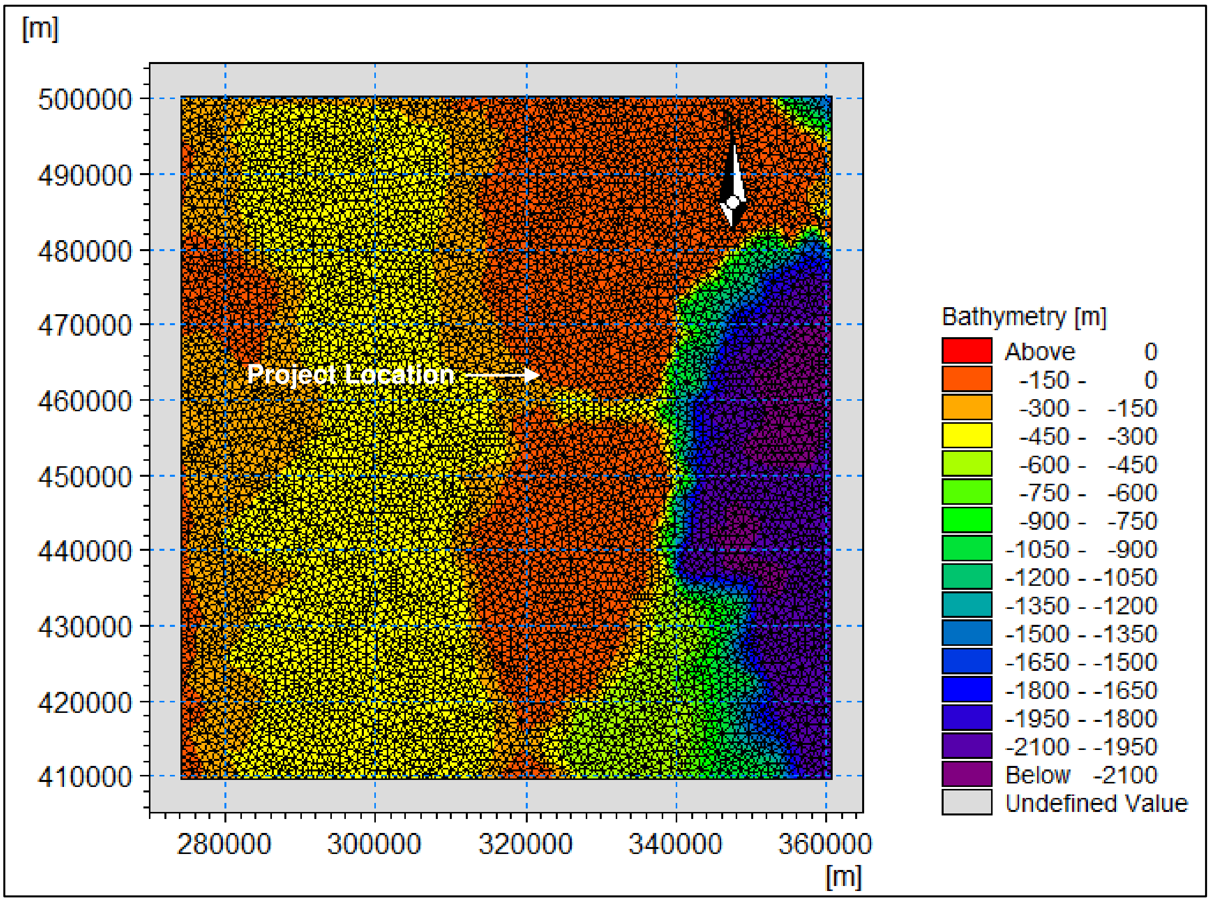

Figure 3.1: Wave Model Bathymetry - Regional

Additionally, a local model was also incorporated to improve the performance and accuracy of results. Then deep sea wind generated waves were transferred to 300m depth by regional model and then analysed wave data were further transferred to the site location by local model. The selected local model which the offshore boundary laid on around 300m depth is shown in Figure 3.2.

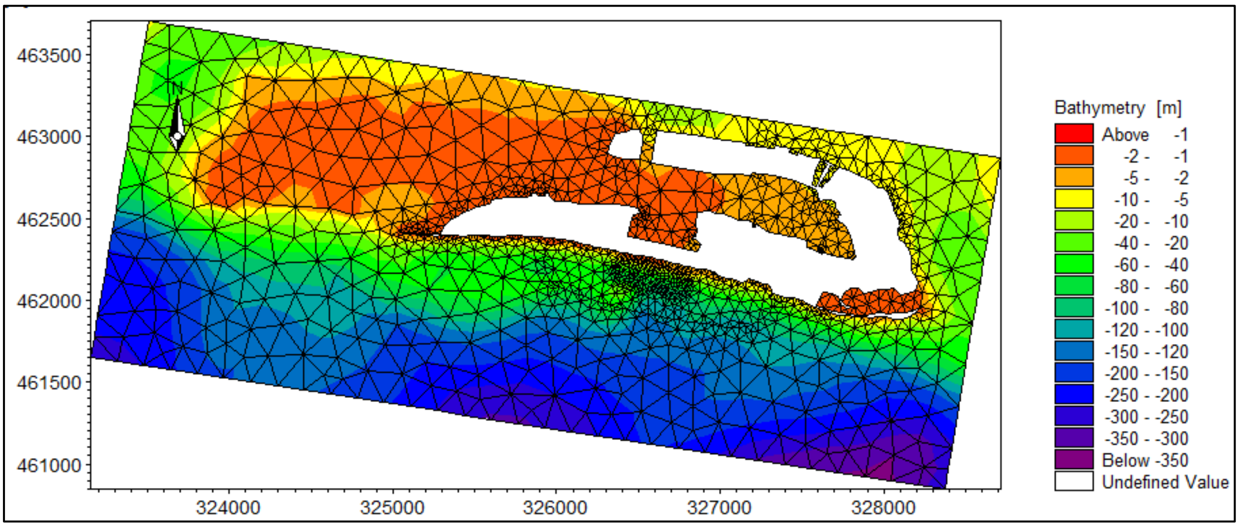

Figure 3.2: Wave Model Bathymetry - Local

3.4 Model Results

The wave analysis details of results obtained from the regional model at 300m depth are given below. The extracted results were analysed considering different seasons such as annual, South-West and North-East monsoon periods. South West monsoon was considered as from May to November while North East as from December to April. Tables 3.1 to 3.6 indicate the percentage of occurrence of waves, and their average peak wave period corresponding to the wave height and direction while Figures 3.3 to 3.5 graphically illustrate the wave height distribution patter in 360° angle.

Table 3.1: Annual Directional Distribution of Wave Height at 300m Depth (Percentage of Occurrence)

Dir (Deg.N) / Hs (m)	0 -- 10	10 -- 20	20 -- 30	30 -- 40	40 -- 50	50 -- 60	60 -- 70	70 -- 80	80 -- 90	90 -- 100	100 -- 110	110 -- 120	120 -- 130	130 -- 140	140 -- 150	150 -- 160	160 -- 170	170 -- 180	180 -- 190	190 -- 200	200 -- 210	210 -- 220	220 -- 230	230 -- 240	240 -- 250	250 -- 260	260 -- 270	270 -- 280	280 -- 290	290 -- 300	300 -- 310	310 -- 320	320 -- 330	330 -- 340	340 -- 350	350 -- 360	Total
0 -- 0.2	0.71	0.88	0.99	1.17	1.36	1.30	1.30	1.05	0.80	0.67	0.47	0.41	0.32	0.33	0.28	0.26	0.25	0.28	0.29	0.36	0.43	0.53	0.62	0.78	0.89	1.01	1.10	1.31	1.20	1.14	1.11	0.98	0.83	0.81	0.73	0.69	27.64
0.2 -- 0.4	0.19	0.32	0.49	0.99	1.73	2.78	3.30	2.53	1.47	0.76	0.43	0.27	0.23	0.17	0.15	0.13	0.14	0.13	0.15	0.18	0.25	0.37	0.58	1.03	1.52	2.41	2.93	2.76	2.04	1.27	0.72	0.46	0.28	0.19	0.16	0.16	33.67
0.4 -- 0.6		0.00	0.01	0.02	0.09	0.44	1.06	0.90	0.41	0.18	0.11	0.07	0.03	0.02	0.01	0.01	0.01	0.02	0.02	0.05	0.12	0.22	0.59	1.59	3.40	4.53	4.29	2.76	1.31	0.41	0.14	0.05	0.01	0.01			22.88
0.6 -- 0.8			0.00	0.00	0.01	0.01	0.03	0.03	0.01	0.00	0.01	0.00	0.00	0.00	0.00			0.00	0.00	0.00	0.01	0.05	0.15	0.52	2.17	3.58	2.84	1.15	0.30	0.04	0.00	0.00	0.00	0.00			10.95
0.8 -- 1			0.00	0.00	0.00		0.00	0.00	0.00	0.00			0.00		0.00	0.00	0.00					0.00	0.03	0.13	0.81	1.56	0.97	0.19	0.03	0.00		0.00		0.00			3.75
1 -- 1.2			0.00	0.00	0.00	0.00										0.00			0.00				0.00	0.01	0.18	0.42	0.19	0.03	0.00		0.00		0.00				0.85
1.2 -- 1.4		0.00	0.00		0.00	0.00										0.00	0.00	0.00							0.02	0.11	0.04						0.00	0.00			0.17
1.4 -- 1.6					0.00			0.00	0.00																0.00	0.01	0.00				0.00	0.00	0.00	0.00			0.03
1.6 -- 1.8				0.00		0.00	0.00		0.00						0.00											0.00	0.00	0.00			0.00	0.00		0.00			0.01
1.8 -- 2					0.00			0.00													0.00		0.00														0.01
2 -- 2.2					0.00	0.00		0.00	0.00										0.00	0.00											0.00			0.00			0.01
Above 2.2		0.00	0.00		0.00	0.00	0.00	0.00	0.00	0.00		0.00	0.00				0.00				0.00		0.00	0.00							0.00		0.00				0.02
Total	0.90	1.20	1.49	2.19	3.19	4.53	5.69	4.52	2.68	1.61	1.02	0.74	0.58	0.52	0.44	0.39	0.41	0.43	0.46	0.59	0.82	1.15	1.97	4.06	8.98	13.64	12.36	8.20	4.87	2.85	1.97	1.49	1.12	1.02	0.90	0.85	100.00

Table 3.2: Annual Directional Distribution of Peak Wave Period at 300m Depth

Dir (Deg.N) / Hs (m)	0 -- 10	10 -- 20	20 -- 30	30 -- 40	40 -- 50	50 -- 60	60 -- 70	70 -- 80	80 -- 90	90 -- 100	100 -- 110	110 -- 120	120 -- 130	130 -- 140	140 -- 150	150 -- 160	160 -- 170	170 -- 180	180 -- 190	190 -- 200	200 -- 210	210 -- 220	220 -- 230	230 -- 240	240 -- 250	250 -- 260	260 -- 270	270 -- 280	280 -- 290	290 -- 300	300 -- 310	310 -- 320	320 -- 330	330 -- 340	340 -- 350	350 -- 360	Average
0 -- 0.2	1.8	1.9	1.9	1.9	2.0	2.0	2.0	2.0	1.9	2.0	1.9	1.8	1.9	1.9	1.8	1.8	2.1	1.9	1.9	1.8	1.7	1.7	1.8	1.8	1.8	1.8	1.9	1.9	1.9	1.9	1.8	1.8	1.8	1.8	1.7	1.7	1.9
0.2 -- 0.4	2.3	2.5	2.5	2.5	2.5	2.6	2.7	2.7	2.7	2.7	2.7	2.8	2.8	2.8	2.8	3.0	3.1	3.2	3.0	3.0	3.0	3.0	3.0	3.0	3.0	3.0	3.0	3.0	2.9	2.8	2.7	2.6	2.5	2.4	2.4	2.4	2.8
0.4 -- 0.6		9.1	7.8	7.0	3.2	3.0	3.1	3.1	3.1	3.2	3.4	3.5	3.3	4.3	7.6	8.5	4.8	8.8	3.6	3.6	3.7	3.8	3.8	3.8	3.8	3.7	3.7	3.6	3.5	3.3	3.4	3.2	3.6	4.9			3.6
0.6 -- 0.8			11.6	10.9	12.4	8.7	7.3	5.3	6.4	5.2	3.5	6.5	13.3	11.5	13.4			19.9	4.0	9.7	4.2	4.2	4.3	4.3	4.2	4.2	4.1	4.0	3.9	3.7	8.9	14.7	13.5	12.9			4.2
0.8 -- 1			13.0	14.1	14.7		10.7	12.2	11.0	12.7			11.8		19.4	7.9	7.0					4.7	5.3	4.6	4.6	4.5	4.4	4.3	4.2	4.1		14.2		12.4			4.5
1 -- 1.2			12.3	10.9	15.9	12.2										12.1			12.3				5.0	5.0	4.9	4.8	4.7	4.6	10.9		13.0		16.3				5.1
1.2 -- 1.4		13.5	12.7		16.6	13.8										13.1	9.8	14.4							5.2	5.1	5.0						14.4	14.0			6.0
1.4 -- 1.6					16.7			14.1	12.8																5.5	5.3	5.2				11.8	14.3	18.8	18.0			9.2
1.6 -- 1.8				13.0		14.2	11.2		14.5						21.2											5.4	5.4	11.6			13.6	16.0		15.8			13.4
1.8 -- 2					15.6			13.0													12.7		18.8														14.8
2 -- 2.2					12.8	13.4		14.7	16.9										10.9	12.2											19.8			14.2			15.3
Above 2.2		17.7	15.1		10.1	12.8	16.4	12.8	15.6	19.6		16.8	13.1				20.9				16.4		15.3	15.4							16.2		15.3				16.3
Average	1.9	2.1	2.3	2.2	2.4	2.5	2.6	2.6	2.6	2.5	2.4	2.3	2.4	2.3	2.5	2.4	2.5	2.5	2.3	2.3	2.4	2.6	3.0	3.3	3.7	3.7	3.5	3.2	2.9	2.5	2.3	2.1	2.0	2.0	1.9	1.8	3.0

Table 3.3: Directional Distribution of Wave Height for South-West Monsoon at 300m Depth (Percentage of Occurrence)

Hs (m) \ Dir (Deg.N)	0 -- 10	10 -- 20	20 -- 30	30 -- 40	40 -- 50	50 -- 60	60 -- 70	70 -- 80	80 -- 90	90 -- 100	100 -- 110	110 -- 120	120 -- 130	130 -- 140	140 -- 150	150 -- 160	160 -- 170	170 -- 180	180 -- 190	190 -- 200	200 -- 210	210 -- 220	220 -- 230	230 -- 240	240 -- 250	250 -- 260	260 -- 270	270 -- 280	280 -- 290	290 -- 300	300 -- 310	310 -- 320	320 -- 330	330 -- 340	340 -- 350	350 -- 360	Total
0 -- 0.2	0.09	0.09	0.08	0.06	0.07	0.03	0.04	0.05	0.07	0.09	0.08	0.08	0.15	0.21	0.24	0.20	0.25	0.31	0.38	0.49	0.60	0.74	0.84	1.13	1.18	1.17	1.19	1.32	1.04	0.79	0.68	0.45	0.30	0.21	0.19	0.10	15.00
0.2 -- 0.4	0.00		0.01	0.01	0.01	0.01	0.01	0.01	0.01	0.01	0.01	0.01	0.03	0.08	0.13	0.15	0.21	0.22	0.27	0.35	0.45	0.65	1.10	1.88	2.55	3.87	4.13	3.52	2.08	1.11	0.57	0.27	0.13	0.04	0.03	0.02	23.96
0.4 -- 0.6			0.01	0.00	0.00		0.01	0.00		0.00	0.00	0.00		0.01	0.01	0.01	0.02	0.03	0.05	0.10	0.23	0.37	1.07	3.00	6.42	8.04	7.35	4.46	2.04	0.66	0.24	0.06	0.00	0.00			34.20
0.6 -- 0.8			0.01	0.01	0.01		0.01							0.00	0.00				0.00	0.00	0.02	0.08	0.31	1.03	4.22	6.25	4.86	1.94	0.57	0.09	0.01						19.41
0.8 -- 1				0.00	0.00		0.00	0.01					0.00			0.00						0.00	0.04	0.22	1.24	2.47	1.63	0.33	0.07	0.01							6.03
1 -- 1.2			0.01	0.00	0.00	0.00													0.00				0.00	0.02	0.19	0.49	0.33	0.05	0.01				0.00				1.10
1.2 -- 1.4			0.00		0.00											0.00		0.01							0.01	0.11	0.07										0.21
1.4 -- 1.6											0.01														0.01	0.02	0.01				0.00	0.00					0.05
1.6 -- 1.8				0.00			0.00		0.00																	0.00	0.00	0.00									0.02
1.8 -- 2					0.01			0.00																													0.01
2 -- 2.2						0.00			0.00										0.00	0.00																	0.01
Above 2.2			0.00		0.00	0.00			0.00														0.00														0.01
Total	0.09	0.09	0.12	0.08	0.10	0.05	0.07	0.07	0.09	0.11	0.10	0.10	0.18	0.30	0.37	0.37	0.49	0.58	0.70	0.95	1.30	1.85	3.36	7.28	15.82	22.44	19.56	11.61	5.80	2.65	1.49	0.79	0.44	0.25	0.22	0.12	100.00

Table 3.4: Directional Distribution of Peak Wave Period for South-West Monsoon at 300m Depth

Hs (m) \ Dir (Deg.N)	0 -- 10	10 -- 20	20 -- 30	30 -- 40	40 -- 50	50 -- 60	60 -- 70	70 -- 80	80 -- 90	90 -- 100	100 -- 110	110 -- 120	120 -- 130	130 -- 140	140 -- 150	150 -- 160	160 -- 170	170 -- 180	180 -- 190	190 -- 200	200 -- 210	210 -- 220	220 -- 230	230 -- 240	240 -- 250	250 -- 260	260 -- 270	270 -- 280	280 -- 290	290 -- 300	300 -- 310	310 -- 320	320 -- 330	330 -- 340	340 -- 350	350 -- 360	Average
0 -- 0.2	1.4	2.5	4.8	2.1	2.4	2.4	1.3	1.4	2.7	1.6	1.8	1.7	2.1	1.9	1.9	1.8	1.8	1.9	1.8	1.8	1.8	1.8	1.8	1.8	1.9	1.9	1.9	1.9	1.9	1.9	1.8	1.8	1.7	2.0	1.6	1.6	1.9
0.2 -- 0.4	2.2		5.3	4.1	6.1	8.6	3.7	10.3	11.5	7.9	2.5	3.7	2.7	2.7	2.8	3.0	2.9	3.1	3.1	3.0	3.0	3.0	3.0	3.0	3.0	3.0	3.0	3.0	2.9	2.9	2.8	2.7	2.5	2.4	2.4	2.4	3.0
0.4 -- 0.6			11.7	9.3	10.1		12.2	7.9		7.9	15.7	8.1		6.8	3.3	5.9	3.8	3.5	3.5	3.7	3.8	3.8	3.8	3.8	3.8	3.7	3.7	3.6	3.5	3.4	3.2	3.1	3.1	13.0			3.7
0.6 -- 0.8			11.5	9.0	9.9		12.7							11.5	17.2				4.0	4.2	4.2	4.2	4.3	4.2	4.2	4.2	4.1	4.0	3.9	3.7	3.6						4.2
0.8 -- 1				14.1	16.1		10.7	12.2					11.8			7.9						4.6	4.7	4.6	4.6	4.5	4.4	4.3	4.2	4.1							4.5
1 -- 1.2			12.3	10.3	13.1	13.0													12.3				4.9	5.0	4.9	4.8	4.7	4.6	10.9				18.7				5.1
1.2 -- 1.4			12.7		16.6											13.1		13.5							5.2	5.1	5.0										5.9
1.4 -- 1.6											14.3														5.5	5.3	5.2				11.8	13.6					8.6
1.6 -- 1.8				13.0			11.2		14.5																	5.4	5.4	11.6									11.1
1.8 -- 2					15.6			13.0																													14.7
2 -- 2.2						13.4			13.1										10.9	12.2																	12.6
Above 2.2			15.8		10.1	12.8			20.0														15.3														11.5
Average	1.5	2.5	6.8	4.0	6.2	7.1	6.0	4.4	5.8	2.6	3.5	2.0	2.4	2.3	2.3	2.6	2.4	2.5	2.5	2.5	2.6	2.7	3.1	3.3	3.7	3.7	3.6	3.3	3.0	2.7	2.4	2.1	2.0	2.2	1.7	1.7	3.4

Table 3.5: Directional Distribution of Wave Height for North East Monsoon at 300m Depth (Percentage of Occurrence)

Hs (m) \ Dir (Deg.N)	0 -- 10	10 -- 20	20 -- 30	30 -- 40	40 -- 50	50 -- 60	60 -- 70	70 -- 80	80 -- 90	90 -- 100	100 -- 110	110 -- 120	120 -- 130	130 -- 140	140 -- 150	150 -- 160	160 -- 170	170 -- 180	180 -- 190	190 -- 200	200 -- 210	210 -- 220	220 -- 230	230 -- 240	240 -- 250	250 -- 260	260 -- 270	270 -- 280	280 -- 290	290 -- 300	300 -- 310	310 -- 320	320 -- 330	330 -- 340	340 -- 350	350 -- 360	Total
0 -- 0.2	1.31	1.73	2.15	2.52	2.85	2.81	2.76	2.01	1.42	1.01	0.65	0.53	0.31	0.28	0.18	0.12	0.16	0.08	0.07	0.07	0.15	0.12	0.07	0.13	0.16	0.20	0.27	0.31	0.33	0.48	0.70	0.87	0.85	0.98	1.04	1.18	30.86
0.2 -- 0.4	0.62	0.98	1.59	3.31	5.87	9.57	11.03	7.95	4.07	1.84	0.87	0.60	0.33	0.22	0.12	0.07	0.04		0.02	0.01	0.02	0.03	0.02	0.07	0.11	0.20	0.31	0.49	0.55	0.51	0.45	0.53	0.43	0.42	0.42	0.46	54.14
0.4 -- 0.6		0.01	0.01	0.07	0.34	1.67	4.06	3.32	1.42	0.62	0.33	0.20	0.05	0.01	0.03	0.01			0.00		0.01	0.02	0.00	0.04	0.20	0.21	0.30	0.17	0.13	0.10	0.07	0.03	0.02	0.01		0.01	13.49
0.6 -- 0.8					0.01	0.01	0.10	0.11	0.01	0.01	0.02	0.00	0.00									0.01	0.00		0.11	0.33	0.18	0.03	0.00		0.00		0.00				0.95
0.8 -- 1																							0.02	0.02	0.16	0.18	0.02							0.00			0.41
1 -- 1.2				0.00												0.00								0.01	0.06	0.01					0.00						0.10
1.2 -- 1.4		0.00																							0.00												0.01
1.4 -- 1.6																																	0.00	0.00			0.01
1.6 -- 1.8															0.00																0.00	0.00					0.01
1.8 -- 2																																					
2 -- 2.2																																		0.00			0.00
Above 2.2								0.00	0.00	0.00							0.00																				0.02
Total	1.94	2.73	3.75	5.89	9.08	14.06	17.95	13.40	6.93	3.48	1.87	1.33	0.69	0.52	0.34	0.20	0.20	0.08	0.10	0.09	0.19	0.17	0.13	0.26	0.79	1.13	1.08	1.00	1.02	1.09	1.23	1.44	1.31	1.43	1.45	1.64	100.00

Table 3.6: Directional Distribution of Peak Wave Period for North East Monsoon at 300m Depth

Hs (m) \ Dir (Deg.N)	0 -- 10	10 -- 20	20 -- 30	30 -- 40	40 -- 50	50 -- 60	60 -- 70	70 -- 80	80 -- 90	90 -- 100	100 -- 110	110 -- 120	120 -- 130	130 -- 140	140 -- 150	150 -- 160	160 -- 170	170 -- 180	180 -- 190	190 -- 200	200 -- 210	210 -- 220	220 -- 230	230 -- 240	240 -- 250	250 -- 260	260 -- 270	270 -- 280	280 -- 290	290 -- 300	300 -- 310	310 -- 320	320 -- 330	330 -- 340	340 -- 350	350 -- 360	Average
0 -- 0.2	1.8	1.9	1.9	1.9	2.0	2.0	2.0	2.0	1.9	2.1	1.8	1.8	1.8	1.8	2.2	1.8	2.4	2.1	2.8	1.9	2.0	1.5	1.9	1.9	1.6	1.8	1.7	1.8	1.9	1.9	1.9	1.8	1.7	1.8	1.8	1.8	1.9
0.2 -- 0.4	2.3	2.4	2.4	2.4	2.5	2.6	2.7	2.7	2.7	2.7	2.7	2.7	2.9	2.8	2.8	2.9	3.1		2.5	2.6	2.9	2.8	3.1	2.8	3.0	2.9	3.0	2.9	2.9	2.8	2.7	2.6	2.5	2.4	2.4	2.3	2.6
0.4 -- 0.6		6.5	5.0	2.9	3.0	3.0	3.0	3.1	3.1	3.1	3.2	3.2	3.3	3.2	7.4	7.2			7.6		3.8	3.9	3.7	3.7	3.8	3.7	3.6	3.5	3.4	3.3	3.7	3.1	3.0	2.9		2.8	3.1
0.6 -- 0.8					3.2	3.3	3.4	3.6	3.4	8.7	3.5	3.6	14.2									4.3	4.5		4.3	4.2	4.1	3.9	3.8		10.0		13.5				4.1
0.8 -- 1																							6.9	4.8	4.6	4.5	4.4							12.4			4.8
1 -- 1.2				14.5												12.1								4.9	4.9	4.9					13.0						6.1
1.2 -- 1.4		13.5																							5.2												9.3
1.4 -- 1.6																																	18.8	18.0			18.4
1.6 -- 1.8															21.2																13.6	13.3					16.0
1.8 -- 2																																					
2 -- 2.2																																		14.2			14.2
2.2 -- 2.4								12.8	11.1	19.6							20.9																				17.5
Average	2.0	2.1	2.2	2.2	2.4	2.5	2.6	2.7	2.6	2.7	2.5	2.5	2.5	2.2	3.1	2.8	3.0	2.1	3.0	2.0	2.2	2.1	3.2	2.7	3.6	3.5	3.1	2.7	2.6	2.4	2.4	2.2	2.1	2.1	1.9	1.9	2.5

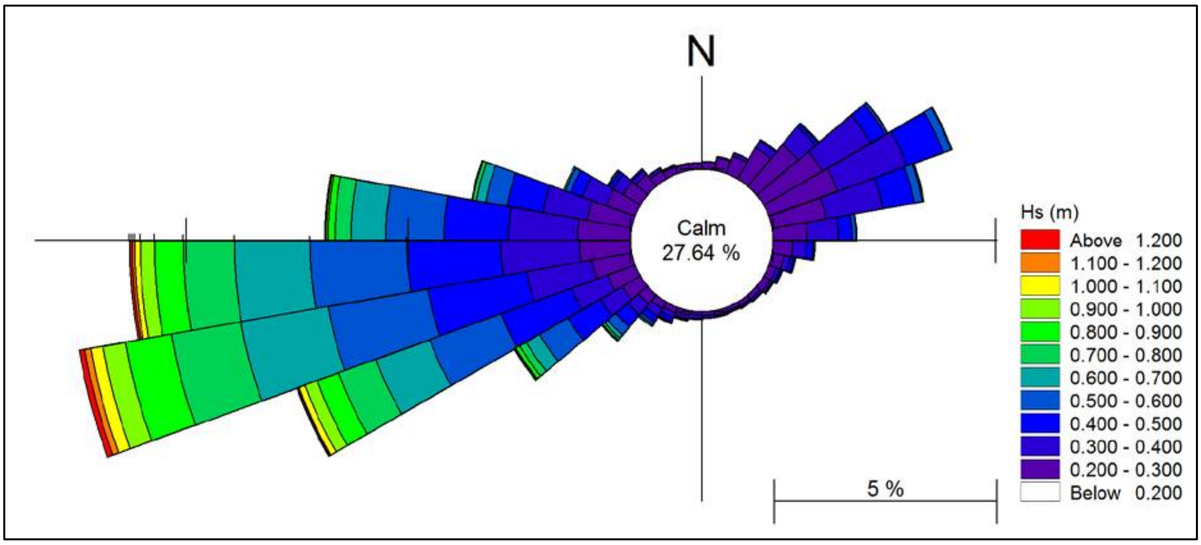

Figure 3.3: Annual Wave Height Distribution at 300m Depth

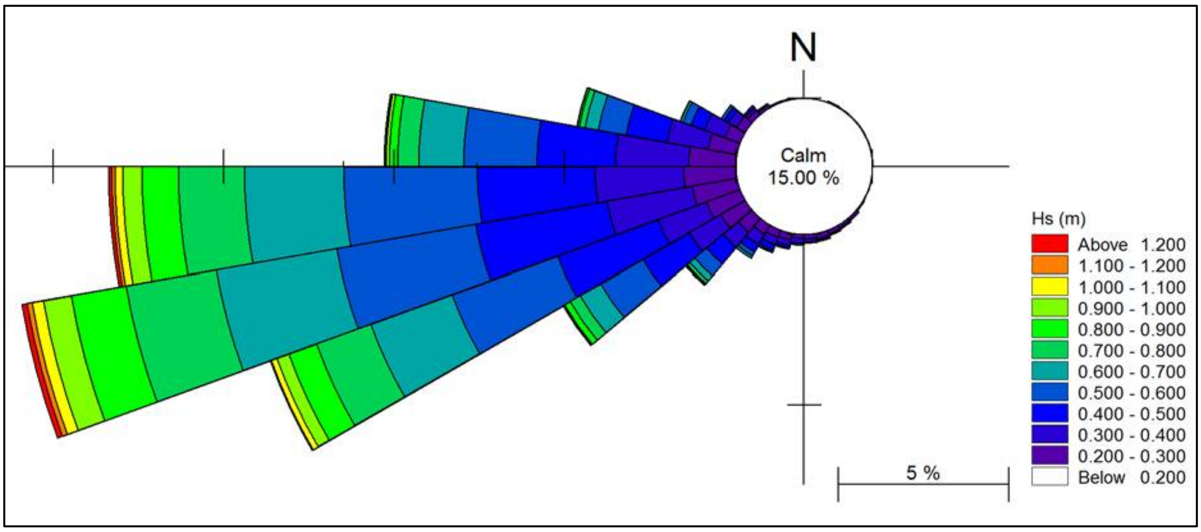

Figure 3.4: Wave Height Distribution for South-West Monsoon at 300m Depth

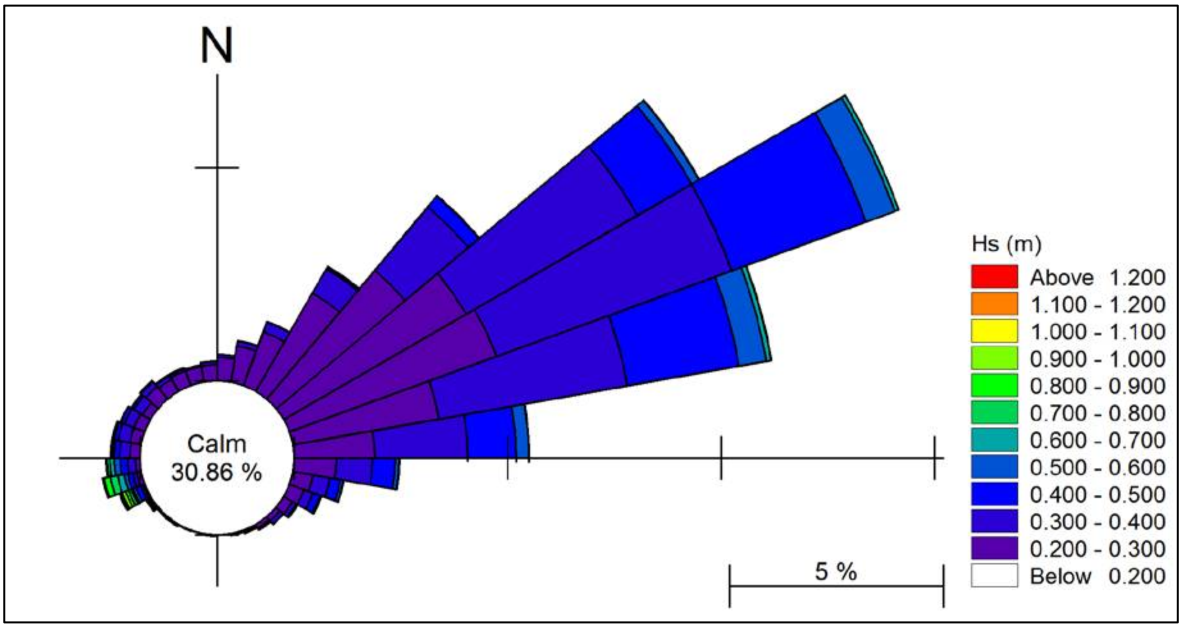

Figure 3.5: Wave Height Distribution for North-East Monsoon at 300m Depth

4 HYDRODYNAMIC MODELLING

In order to compute water circulation with effect of tidal flow, wave and wind in and around the study area, a hydrodynamic model required to be carried out. Hence, the numerical model, MIKE 21 HD was used in this process.

4.1 MIKE 21 Hydrodynamic Model System

MIKE 21 HD (Flexible Mesh) model developed by Danish Hydraulic Institute was used for the simulation. It is a modelling system for 2D free-surface flows and applicable to the simulation of hydraulic and environmental phenomena in lakes, rivers, estuaries, bays, coastal areas and seas in response to a variety of forcing functions including tide, wind, wave and river flow. The HD module allows you to specify a variety of hydrographic boundary conditions, initial conditions, bed resistance and wind forcing. It also allows you to include different types of sources and sinks as well as a number of different structures. It provides the hydrodynamic basis for the computations performed in the environmental hydraulics and sediment transport modules.

4.2 MIKE 21 HD Model Set Up

4.2.1 Model Bathymetry

Same as the wave model, Admiralty charts and bathymetry data provided by the client were used for the development of model bathymetry. Since tidal variation would be applied as main boundary condition for the regional model, availability of tidal data was considered when setting up the model. Tidal boundaries were developed using MIKE 21 Toolbox Tide developer considering 25km away from Thilafushi in North and South directions, and 45km in West and East direction. Therefore the regional model covers the model area of 50km in north-south way and 90km east-west way. Figure 4.1 illustrates the bathymetry of regional model and position of the local model on it. Local model was selected considering the bathymetry, and kept offshore boundary at 300m depth.

Triangular flexible mesh was generated by MIKE 21 Bathymetry Creator Tool while considering finer mesh size for more concern area. The UTM 43 coordinate system was used for (x, y) coordinates and Mean Sea Level (MSL) was used as the elevation datum. The local bathymetry with mesh is given in Figure 4.2.

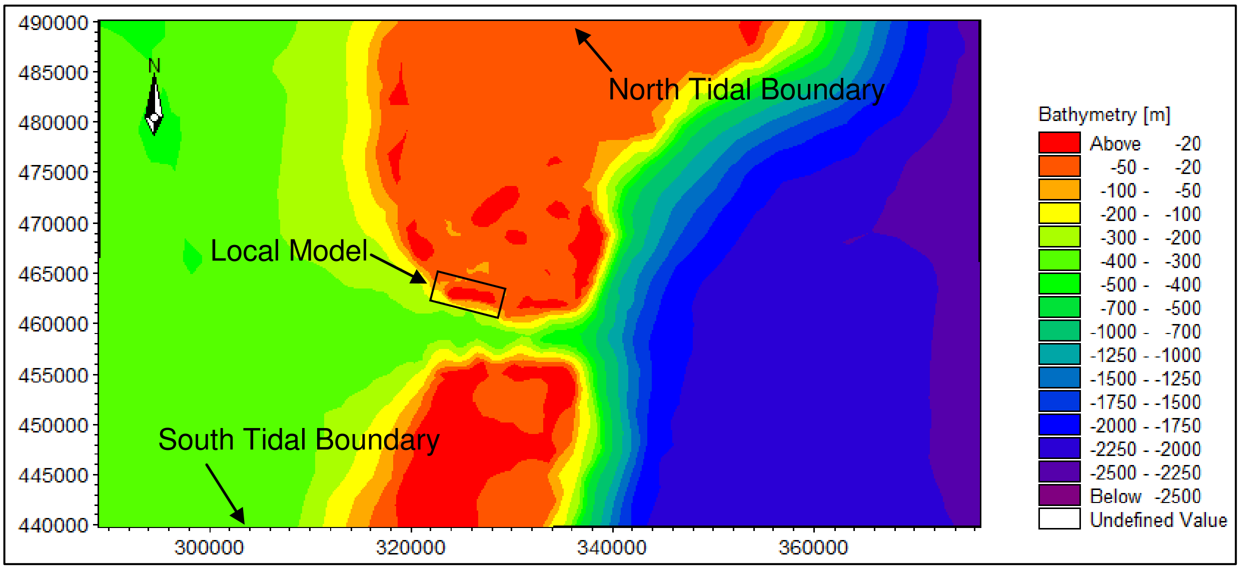

Figure 4.1: Bathymetry for Regional Hydrodynamic Model

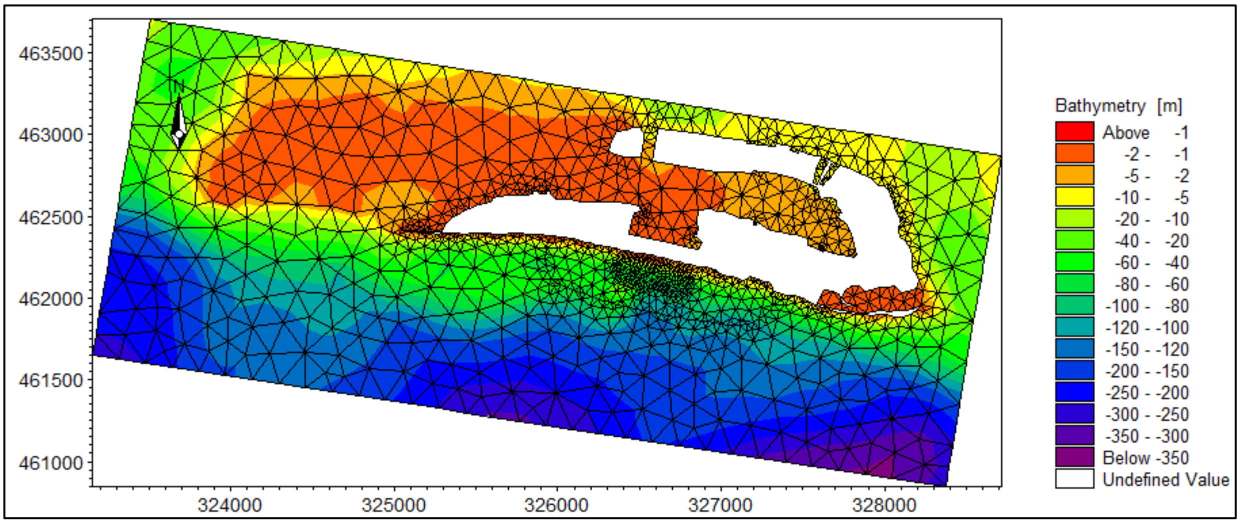

Figure 4.2: Bathymetry for Local Hydrodynamic Model

4.2.2 Simulation Period

The regional model was run for one month period for each South-West and North-East monsoon and the local model was run for three days for each monsoon which covering spring and neap tide. The regional model was run with the time step of 3s and the local model with 1s.

4.2.3 Boundary Conditions

The tide levels of the boundaries are used as boundary conditions for regional model. Time series of water levels were predicted using MIKE 21 Toolbox Tide developer for north and south tidal boundaries as indicated in Figure 4.1. Representative predicted tidal plots in north and south boundaries for few days in South-West Monsoon are shown in Figures 4.3 and 4.4.

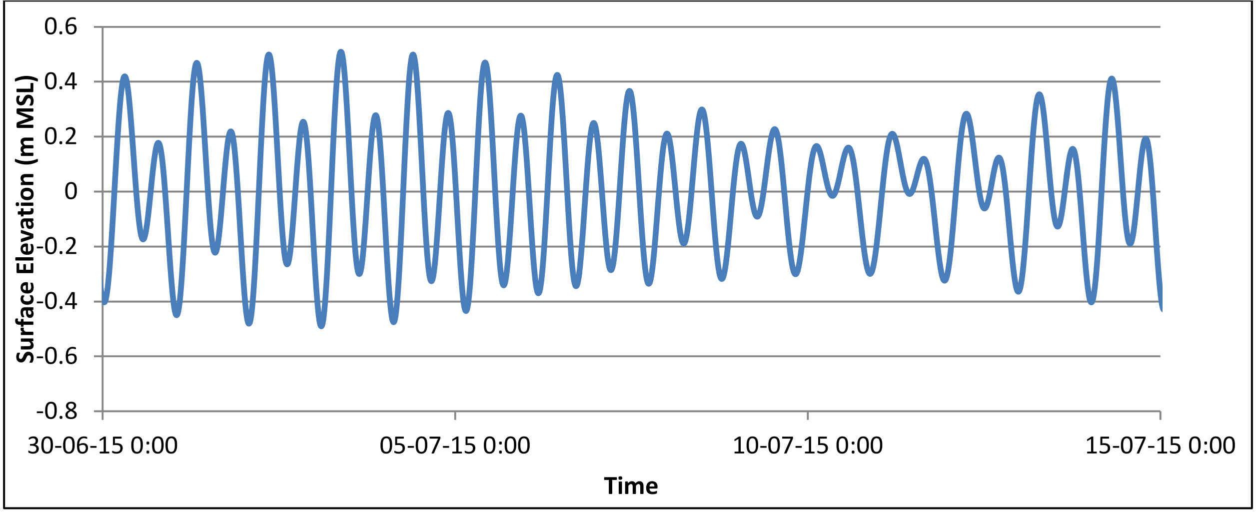

Figure 4.3: Predicted Tide in North Boundary

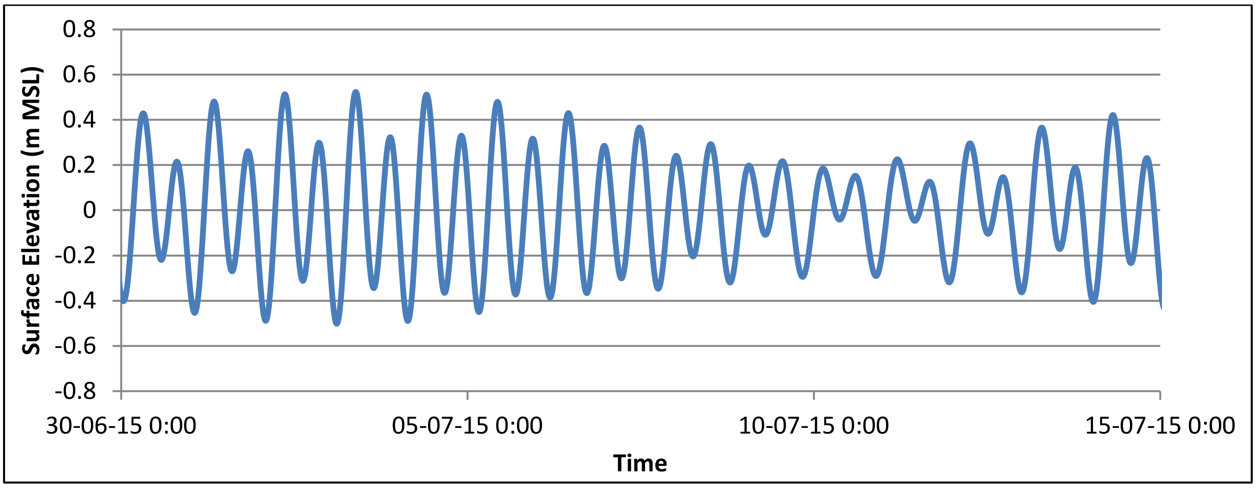

Figure 4.4: Predicted Tide in South Boundary

Water levels and discharges extracted from regional model at the boundaries of the local model were used as boundary conditions for the local model.

4.2.4 Wave and Wind Conditions

Local model was run for average wave/wind condition for both monsoons. The average condition was selected considering 50% of occurrence line of wave height of the wave data extracted at 300m depth from wave transformation model (MIKE 21 SW). In this process, most dominant directional bands were selected for the calculations (as coloured in Table 3.3 to 3.6). Same as wave, 50% of occurrence line of wind speed of UKMO wind data was selected to obtain corresponding wind speed. The selected wave and wind conditions are given in following table and both wind and wave conditions were applied at the same time in the model for each monsoon.

Table 4.1: Applied Wave/Wind Conditions for the Local Hydrodynamic Model

Monsoon	Wave Condition			Wind Condition	
	Hs (m)	Tp (s)	Direction (deg)	Speed (m/s)	Direction (deg)
SW	0.49	3.6	260	5.75	270
NE	0.26	2.4	60	5.02	55

4.3 MIKE 21 HD Model Calibration

Calibration was done for predicted tide levels at Male considering the variation of surface elevations. Figure 4.5 shows the water level comparison between model values and predicted tide at male. The bed roughness was used as the calibration parameter and Manning's Number of 32 was set as the suitable values for the calibration.

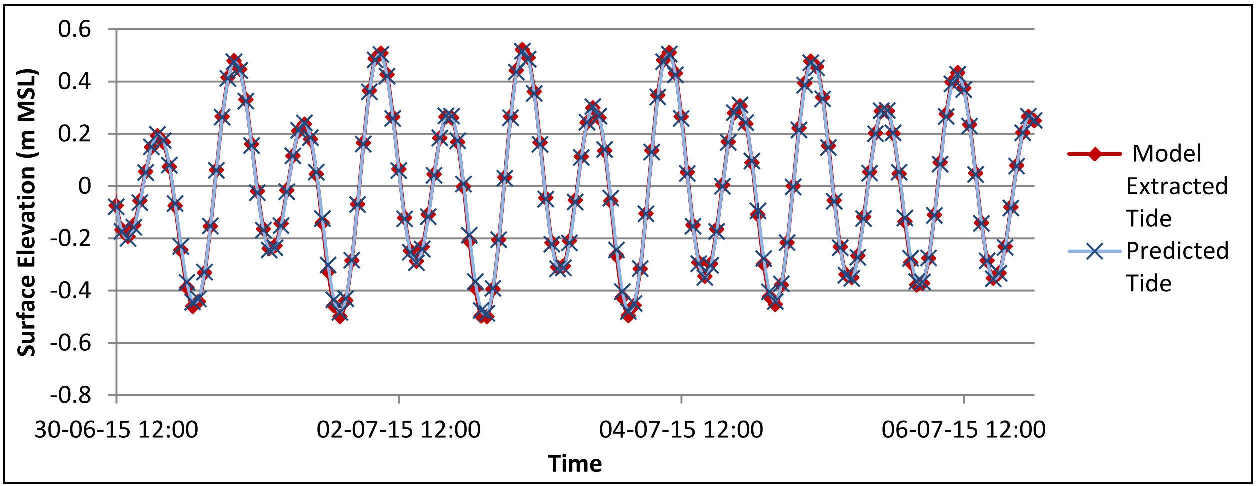

Figure 4.5: Calibration with Predicted Tide at Male

4.4 MIKE 21 HD Results

The main objective of the HD modelling is to observe the flow pattern in the site area and find out the effective current flow for thermal dispersion at outfall. Hence current speeds and directions were extracted at the outfall location (Figure 4.6) for both monsoon periods and spring and neap tidal conditions. The average current speed and direction for different conditions are given in Table 4.2. Further variations of current pattern at outfall area are given in Annex A.

According to the results, it can be observed that the wave condition is not significantly affected for the current at outfall location; it is basically tide dominant. The direction of current varies almost 180 degree with ebb and flood conditions, but Table 4.2 gives direction values only considering westward current flow condition.

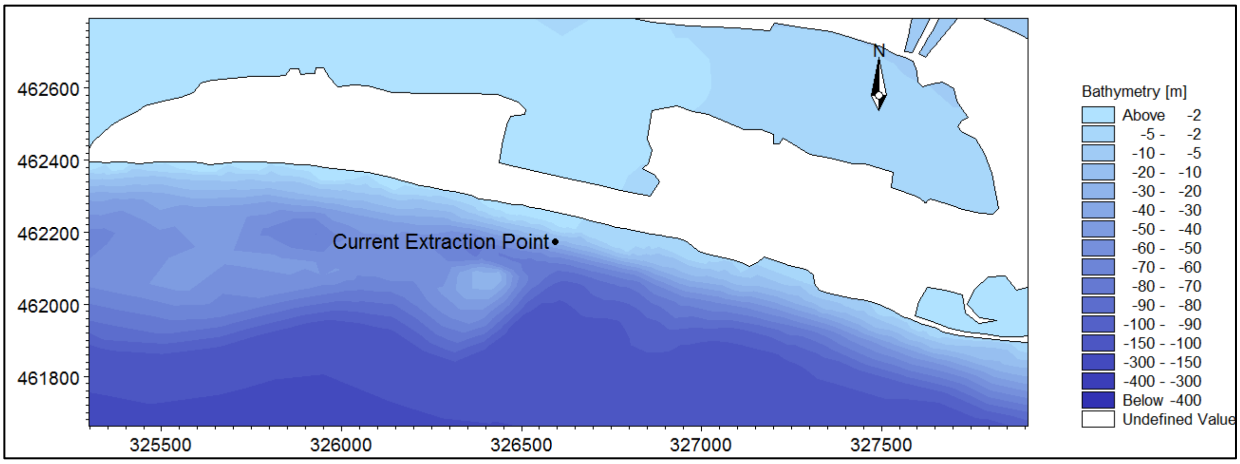

Figure 4.6: Current Extracted Points

Table 4.2: Average Current Condition at Extracted Point

Monsoon	Tidal Condition	Current Speed (m/s)	Direction (deg)
SW	Neap Tide	0.10	277
	Spring Tide	0.22	280
NE	Neap Tide	0.10	280
	Spring Tide	0.20	271

5 THERMAL DISPERSION MODELLING

5.1 Introduction

The proposed incinerator will use sea water as the coolant and discharge hot water back to the sea. Inevitably, the temperature of water discharged is above the ambient. As temperature is one of the most important environmental variables, discharging water of such temperature will have significant impact to the aquatic organisms and to the local biological and biogeochemistry of the ocean. Impacts of high water temperature discharge are such as:

- Coral bleaching
- Reduction of dissolved oxygen level
- Stimulation of phytoplankton and benthic algal growth
- Alteration in ecosystem which affects the mortality and reproduction
- Alteration of thermal structure of the ocean, current patterns, surface wave patterns

In this modelling process, initial dilution is estimated using a near field model (CORMIX). Thereafter using its results depth average diluted thermal factors are obtained and fed them to a far field model (MIKE 21 HD Thermal Dispersion). Finally spreading of thermal plume in 2D plain can be obtained.

5.2 Simulation Scenarios

Three different flow rates for three different excess temperature are required to consider in the simulations. In order to find out best location (depth) for the outfall, three different depths are proposed for the simulations. In addition, two different monsoon and tidal conditions are also considered. Therefore all together 36 number of scenarios are required to simulate. All simulation scenarios are given in the following table.

Table 5.1: Simulation Scenarios

Sc. ID	Monsoon	Tide	Excess Temperature (°C)	Flow Rate (m^3/h)	Depth at Discharge (m)
NE_S_01	North-East	Spring	2.5	16.56	10
NE_S_02					20
NE_S_03					30
NE_S_04			5	8.28	10
NE_S_05					20
NE_S_06					30
NE_S_07			10	6.21	10
NE_S_08					20
NE_S_09					30
NE_N_01		Neap	2.5	16.56	10
NE_N_02					20
NE_N_03					30
NE_N_04			5	8.28	10
NE_N_05					20
NE_N_06					30
NE_N_07			10	6.21	10
NE_N_08					20
NE_N_09					30
SW_S_01	South-West	Spring	2.5	16.56	10
SW_S_02					20
SW_S_03					30
SW_S_04			5	8.28	10
SW_S_05					20
SW_S_06					30
SW_S_07			10	6.21	10
SW_S_08					20
SW_S_09					30
SW_N_01		Neap	2.5	16.56	10
SW_N_02					20
SW_N_03					30
SW_N_04			5	8.28	10
SW_N_05					20
SW_N_06					30
SW_N_07			10	6.21	10
SW_N_08					20
SW_N_09					30

5.3 Near Field Modelling

The given outfall pipe diameter is 300mm. Accordingly discharge velocity of plume is between 0.065m/s and 0.0244m/s which are significantly low compared to the sea current at location. It will be released close to the sea bottom. Since the density of the heated plume is less it will act as negatively buoyant discharges and tends to move upwards. The initial momentum of the discharge will lead to a very turbulent flow that will attempt to mix the fluid over the full depth available. This mixing will be resisted by the fact that the discharge is buoyant. The mixing will also cause ambient fluid to be entrained into the jet, reducing its momentum and temperature. This initial momentum is very important and generally reduces the excess temperature by a factor of 2 to 3 over a distance of a few meters. Once the discharge momentum has been reduced below a certain limit due to the dilution, the mixing will cease to be the dominant factor and the discharge will transform into what is generally known as a plume. After this the discharge enters the far field. To examine the near field behaviour of the heated plume CORMIX mixing zone model is used.

5.3.1 Cormix Modelling System

The CORMIX is a mixing zone model and decision support system for environmental impact assessment of regulatory mixing zones resulting from continuous point source discharges (Doneker & Jirka 2007). It is a computer-aided-design (CAD) developed by the Defrees Hydraulic Laboratory at Cornell University, Ithaca, New York, in cooperation of USEPA for studying aqueous pollutant discharges into a range of water bodies, design and mixing zone analysis (Doneker & Jirka 2007). The role of boundary interaction is the emphasis of the system for predicting steady-state mixing behaviour and plume geometry (Doneker & Jirka 2007).

Simulation model selection in CORMIX is controlled by the Graphical user interface (GUI) and mixing zone rule-based expert systems technology. Description of discharge and ambient conditions are specified as input data in the GUI. Based on the inputs, the most appropriate hydrodynamic simulation model is determined. CORMIX employs the length-scaled rule-based system for classification of flow regimes and uses the length scale for predicting the initial dilution. CORMIX simplifies the characteristics of each stage in the steady-state condition and predicts the plume dilution by using some empirical equations (Etemad-Shahidi & Azimi 2007).

CORMIX is applicable to wide range of problems from a simple single submerge pipe discharge into a small stream with rapid cross-sectional mixing to a complicated multiport diffuser installation in deeply-stratified coastal water. However, there is lack of applicability in highly unsteady ambient flow conditions that are prone to locally recirculating flows (Doneker & Jirka 2007).

The main aim is to obtain an estimation of spreading of heated plume around the discharge. The model set up used the excess temperature as a tool to access the change in temperature level. Based on the requirement, four different water depths were considered for outfall and simulations were carried out accordingly for considering all the relative environmental conditions.

5.3.2 Model Simulations

As discussed earlier dilution process can be divided into a primary jet dilution in the so-called **near-field** and a subsequent natural dilution in the **far-field**. The natural dilution (far field) is influenced by waves, currents and environment conditions.

In general near field of an outfall is governed by the initial jet characteristics of the plume and outfall geometry. In this case, horizontal single port discharge is considered in the modelling simulations. The density of effluent was varied from 1017m^3/kg to 1020m^3/kg according to the excess temperature and the ambient density of the sea water is considered as 1025m^3/kg. Ambient temperature level is assumed as 28°C. Simulations were carried out for list of scenarios given in Table 5.1.

5.3.3 CORMIX Model Results

Visualization of the effluent discharged from the port and rising to the surface in a cross flow at near-field region is given below for the simulation of North-East monsoon with neap tide and excess temperature 10°C and depth of discharge 10m (Sc. ID: NE_N_07). Both plan view and the elevation of the plume of for this scenario are given below and 3D view plots for rest of simulations are given in Annex B.

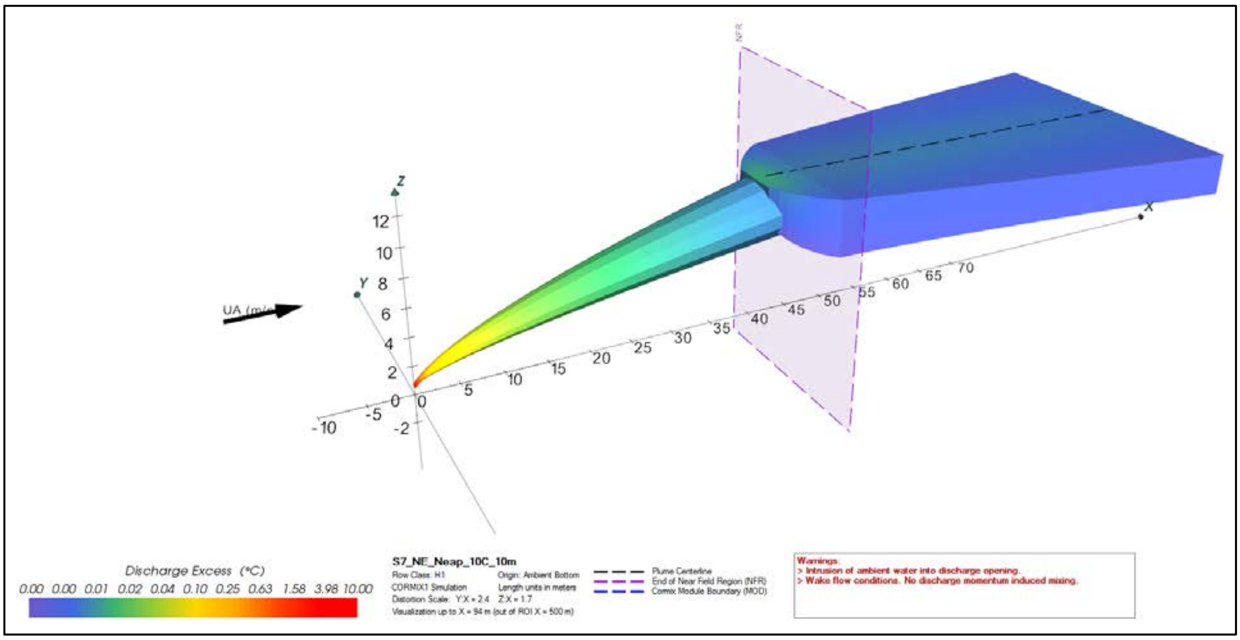

Figure 5.1: Visualization of the Effluent Discharged from the Port and Rising to the Surface at Near-Field Region (3D View)

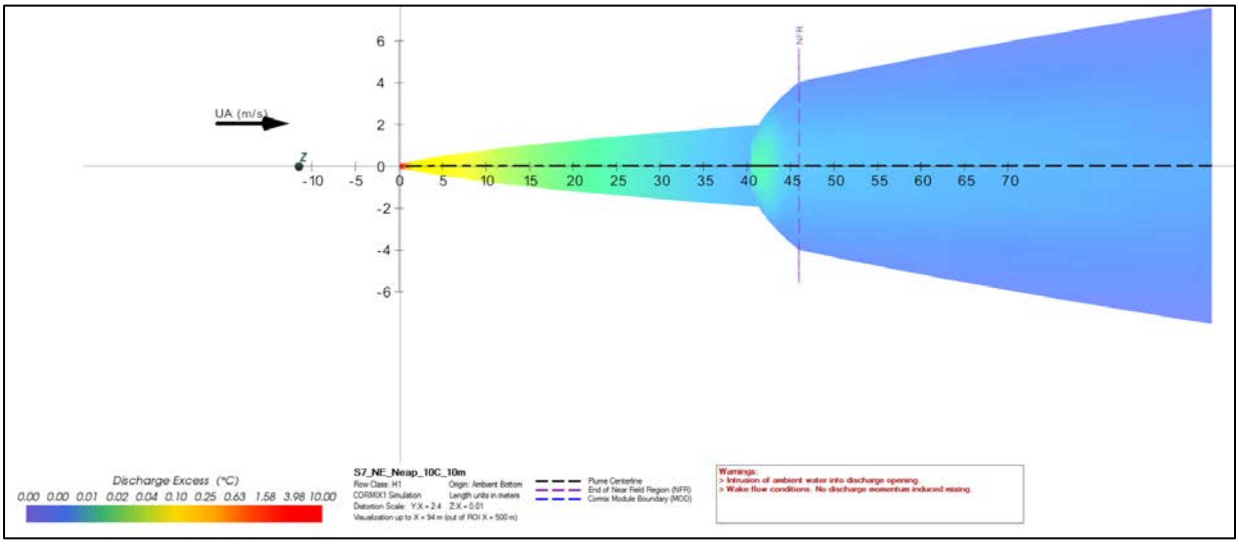

Figure 5.2: Visualization of the Effluent Discharged from the Port and Rising to the Surface in a Cross Flow at Near-Field Region. (Plan View)

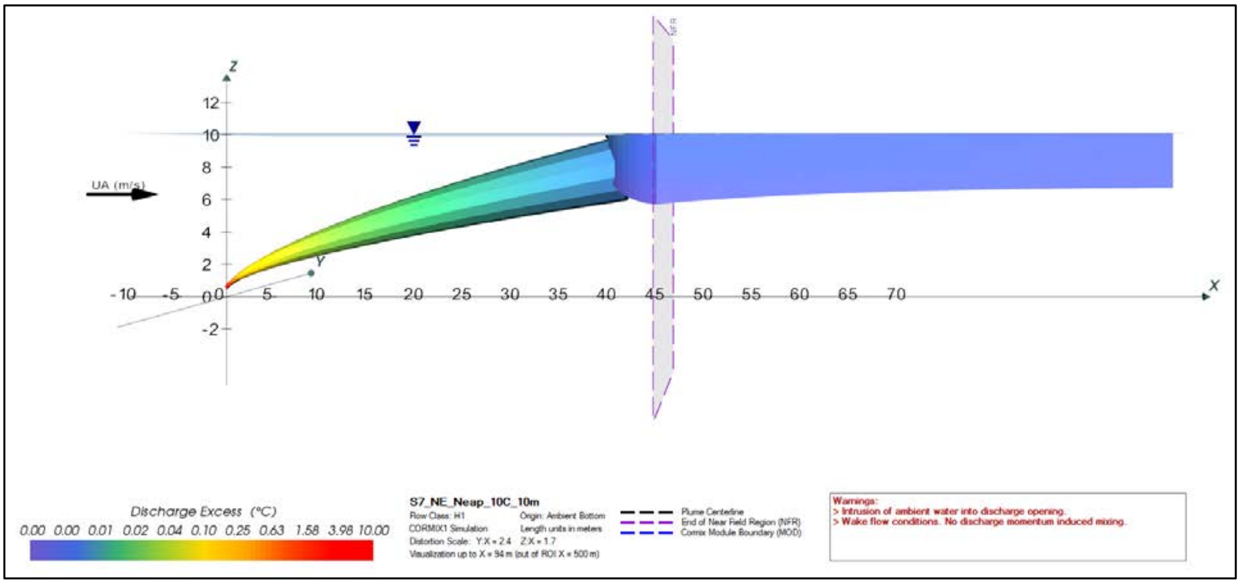

Figure 5.3: Visualization of the Effluent Discharged from the Port Spreading at Near-Field Region. (Elevation)

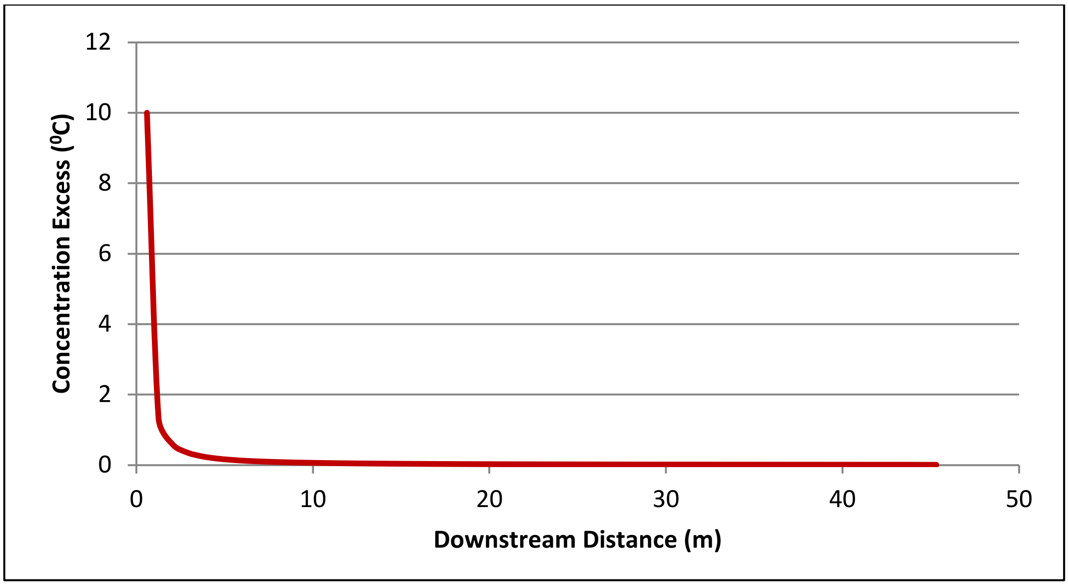

Figure 5.4: Excess Concentration vs. Downstream Distance

5.3.4 Discussion

According to the results of above scenario, relatively high influence can be observed with low depth release, high temperature plume and low current speed. Hence plume discharge at 10m depth with 10°C excess temperature at neap tidal condition is the most influence scenario in near-field modelling. There are two scenario which satisfy these condition; scenario IDs of those are **NE_N_07** and **SW_N_07**. Hence the above selected scenario is one of most influential condition among all scenarios. Even with this most influential condition, high dilution can be observed due to low flow rate of effluent. The excess temperature reduces to less than 1°C within few meters of downstream distance. Therefor effect on coastal environment with this discharge is negligible.

5.4 Far Field Modelling

As discussed earlier two models were used to assess the dispersion pattern of the heat plume, one for the near field and one for the far field. The use of the semi-empirical length scale model, CORMIX, for the near field is described in Section 5.3.

As the turbulent plume travels further away from the discharge location, the jet characteristics become less important and three dimensional treatment of thermal dispersion is nearly changed to two dimensional treatments. Then in order to simulate the current phenomena, it is possible to use two-dimensional models. MIKE 21 Hydrodynamic Model combine with Thermal Dispersion Tool has been used for hydrodynamic and thermal dispersion simulation in far field region.

5.4.1 Input Data

All input parameters used in local hydrodynamic model (as given in Chapter 4) are used for thermal dispersion modelling. Therefore two deferent monsoon conditions (South-West and North-East) and two different tidal conditions (Spring and Neap) are taken into consideration in the simulation. In addition, heat plume discharge boundary for far-field simulation is establish using the near-field model (CORMIX) results. The excess temperature was extracted in mean water depth from CORMIX model and given as an input data for MIKE 21 HD thermal dispersion model. The excess temperature extracted for different scenarios are given in Table 5.2.

Table 5.2: Input Excess Temperature for Far-Field Model

Sc. ID	Monsoon	Tide	Excess Temperature (°C)	Flow Rate (m^3/h)	Depth at Discharge (m)	Excess Temperature at Average Depth(°C)
NE_S_01	North-East	Spring	2.5	16.56	10	0.015
NE_S_02					20	0.002
NE_S_03					30	0.001
NE_S_04			5	8.28	10	0.006
NE_S_05					20	0.002
NE_S_06					30	0.001
NE_S_07			10	6.21	10	0.011
NE_S_08					20	0.004
NE_S_09					30	0.002
NE_N_01		Neap	2.5	16.56	10	0.015
NE_N_02					20	0.004
NE_N_03					30	0.002
NE_N_04			5	8.28	10	0.016
NE_N_05					20	0.004
NE_N_06					30	0.002
NE_N_07			10	6.21	10	0.024
NE_N_08					20	0.005
NE_N_09					30	0.002
SW_S_01	South-West	Spring	2.5	16.56	10	0.007
SW_S_02					20	0.002
SW_S_03					30	0.001
SW_S_04			5	8.28	10	0.005
SW_S_05					20	0.001
SW_S_06					30	0.001
SW_S_07			10	6.21	10	0.007
SW_S_08					20	0.002
SW_S_09					30	0.001
SW_N_01		Neap	2.5	16.56	10	0.016
SW_N_02					20	0.004
SW_N_03					30	0.002
SW_N_04			5	8.28	10	0.016
SW_N_05					20	0.004
SW_N_06					30	0.002
SW_N_07			10	6.21	10	0.024
SW_N_08					20	0.005
SW_N_09					30	0.002

5.4.2 Model Results and Discussion

Since the discharge flow rate is considerably low, high dilution can be observed at outfall area. Hence the mean depth excess temperature is very low. However the extracted values were added to the far-field model and obtained the results.

High influence can be observed at low depth discharge same as near-field model, but high heat distribution can also be observed for high effluent flow rate condition even it has low excess temperature. As an example Sc. ID: NE_S_01 has excess temperature 2.5°C in the effluent, but it has $16.56 m^3/h$ flow rate which is comparatively high. Therefore results of this scenario shows high heat distribution. Further scenarios with neap tidal condition shows higher influence with its low current speed than spring tide. According to these conditions high influence scenarios are;

a) NE_S_01
b) NE_N_01
c) NE_N_07
d) SW_S_01
e) SW_N_01
f) SW_N_07

As an example Sc. ID: NE_N_07 has been used for further discussion which was critical in near-field model too. Figure 5.5 and 5.6 show the temperature variation in 2D plain for this high influence scenario when current directed westward and eastward respectively. According to the results, the excess temperature level reduces $5x10^{-6}$ °C within the 90m rage from the discharge point for both cases. However $5x10^{-6}$ °C excess temperature is very low temperature and negligible in coastal environment. Therefore thermal dispersion is very high even in a high influence scenario and it will be a very low effect to the coastal environment. Thermal dispersion plots for all scenarios are given in Annex C.

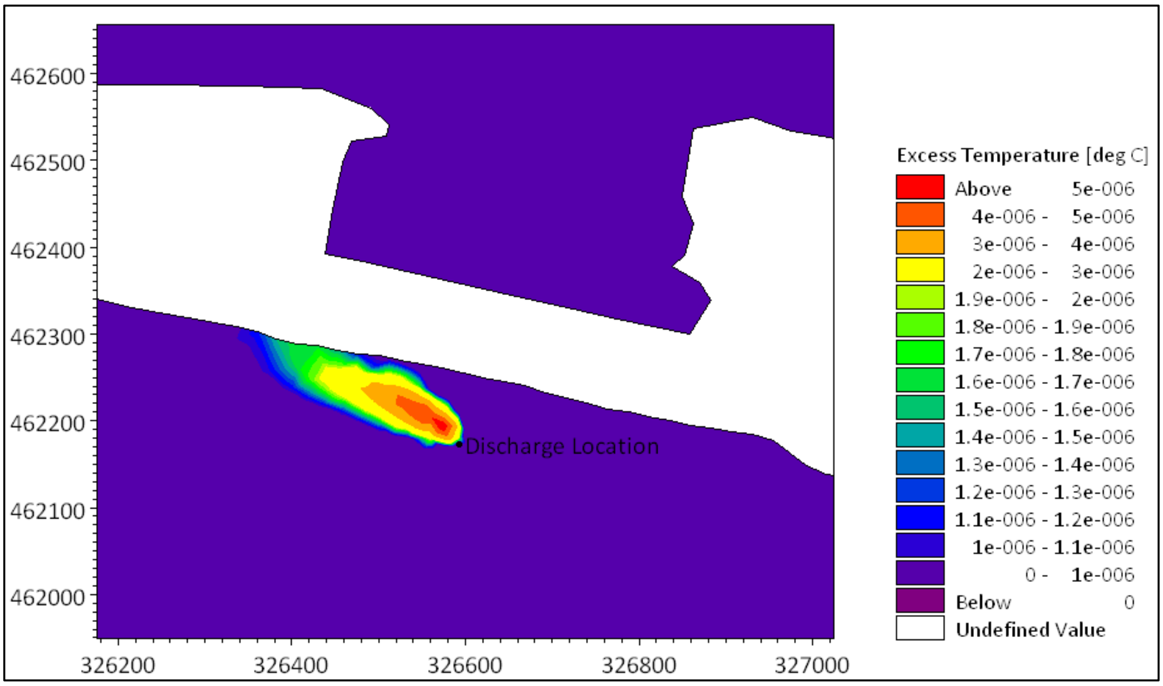

Figure 5.5: Thermal Dispersion towards West at Scenario NE_N_07

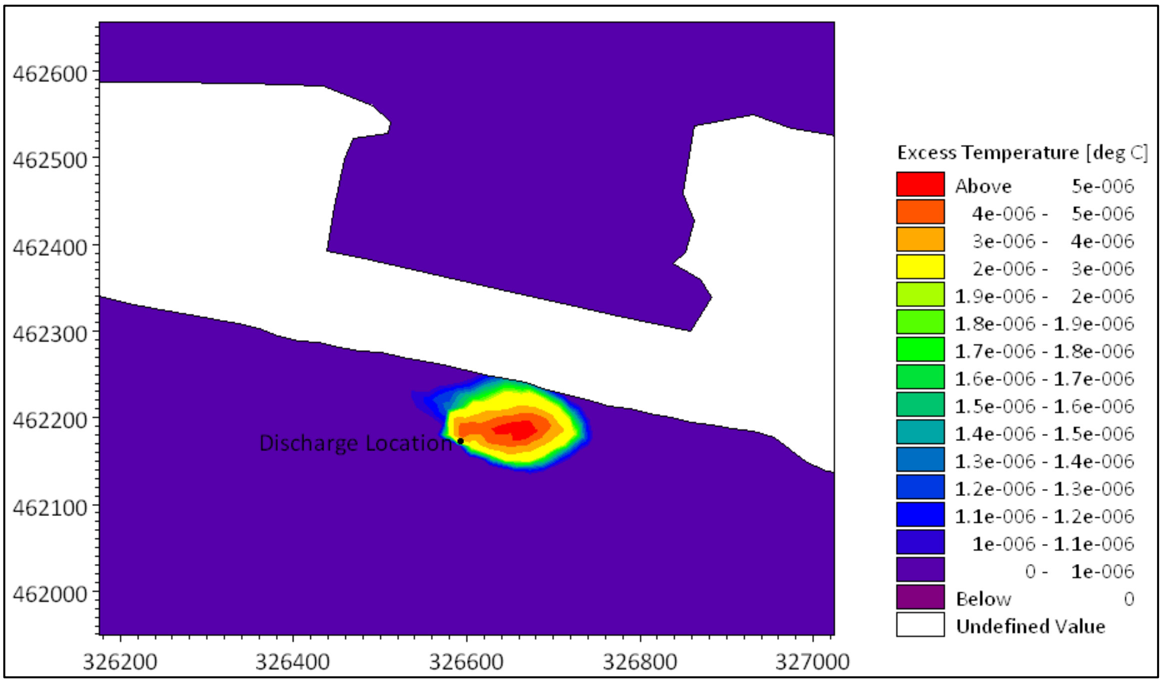

Figure 5.6: Thermal Dispersion towards East at Scenario NE_N_07

6 SUMMARY AND CONCLUSION

- In order to find out thermal dispersion in coastal environment for outfall of hot water plume of a proposed incinerator at Thilafushi Island, a set of numerical model simulation was carried out for different design conditions and seasonal conditions.
- Measured data as well as reliable predicted data were utilized as model inputs, and analysed them before applied to the model.
- MIKE 21 SW model was used to establish the wave condition at site for different monsoon periods (South-West and North-East) and MIKE 21 HD model was used to obtain the current condition at discharge location. Further both spring and neap tidal conditions were simulated separately; and about 0.2m/s and 0.1m/s average current speed were obtained at the discharge point for spring and neap tide respectively. Wave condition was not significantly affected on current condition at discharge point.
- Two modelling system were used thermal dispersion modelling, namely CORMIX model for **near-field** dispersion and MIKE 21 HD coupled with thermal dispersion tool for **far-field** dispersion.
- According to near-field model results,
  - High dilution can be observed due to low flow rate of effluent.
  - High temperature reduction was observed within few meters from released point. Even in one of most influential scenario (Sc. ID: NE_N_07) which has low depth of discharge (10m), high excess temperature (10°C) and low current speed (0.1m/s), temperature reduces to 1°C within 3m of range.
- Results obtained from near-field model were used as input parameter for far-field model.
- Far-field model results represent the temperature spreading in 2D plain for different scenarios.
- According to far-field model results,
  - High heat distribution can be observed with high effluent flow rate, but excess temperature is very low and negligible in coastal environment.
  - Same as the near-field model low depth discharge creates some influence comparative to the other conditions.

ANNEX A

Current Speed Vector Plots

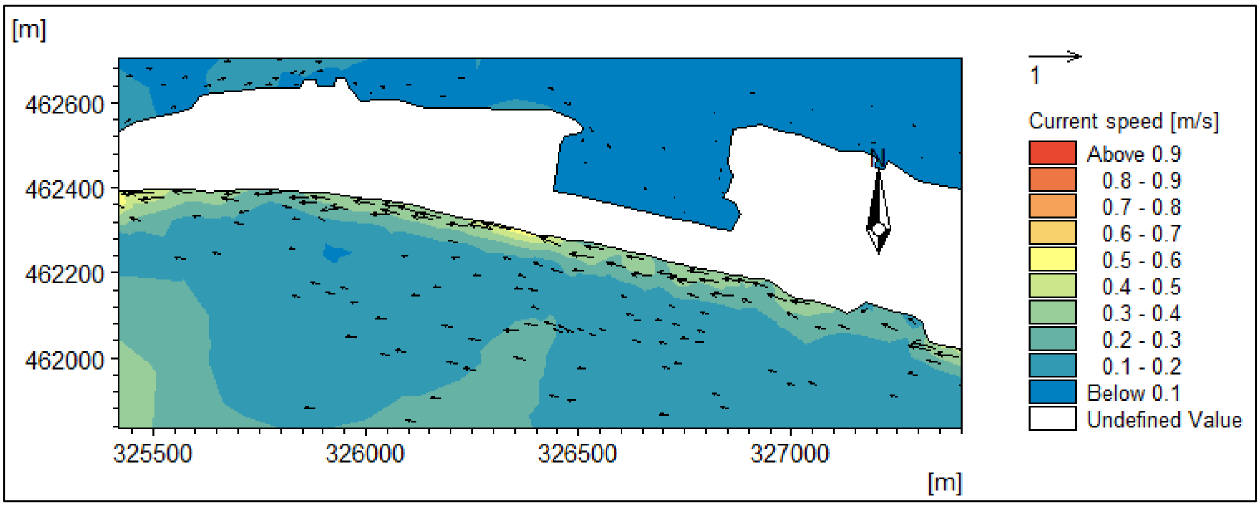

Figure A.1: SW Monsoon, Spring Tide, Average Condition

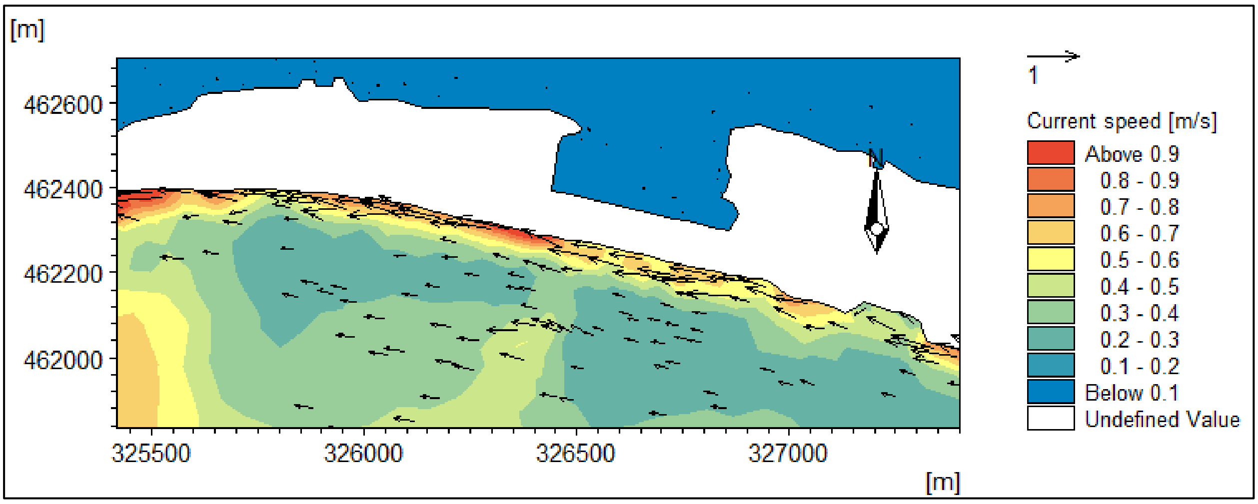

Figure A.2: SW Monsoon, Spring Tide, Maximum Condition

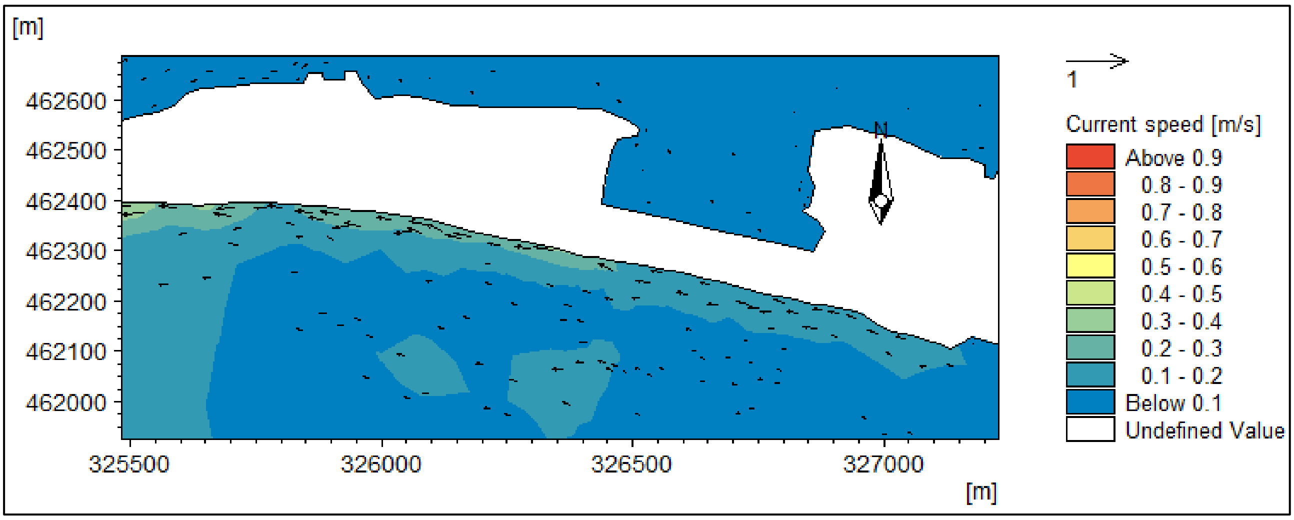

Figure A.3: SW Monsoon, Neap Tide, Average Condition

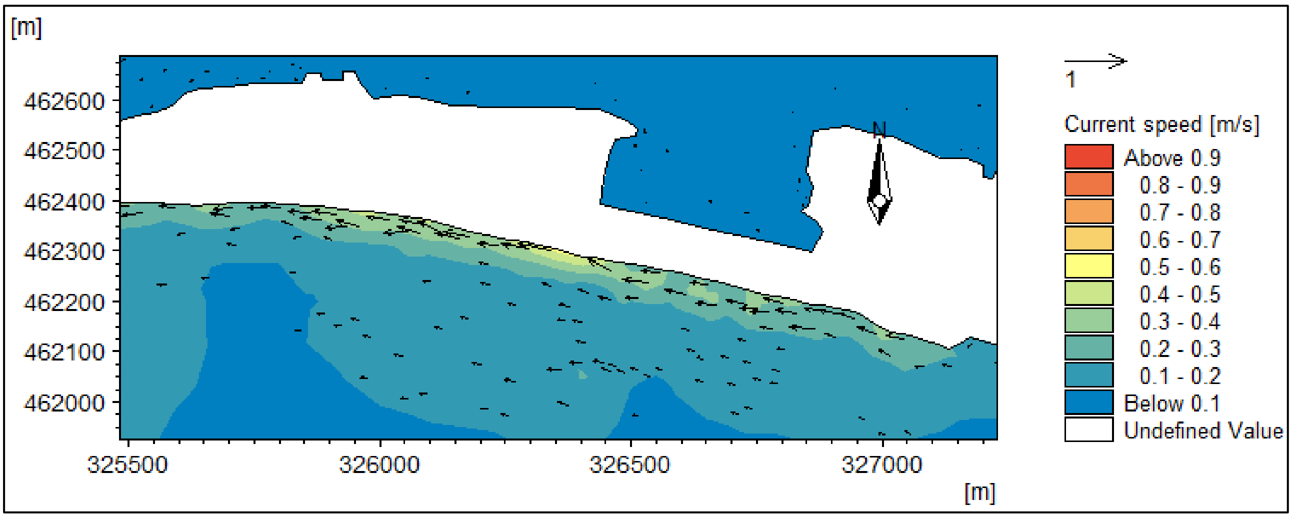

Figure A.4: SW Monsoon, Neap Tide, Maximum Condition

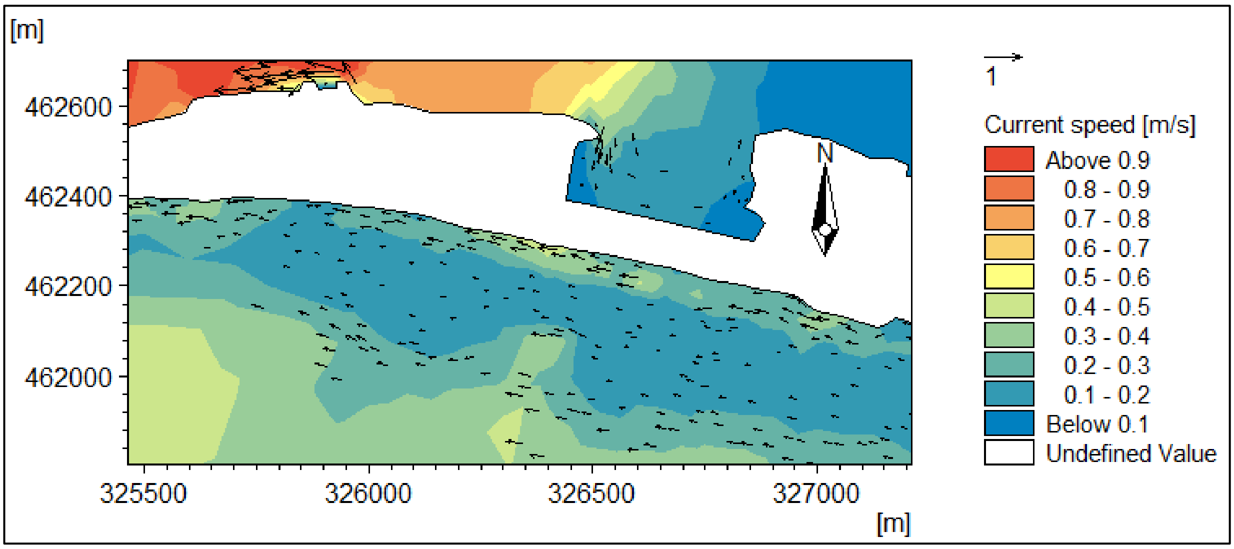

Figure A.5: NE Monsoon, Spring Tide, Average Condition

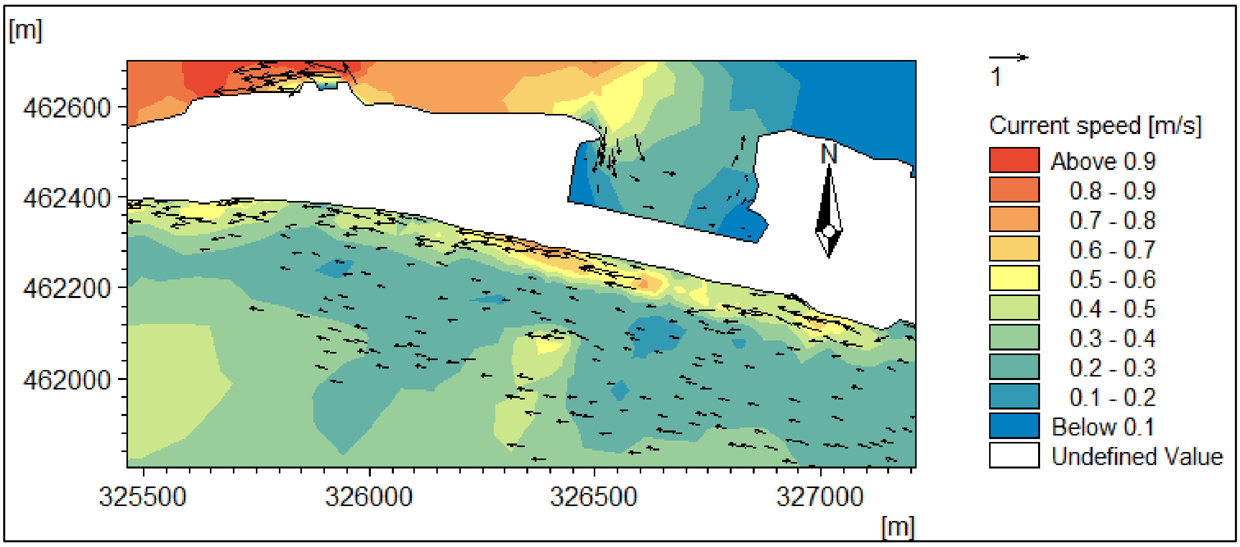

Figure A.6: NE Monsoon, Spring Tide, Maximum Condition

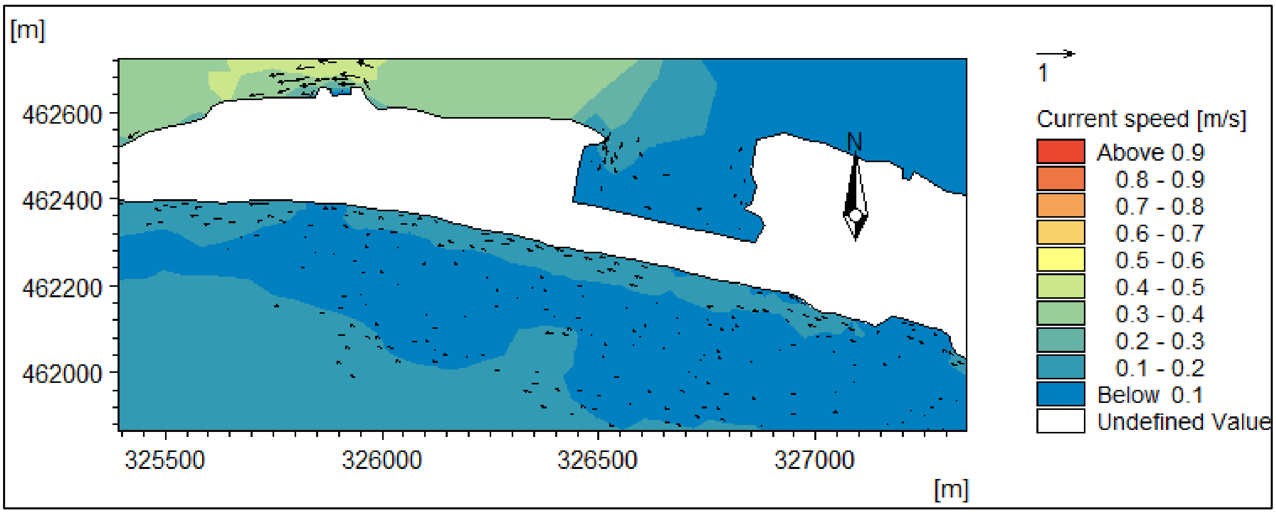

Figure A.7: NE Monsoon, Neap Tide, Average Condition

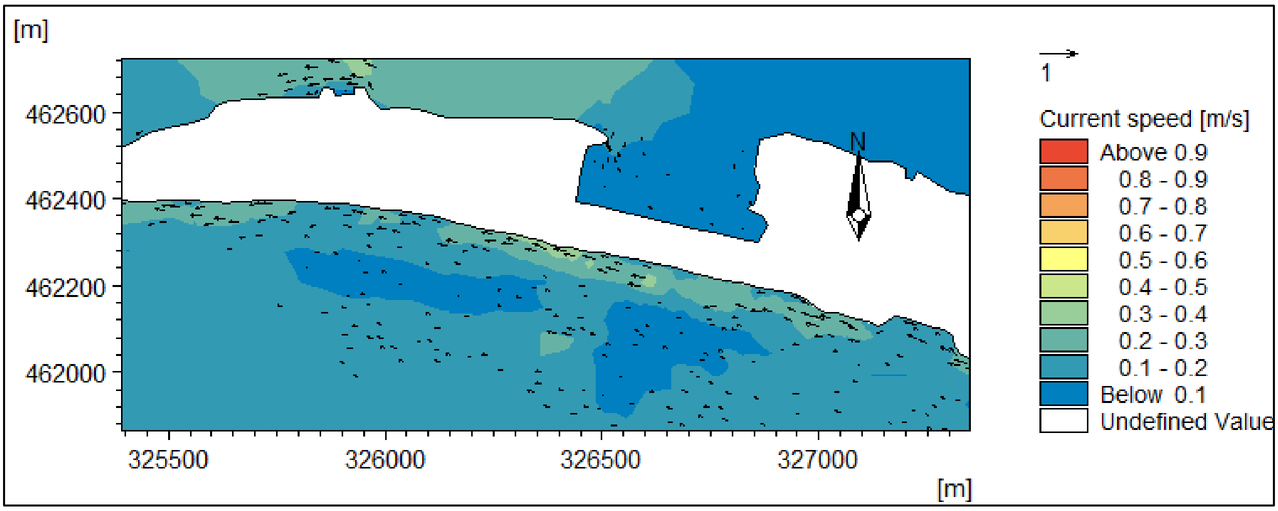

Figure A.8: NE Monsoon, Neap Tide, Maximum Condition

ANNEX B

Heat Dissipation in Near Field (CORMIX)

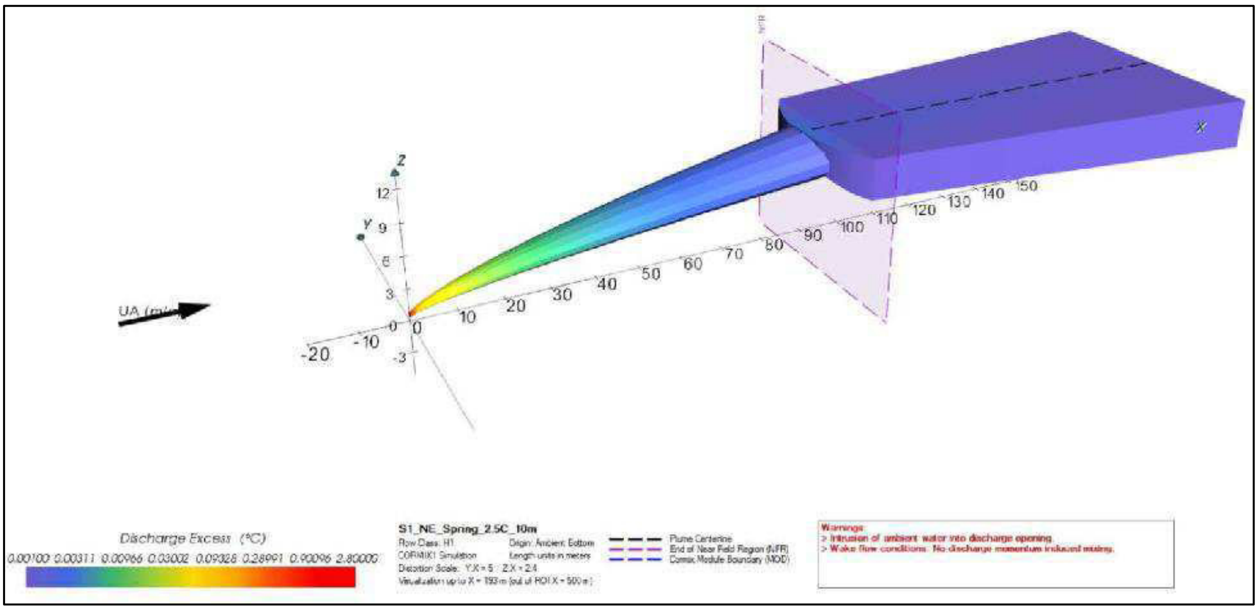

Figure B1: NE_S_01_ (Ex. Temp.=2.5°C, Flow Rate=16.56 m^3/h, Depth=10m)

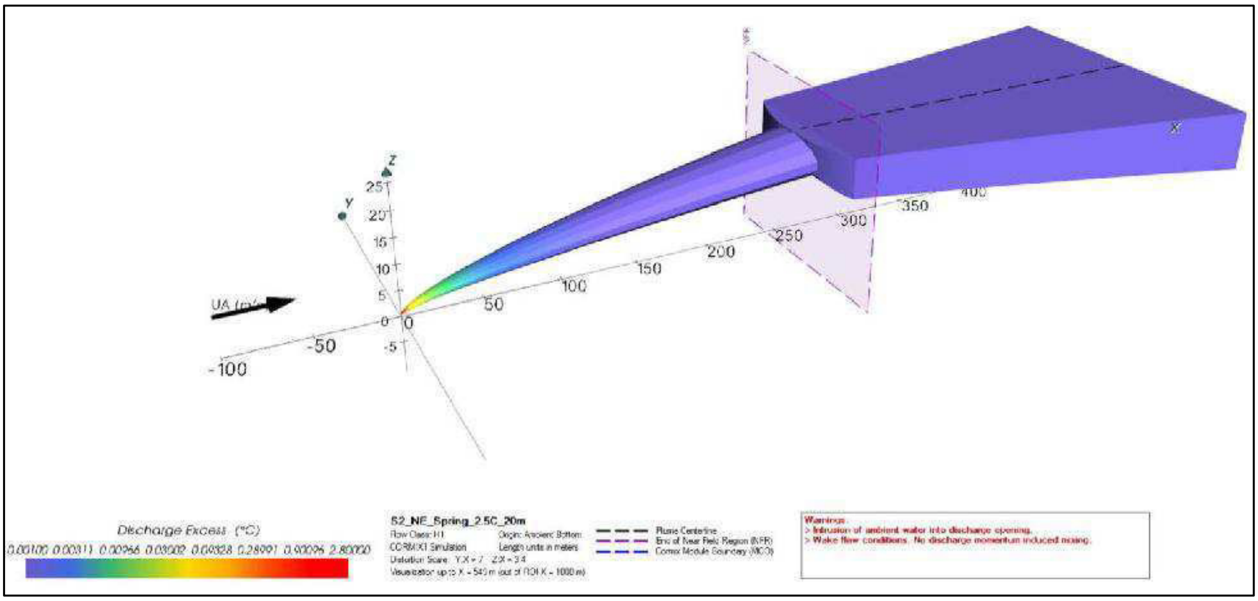

Figure B2: NE_S_02_ (Ex. Temp.=2.5°C, Flow Rate=16.56 m^3/h, Depth=20m)

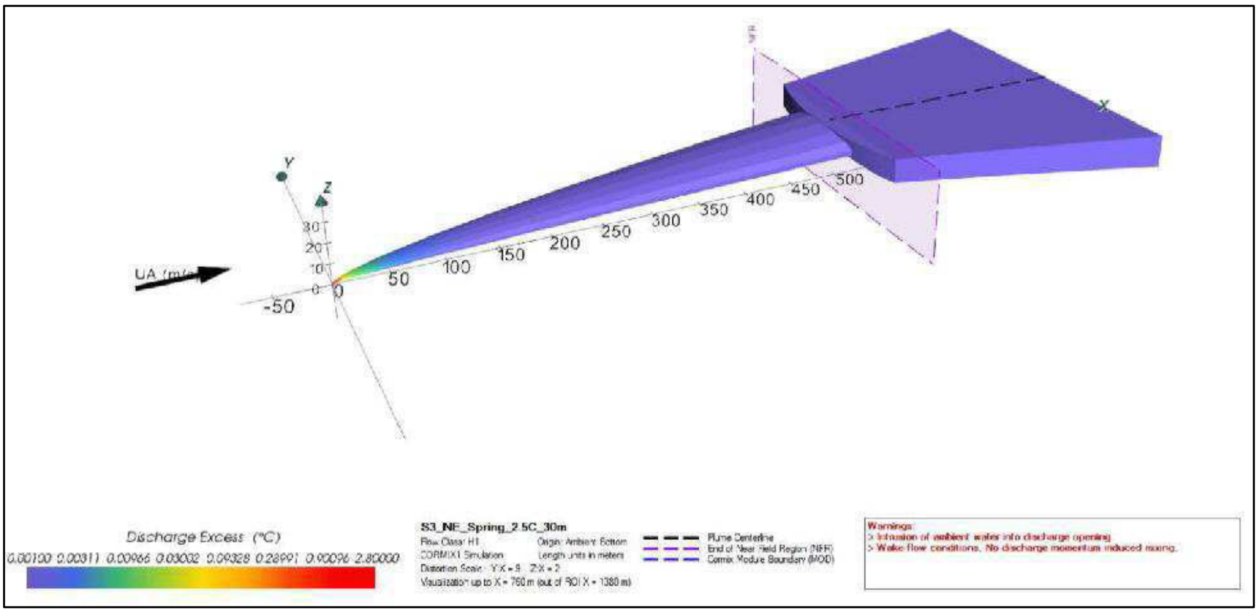

Figure B3: NE_S_03_ (Ex. Temp.=2.5°C, Flow Rate=16.56 m^3/h, Depth=30m)

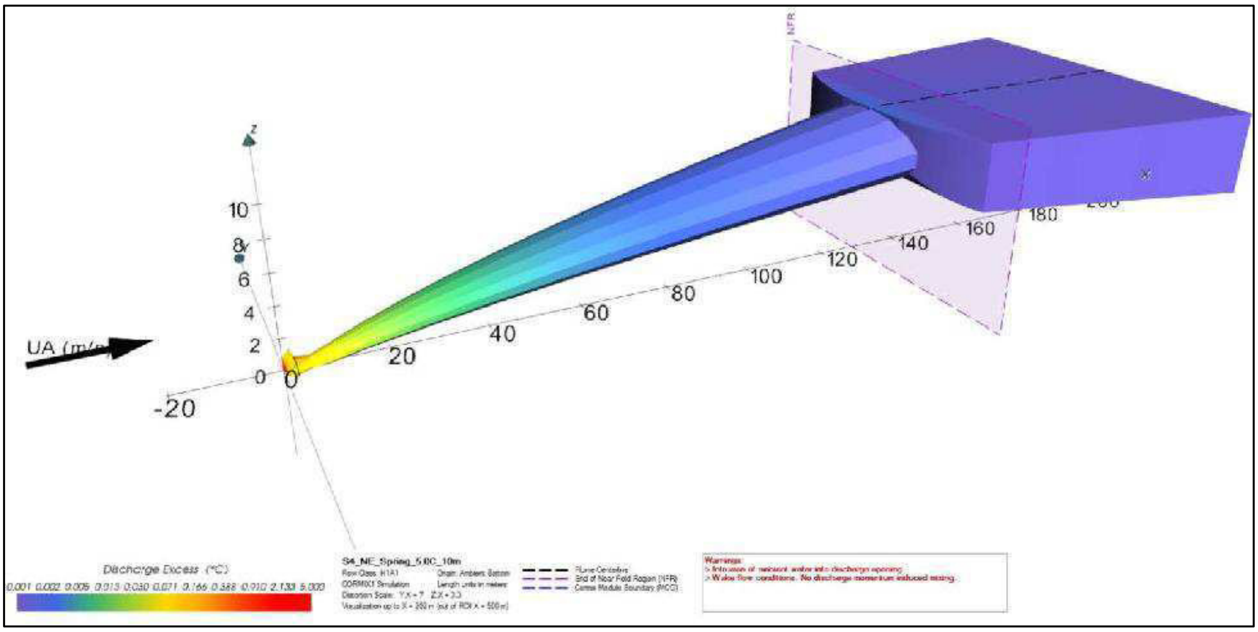

Figure B4: NE_S_04_ (Ex. Temp.= 5°C, Flow Rate=8.28 m^3/h, Depth=10m)

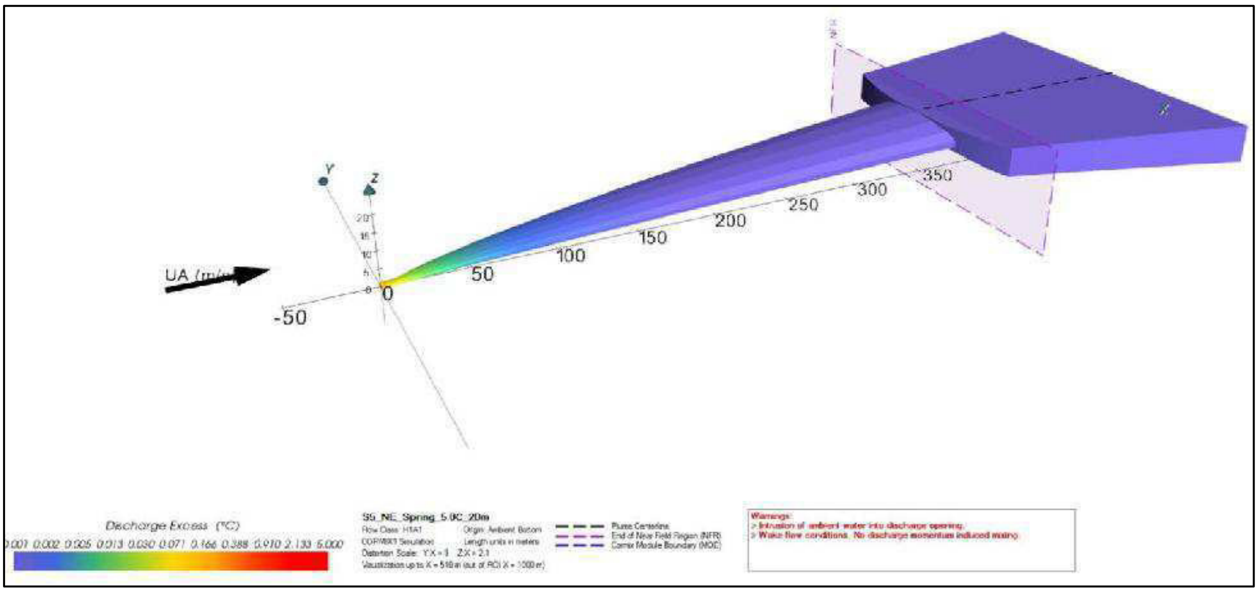

Figure B5: NE_S_05_ (Ex. Temp.= 5°C, Flow Rate=8.28 m^3/h, Depth=20m)

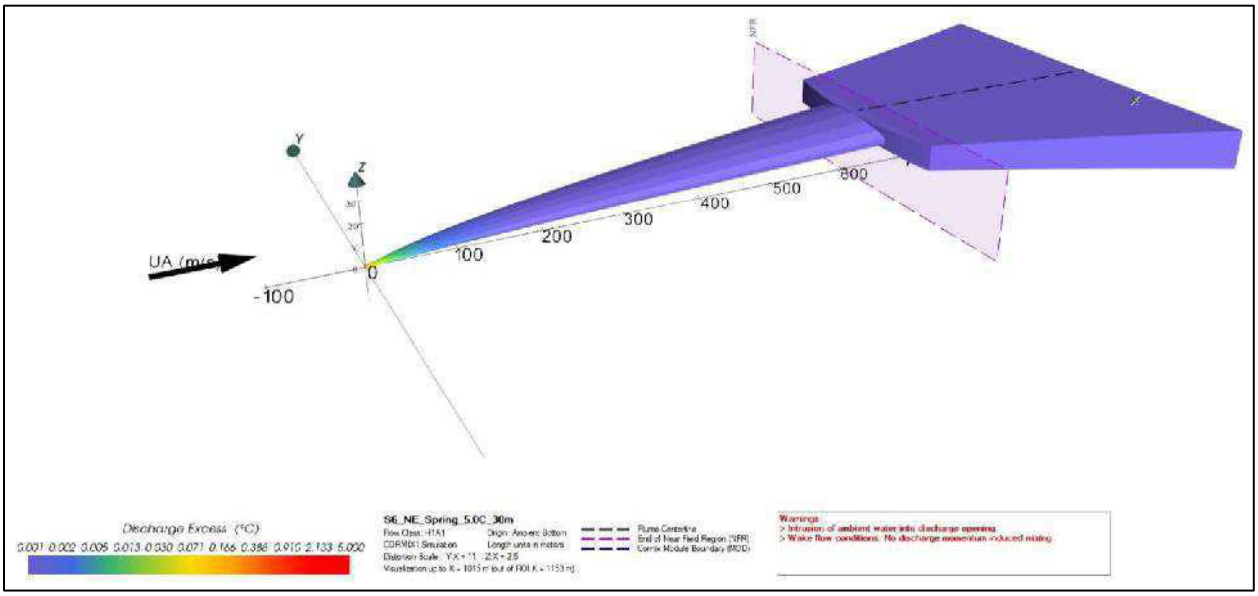

Figure B6: NE_S_06_ (Ex. Temp.= 5°C, Flow Rate=8.28 m^3/h, Depth=30m)

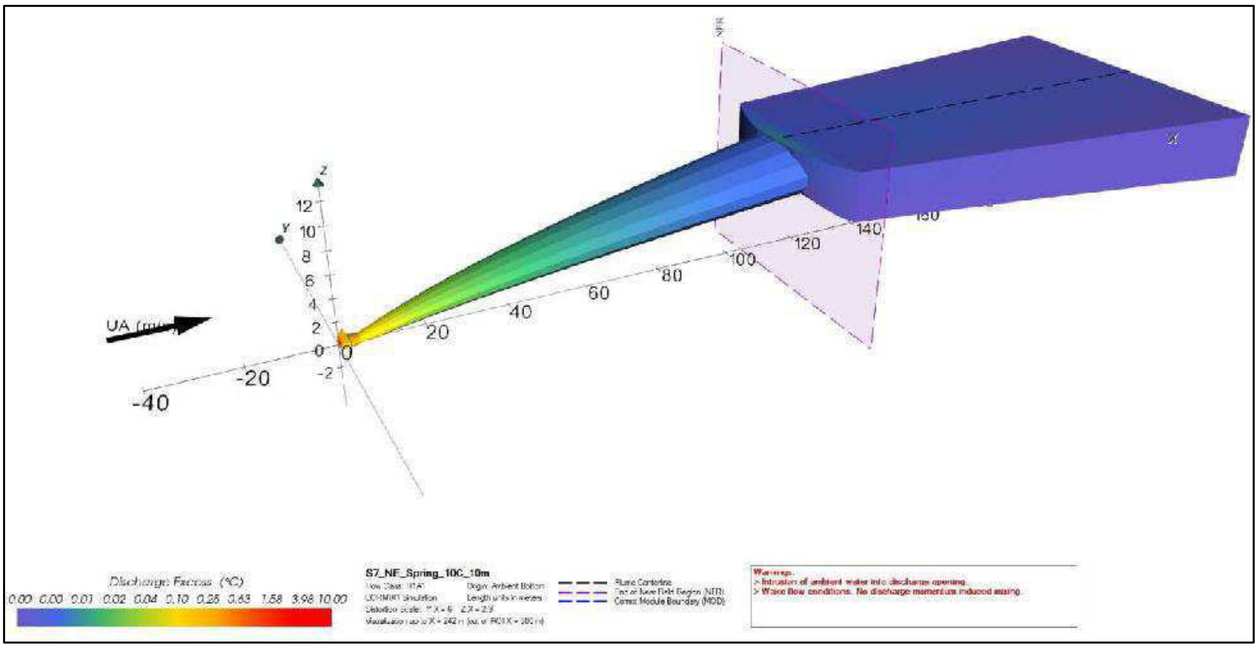

Figure B7: NE_S_07_ (Ex. Temp.= 10°C, Flow Rate=6.21 m^3/h, Depth=10m)

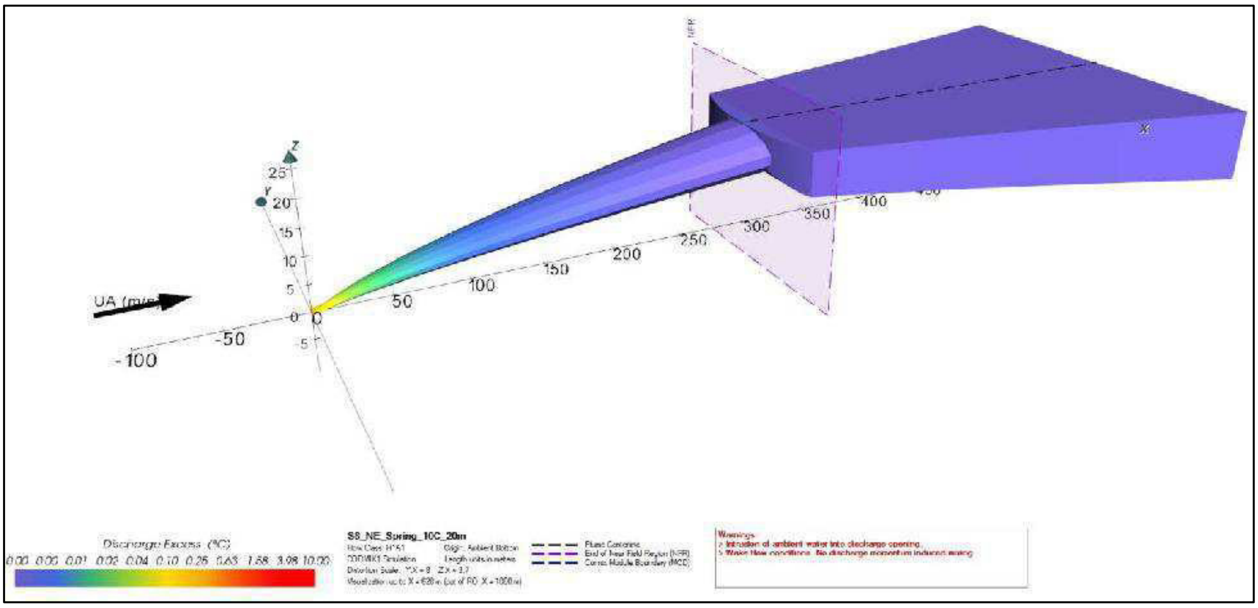

Figure B8: NE_S_08_ (Ex. Temp.= 10°C, Flow Rate=6.21 m^3/h, Depth=20m)

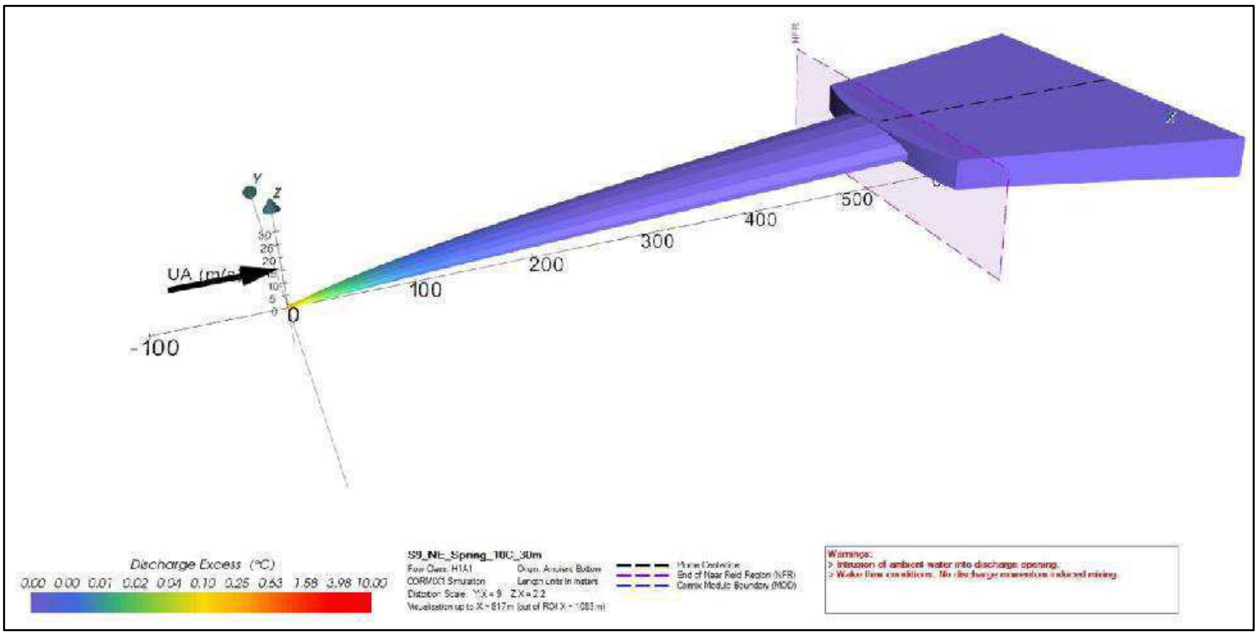

Figure B9: NE_S_09_ (Ex. Temp.= 10°C, Flow Rate=6.21 m^3/h, Depth=30m)

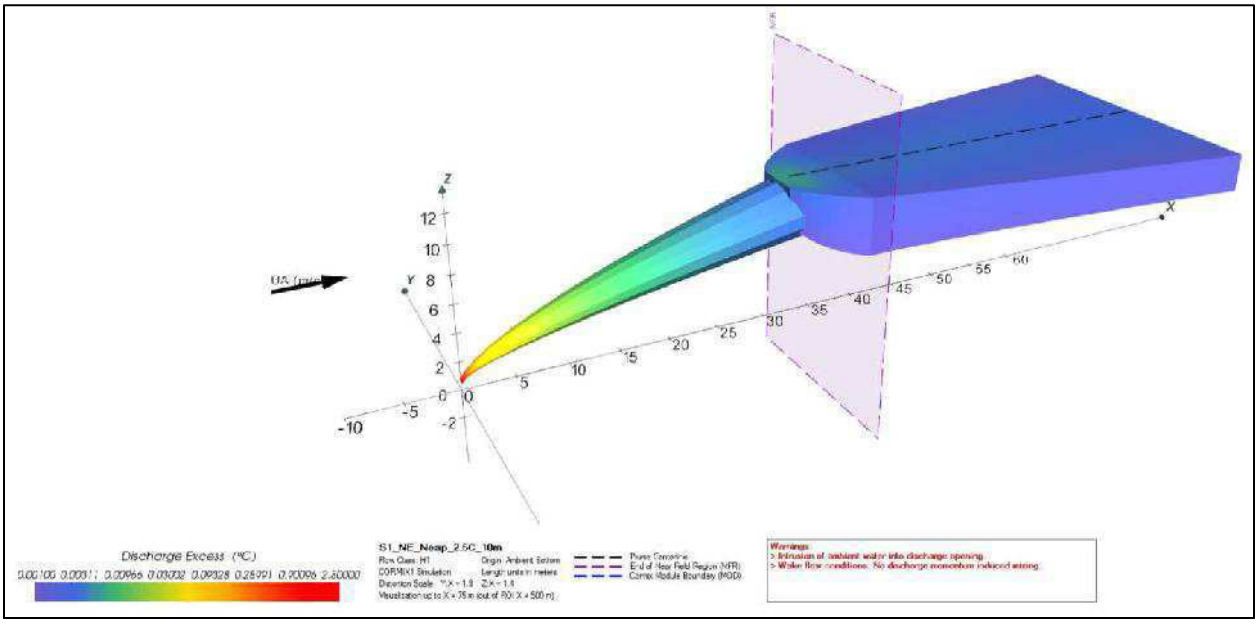

Figure B10: NE_N_01_ (Ex. Temp.= 2.5°C, Flow Rate=16.56 m^3/h, Depth=10m)

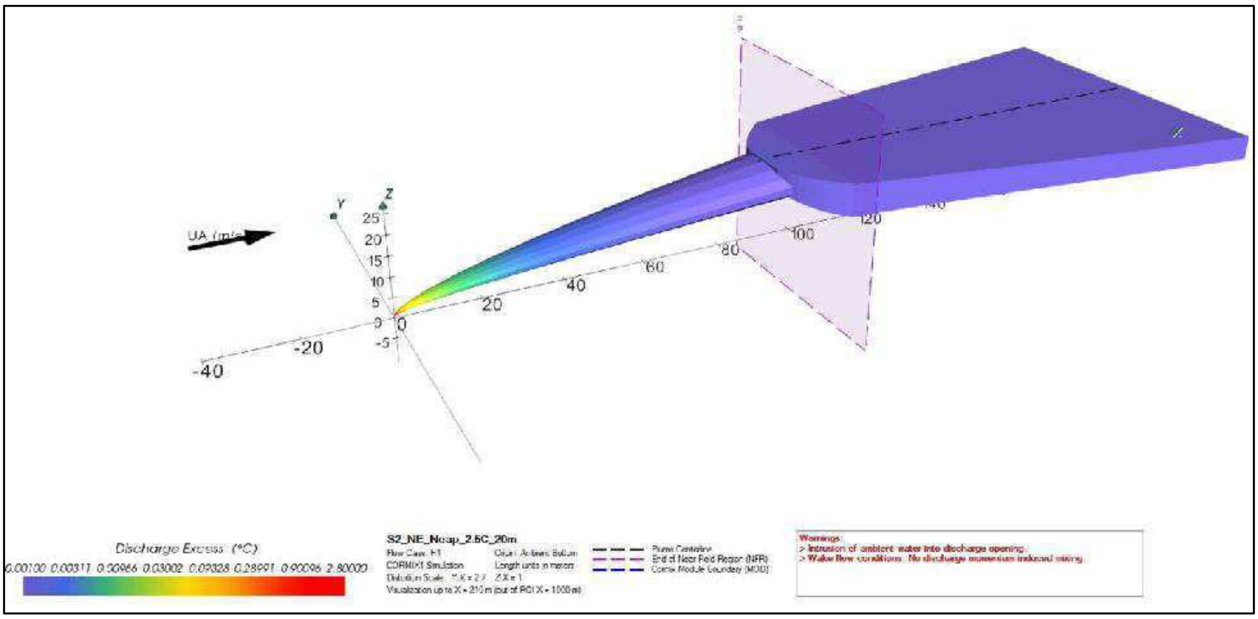

Figure B11: NE_N_02_ (Ex. Temp.= 2.5°C, Flow Rate=16.56 m^3/h, Depth=20m)

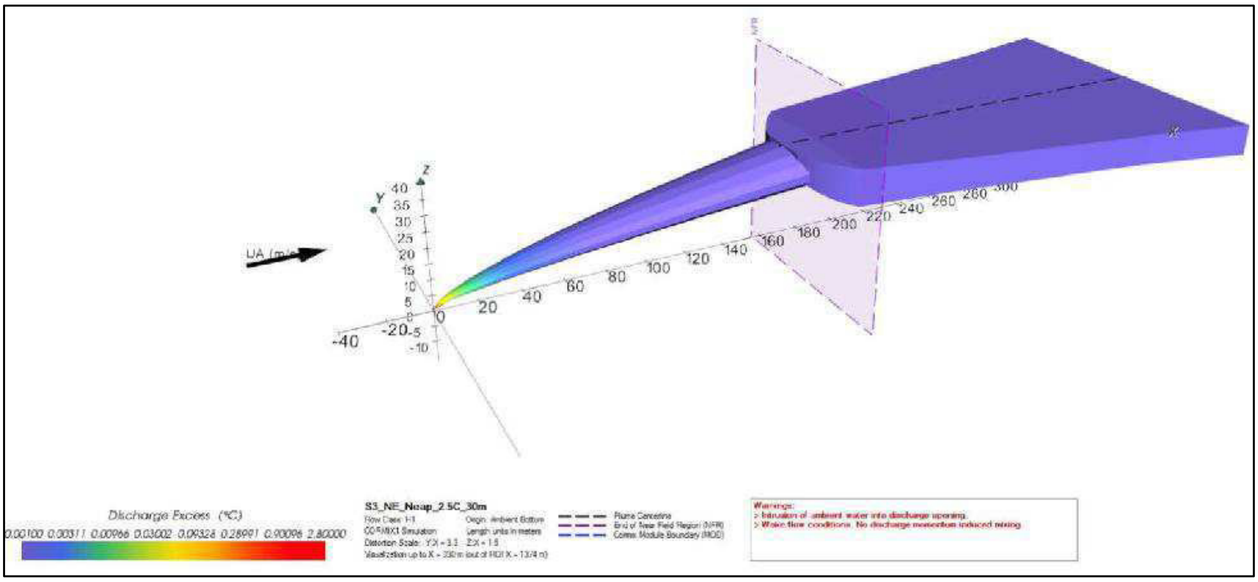

Figure B12: NE_N_03_ (Ex. Temp.= 2.5°C, Flow Rate=16.56 m^3/h, Depth=30m)

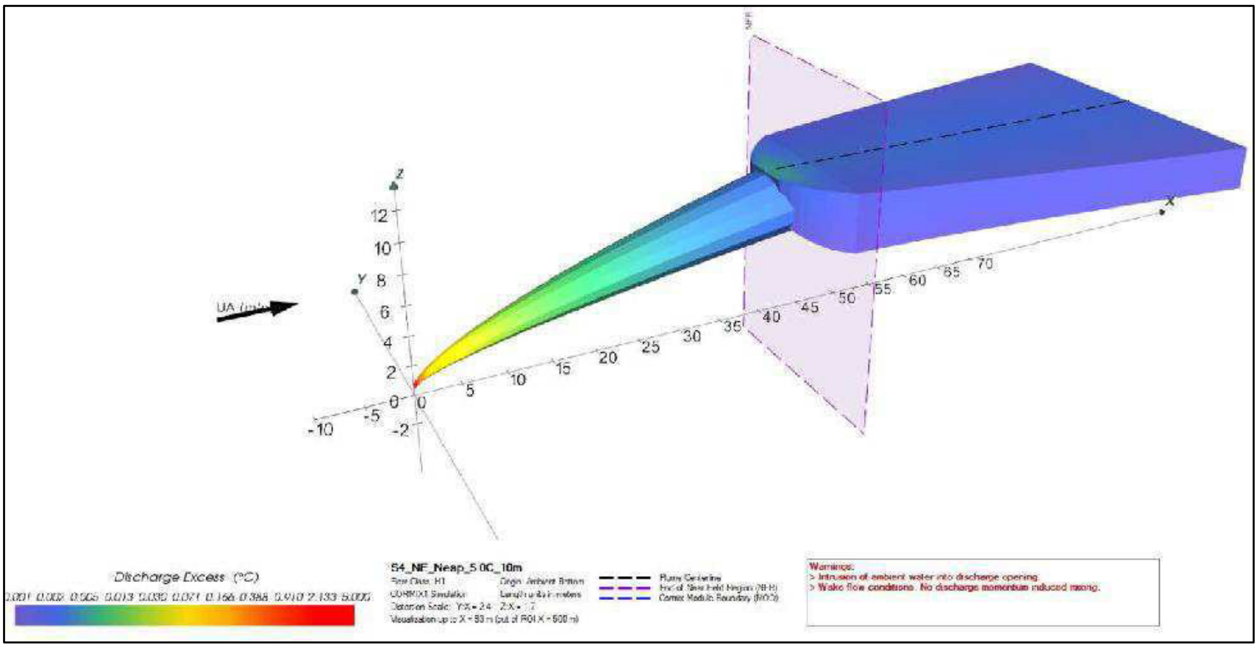

Figure B13: NE_N_04_ (Ex. Temp.= 5°C, Flow Rate=8.28 m^3/h, Depth=10m)

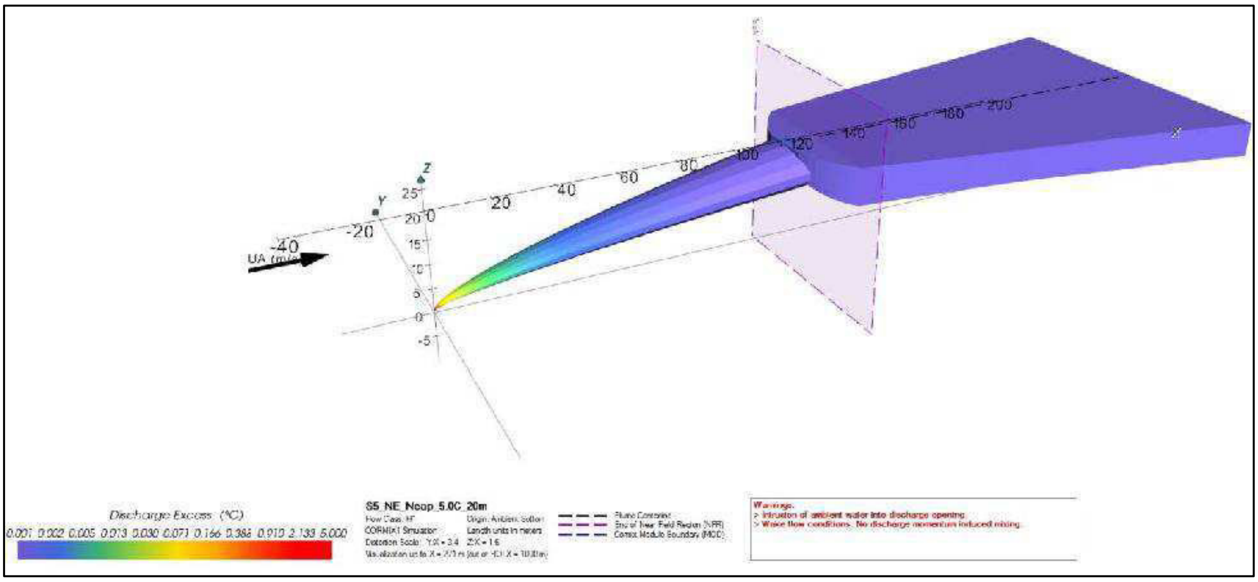

Figure B14: NE_N_05_ (Ex. Temp.= 5°C, Flow Rate=8.28 m^3/h, Depth=20m)

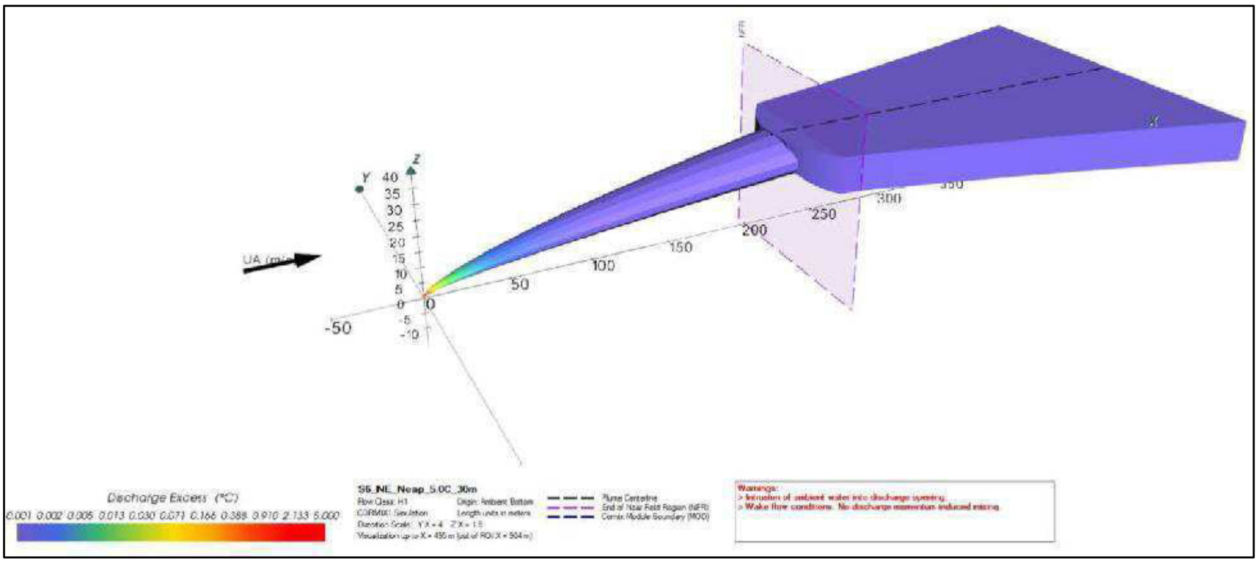

Figure B15: NE_N_06_ (Ex. Temp. = 5°C, Flow Rate=8.28 m^3/h, Depth=30m)

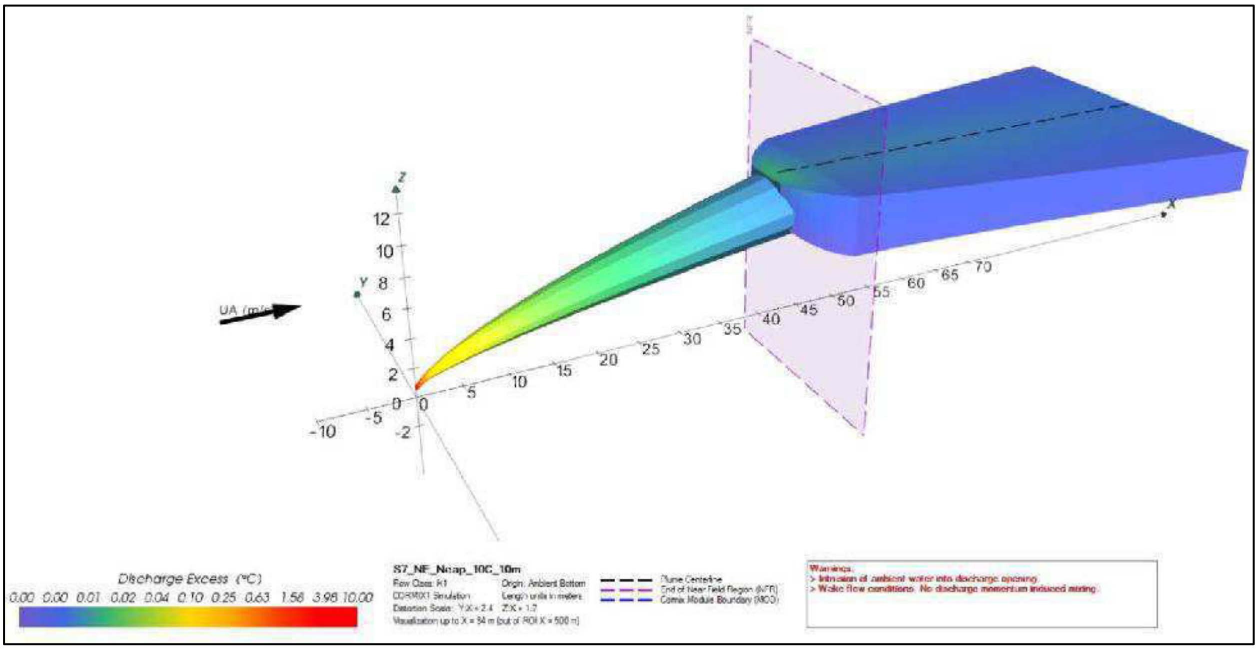

Figure B16: NE_N_07_ (Ex. Temp. = 10°C, Flow Rate=6.21 m^3/h, Depth=10m)

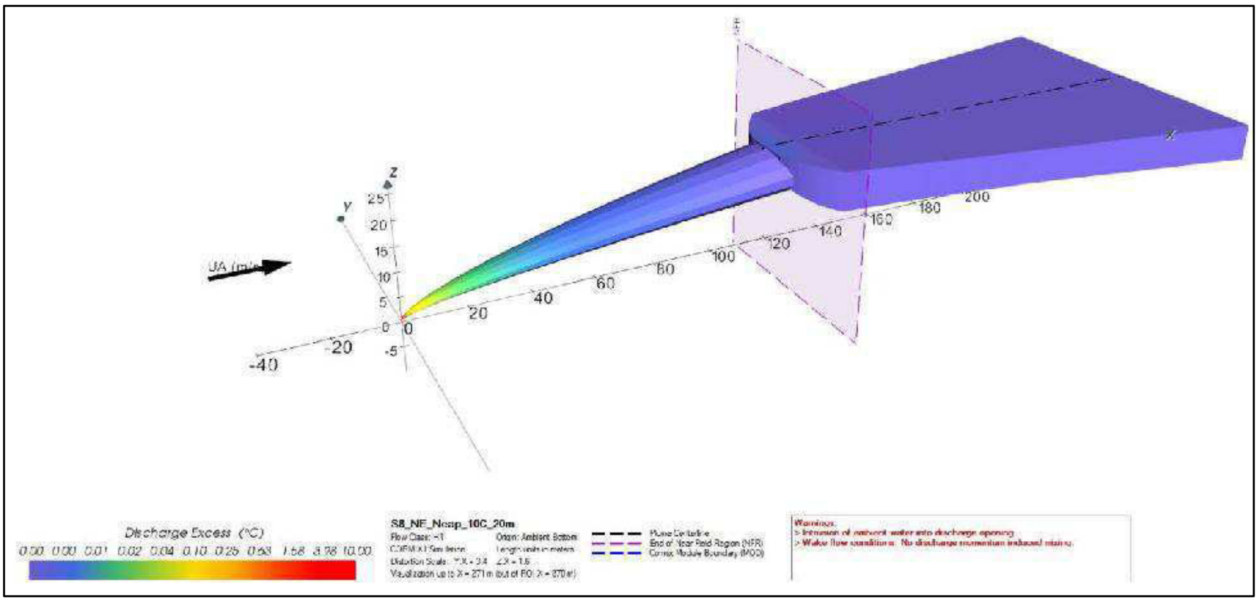

Figure B17: NE_N_08_ (Ex. Temp. = 10°C, Flow Rate=6.21 m^3/h, Depth=20m)

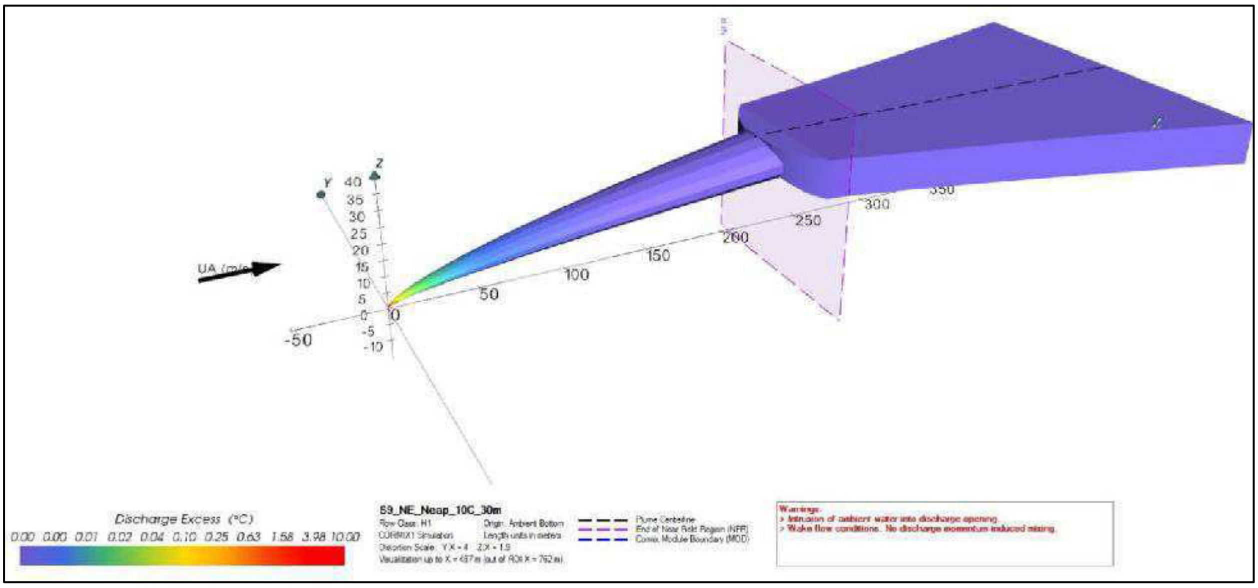

Figure B18: NE_N_09_ (Ex. Temp. = 10°C, Flow Rate=6.21 m^3/h, Depth=30m)

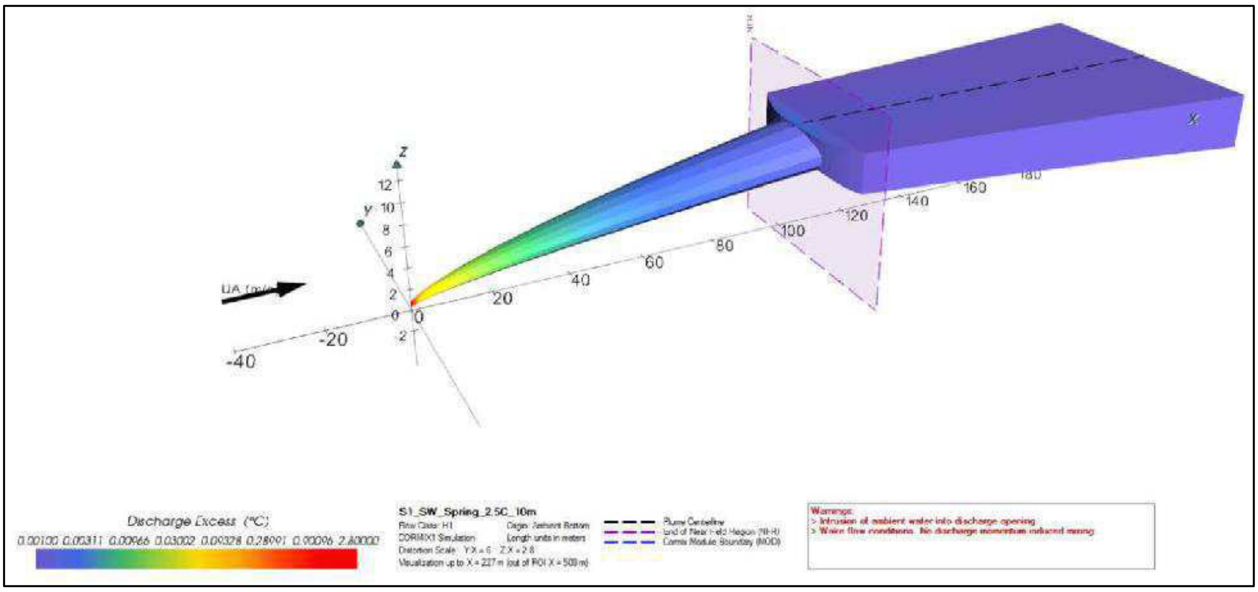

Figure B19: SW_S_01_ (Ex. Temp. = 2.5°C, Flow Rate=16.56 m^3/h, Depth=10m)

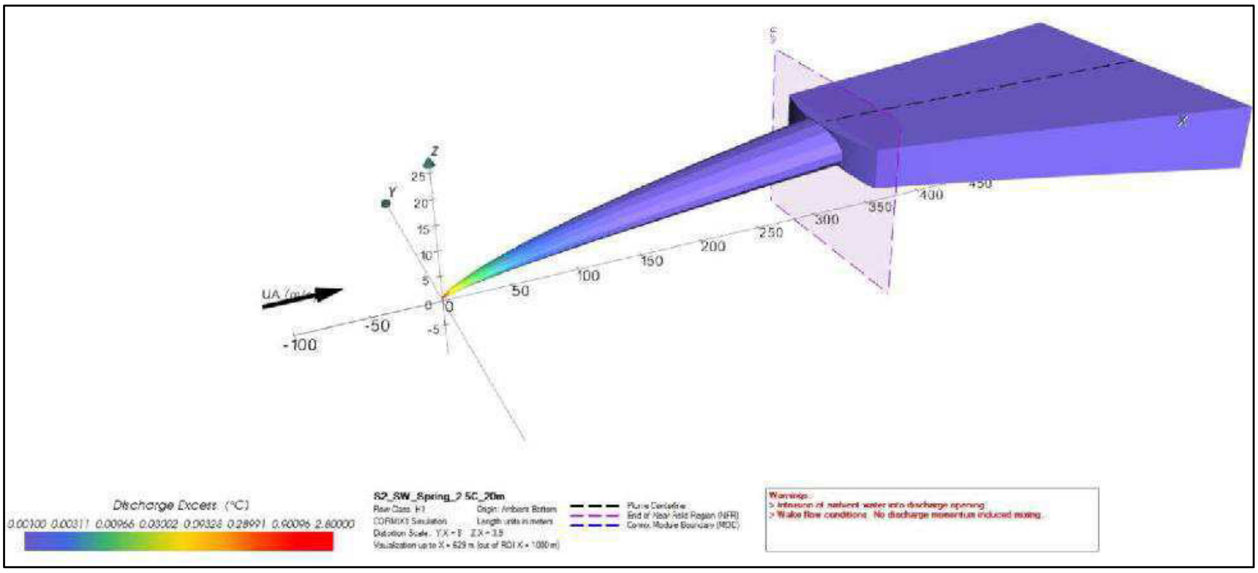

Figure B20: SW_S_02_ (Ex. Temp. = 2.5°C, Flow Rate=16.56 m^3/h, Depth=20m)

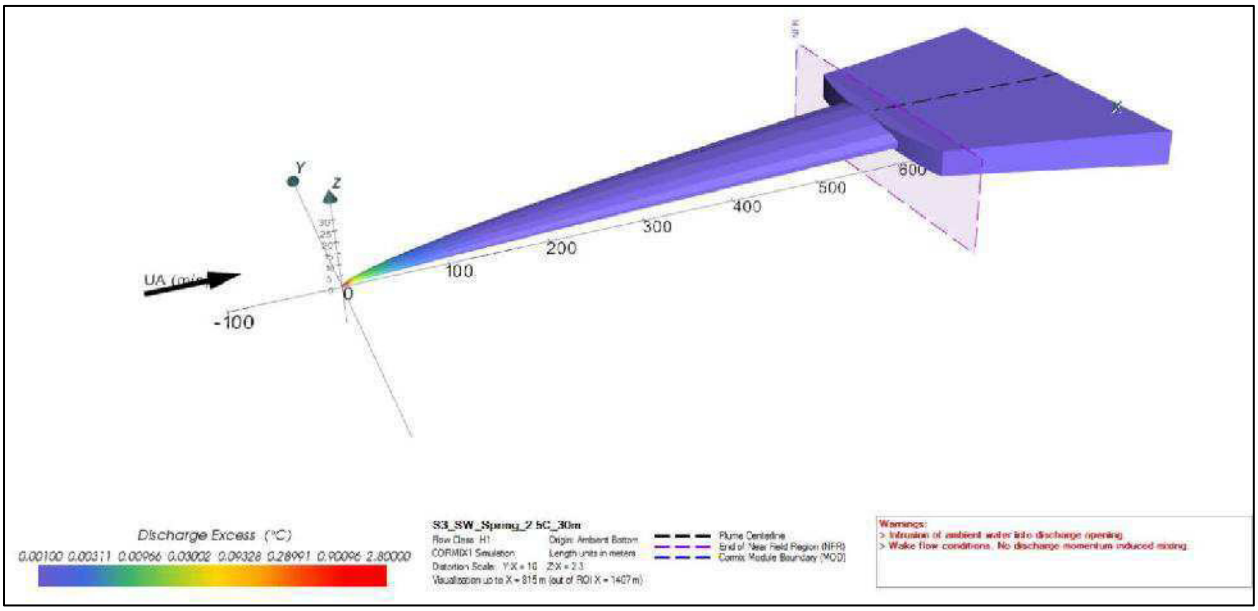

Figure B21: SW_S_03_ (Ex. Temp. = 2.5°C, Flow Rate=16.56 m^3/h, Depth=30m)

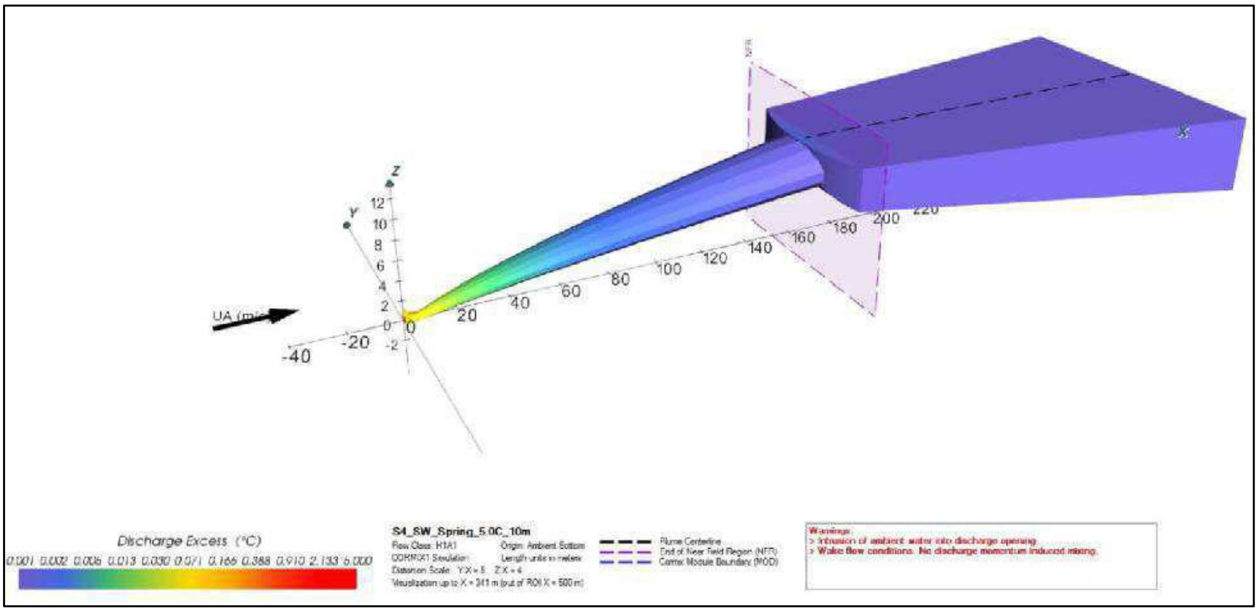

Figure B22: SW_S_04_ (Ex. Temp. = 5°C, Flow Rate=8.28 m^3/h, Depth=10m)

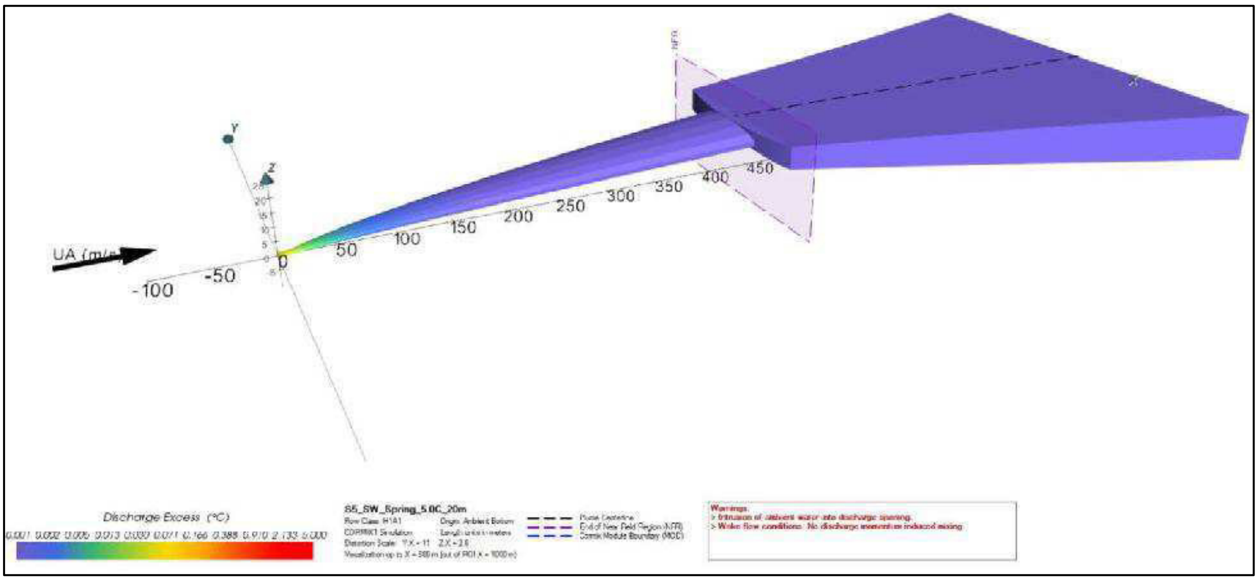

Figure B23: SW_S_05_ (Ex. Temp. = 5°C, Flow Rate=8.28 m^3/h, Depth=20m)

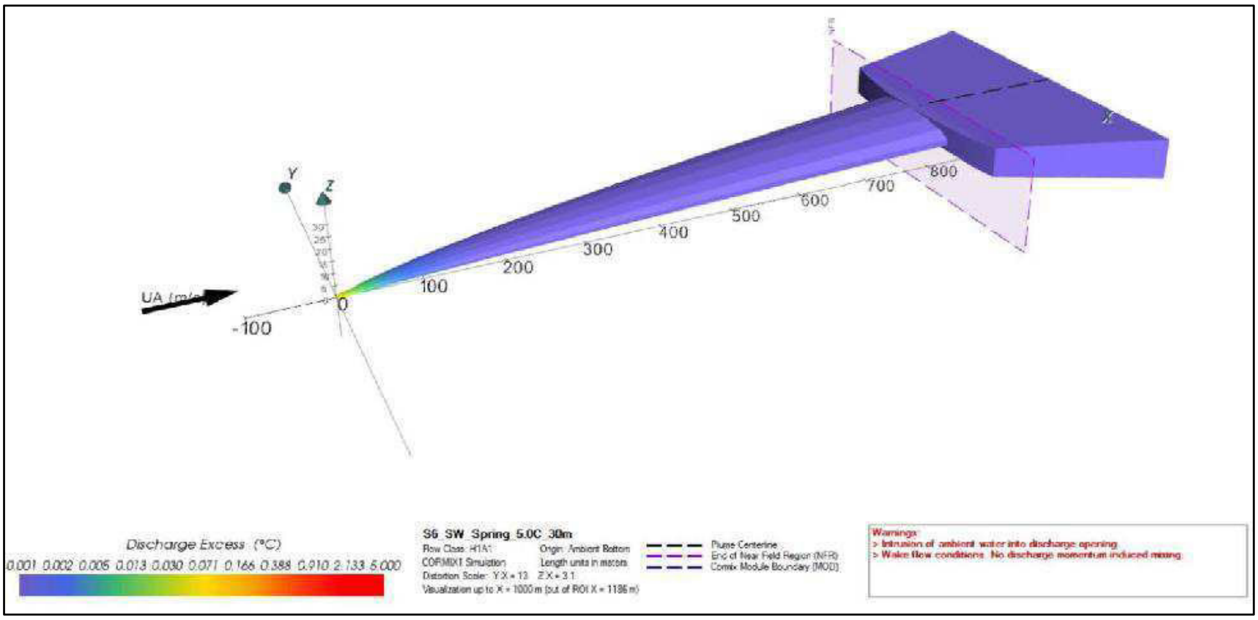

Figure B24: SW_S_06_ (Ex. Temp. = 5°C, Flow Rate=8.28 m^3/h, Depth=30m)

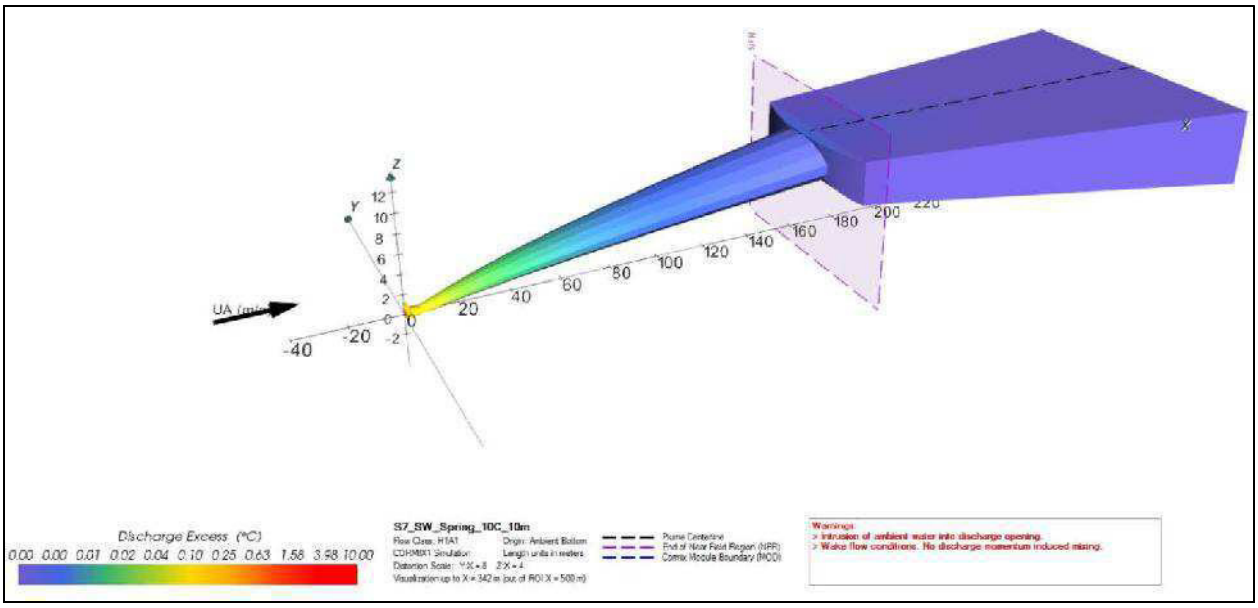

Figure B25: SW_S_07_ (Ex. Temp. = 10°C, Flow Rate=6.21 m^3/h, Depth=10m)

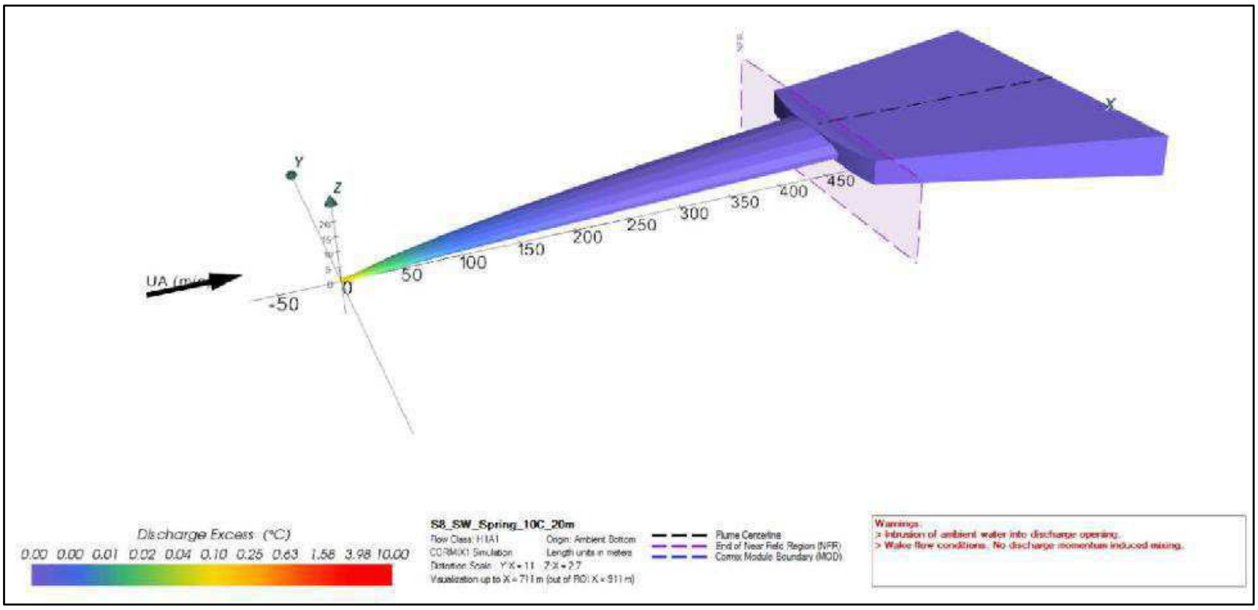

Figure B26: SW_S_08_ (Ex. Temp. = 10°C, Flow Rate=6.21 m^3/h, Depth=20m)

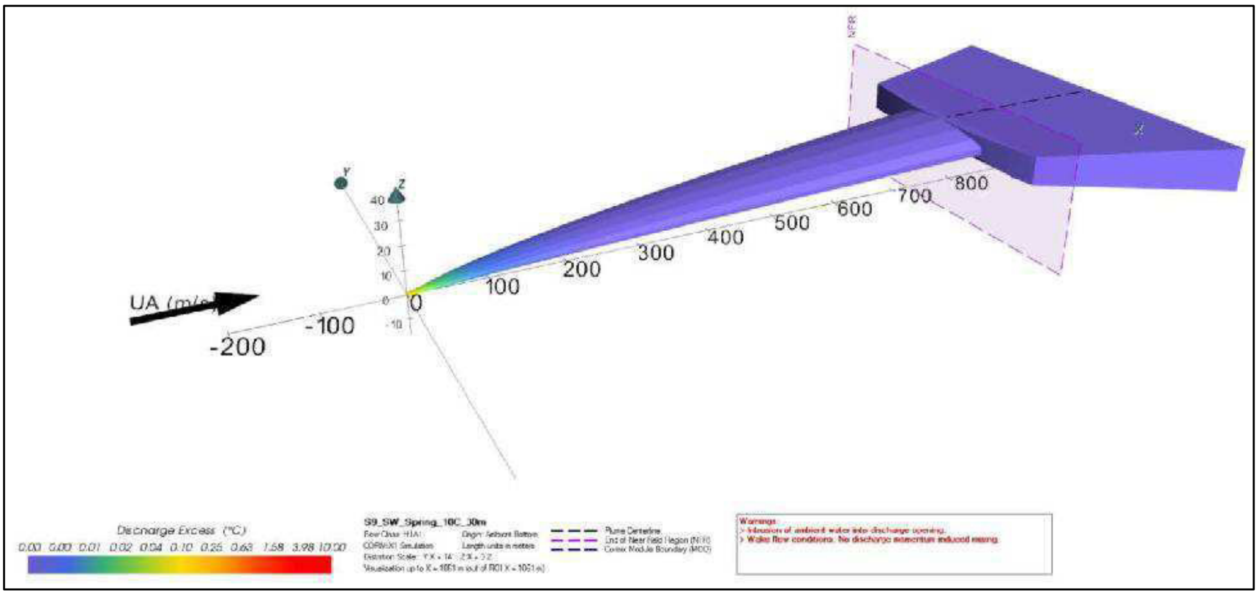

Figure B27: SW_S_09_ (Ex. Temp. = 10°C, Flow Rate=6.21 m^3/h, Depth=30m)

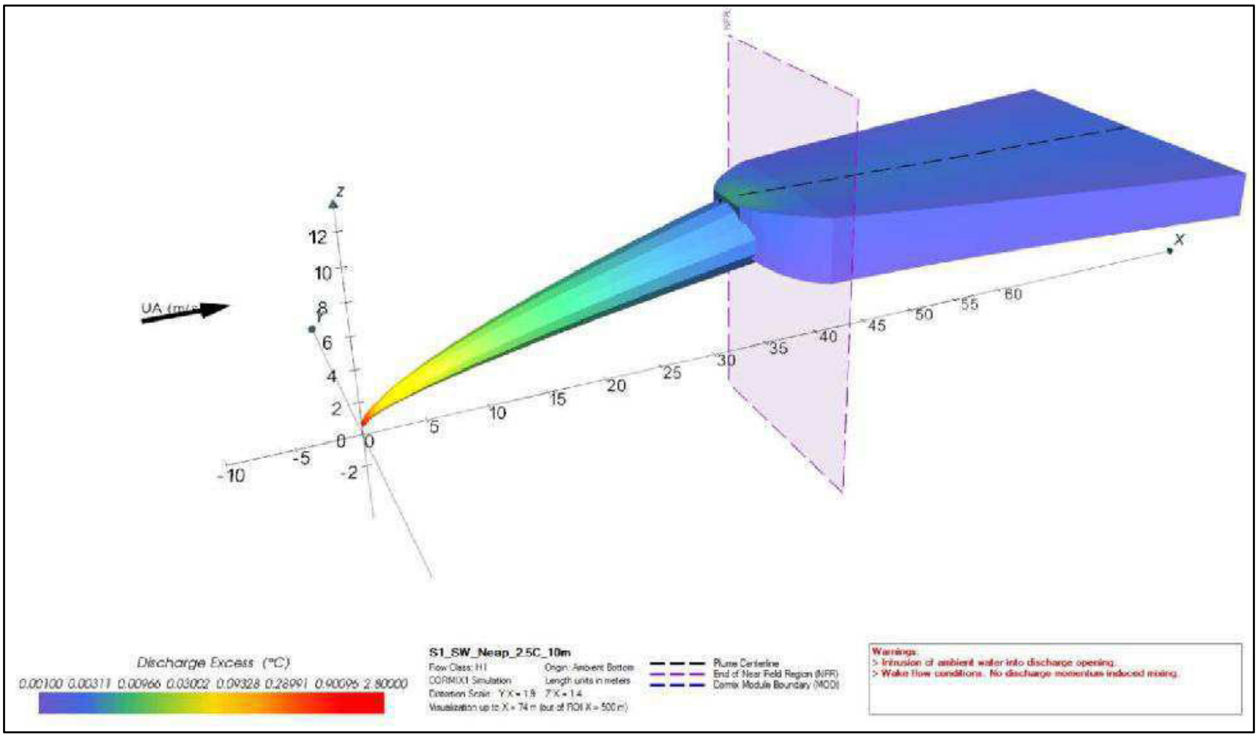

Figure B28: SW_N_01_ (Ex. Temp. = 2.5°C, Flow Rate=16.56 m^3/h, Depth=10m)

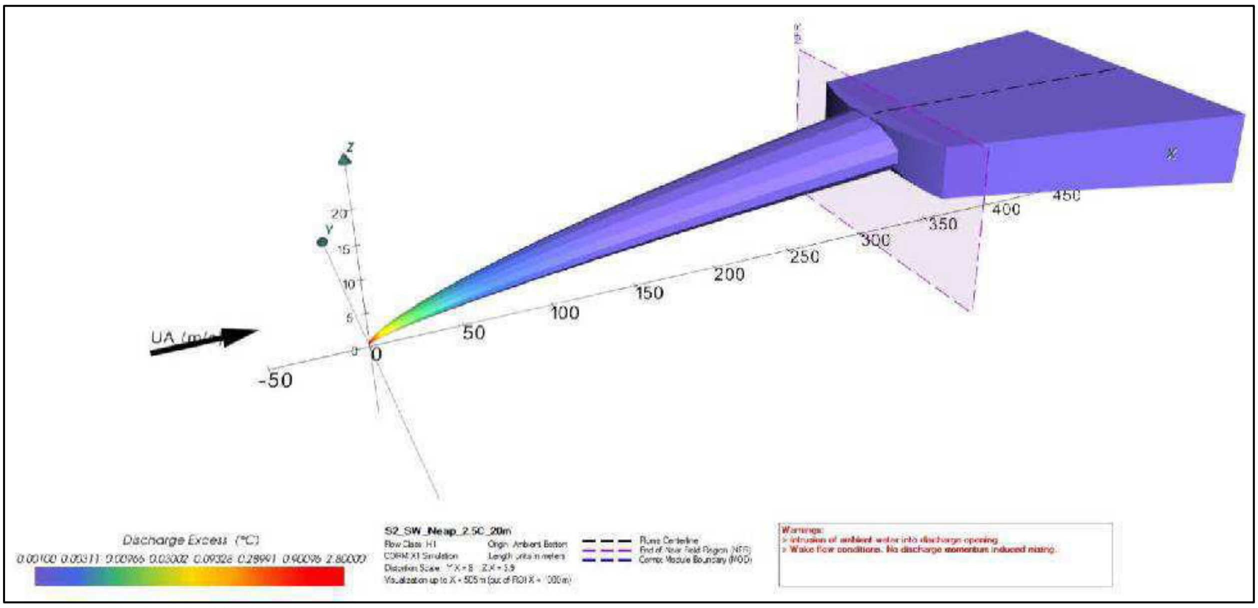

Figure B29: SW_N_02_ (Ex. Temp. = 2.5°C, Flow Rate=16.56 m^3/h, Depth=20m)

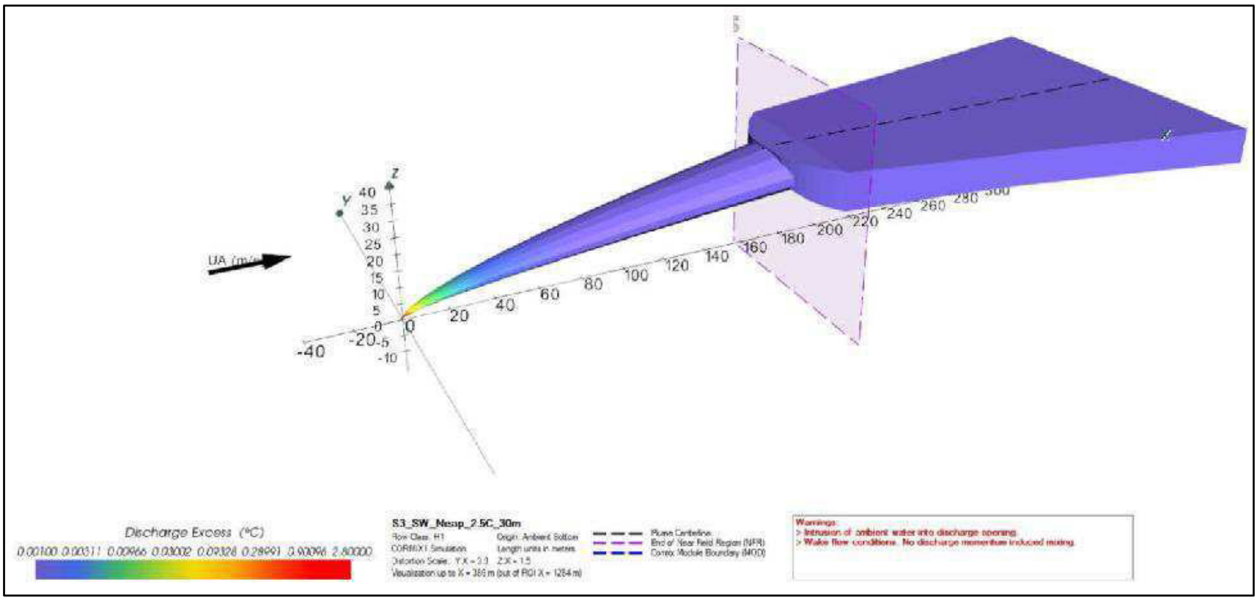

Figure B30: SW_N_03_ (Ex. Temp. = 2.5°C, Flow Rate=16.56 m^3/h, Depth=30m)

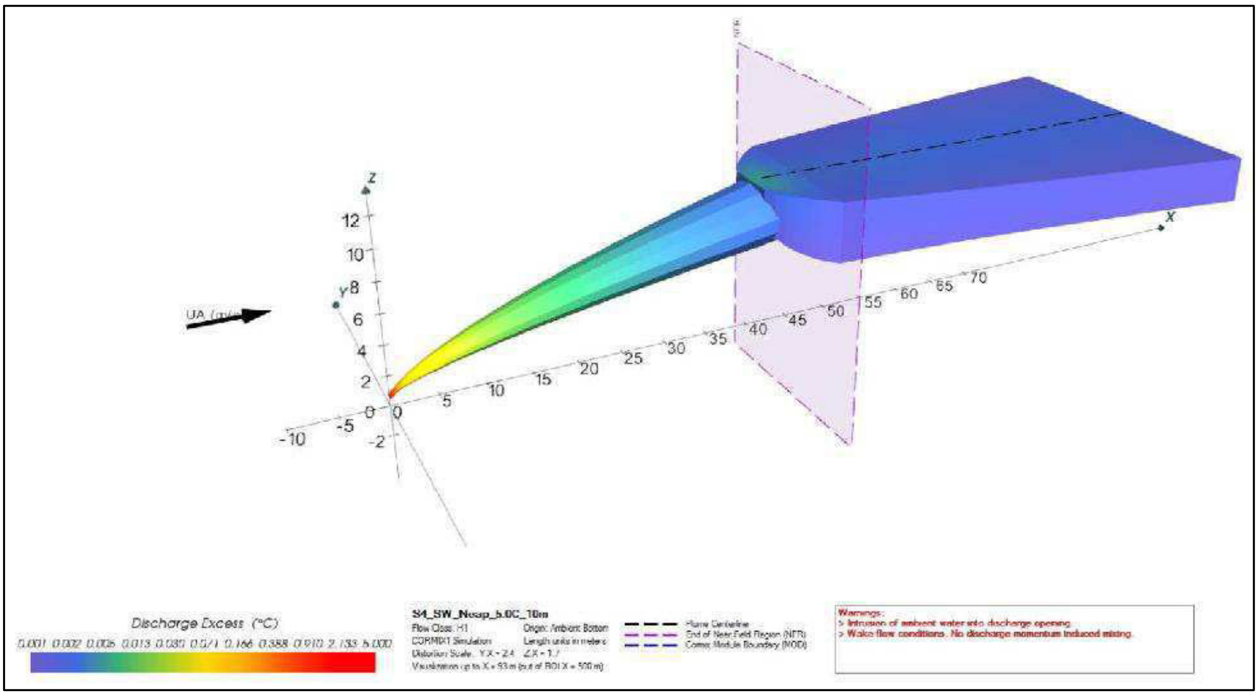

Figure B31: SW_N_04_ (Ex. Temp. = 5°C, Flow Rate=8.28 m^3/h, Depth=10m)

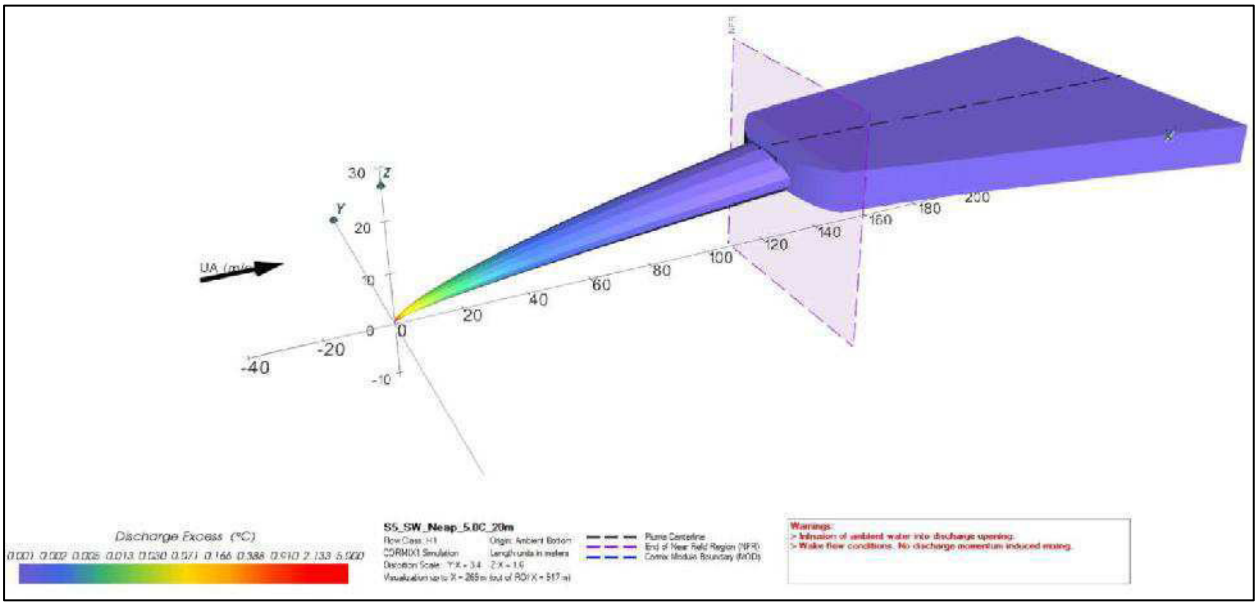

Figure B32: SW_N_05_ (Ex. Temp. = 5°C, Flow Rate=8.28 m^3/h, Depth=20m)

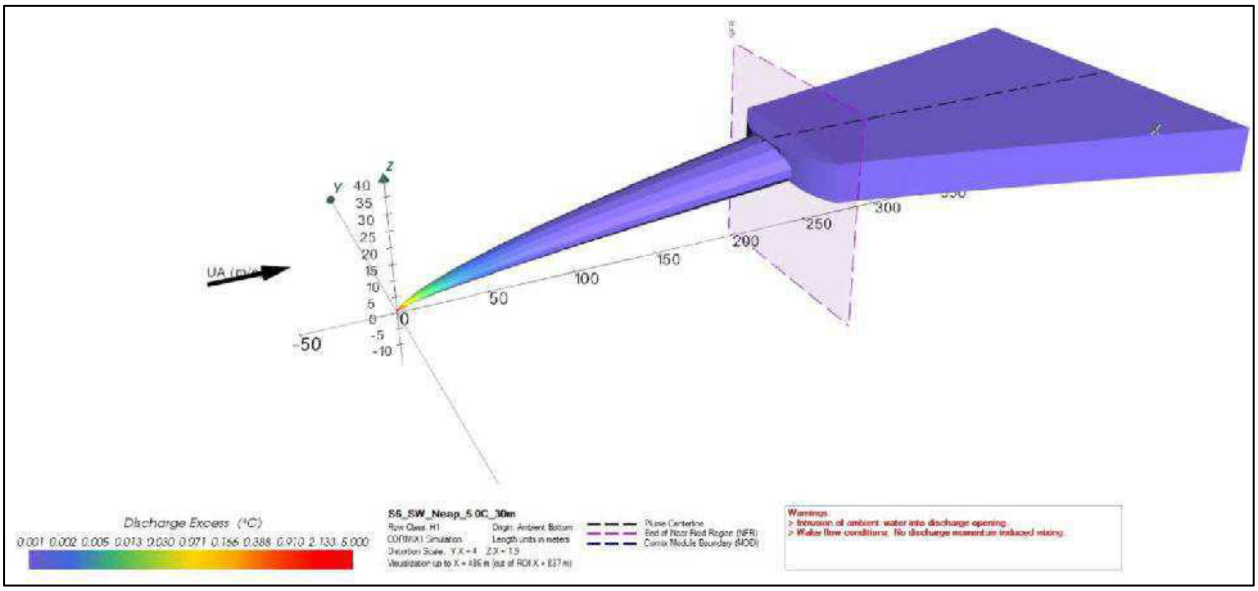

Figure B33: SW_N_06_ (Ex. Temp. = 5°C, Flow Rate=8.28 m^3/h, Depth=30m)

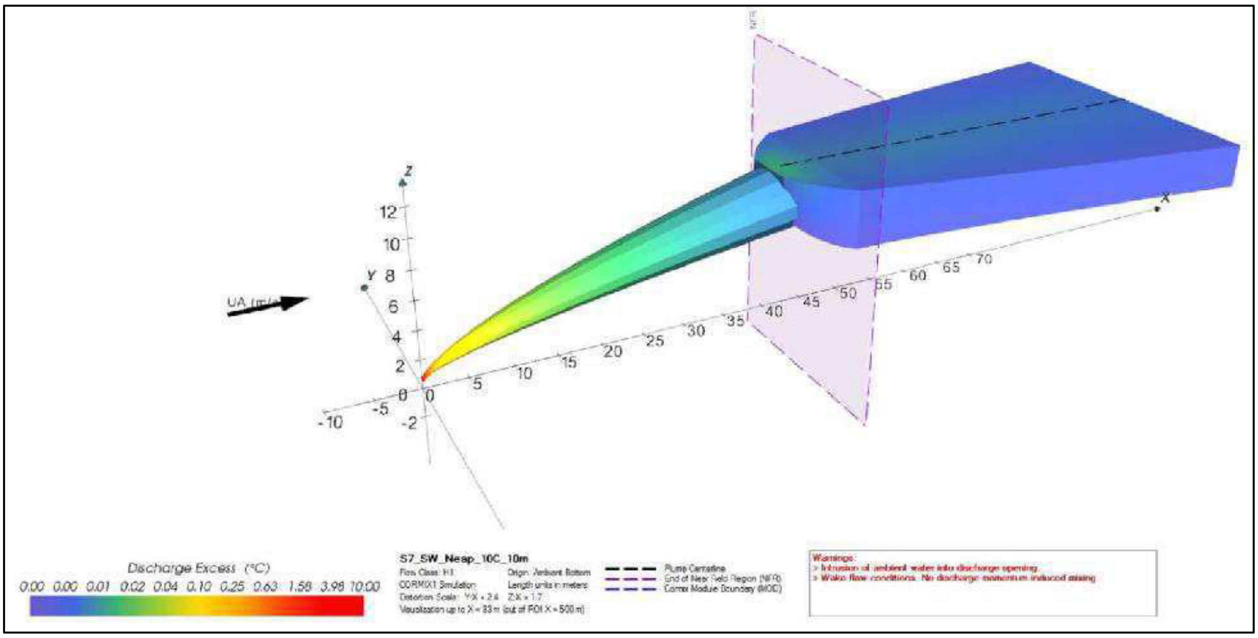

Figure B34: SW_N_07_ (Ex. Temp. = 10°C, Flow Rate=6.21 m^3/h, Depth=10m)

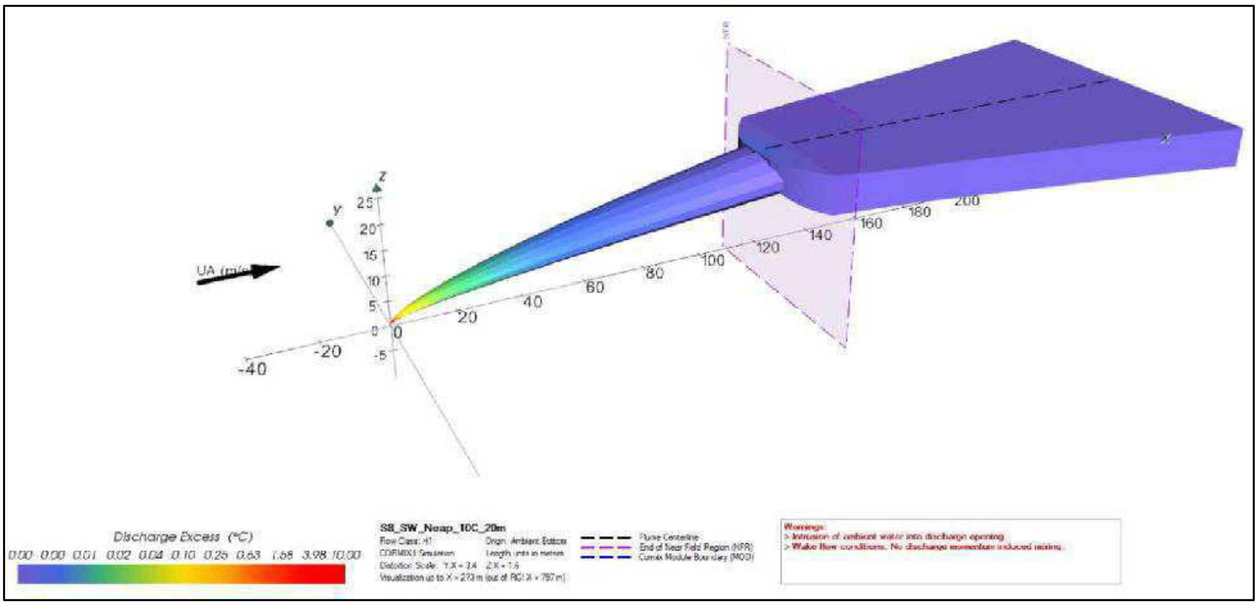

Figure B35: SW_N_08_ (Ex. Temp. = 10°C, Flow Rate=6.21 m^3/h, Depth=20m)

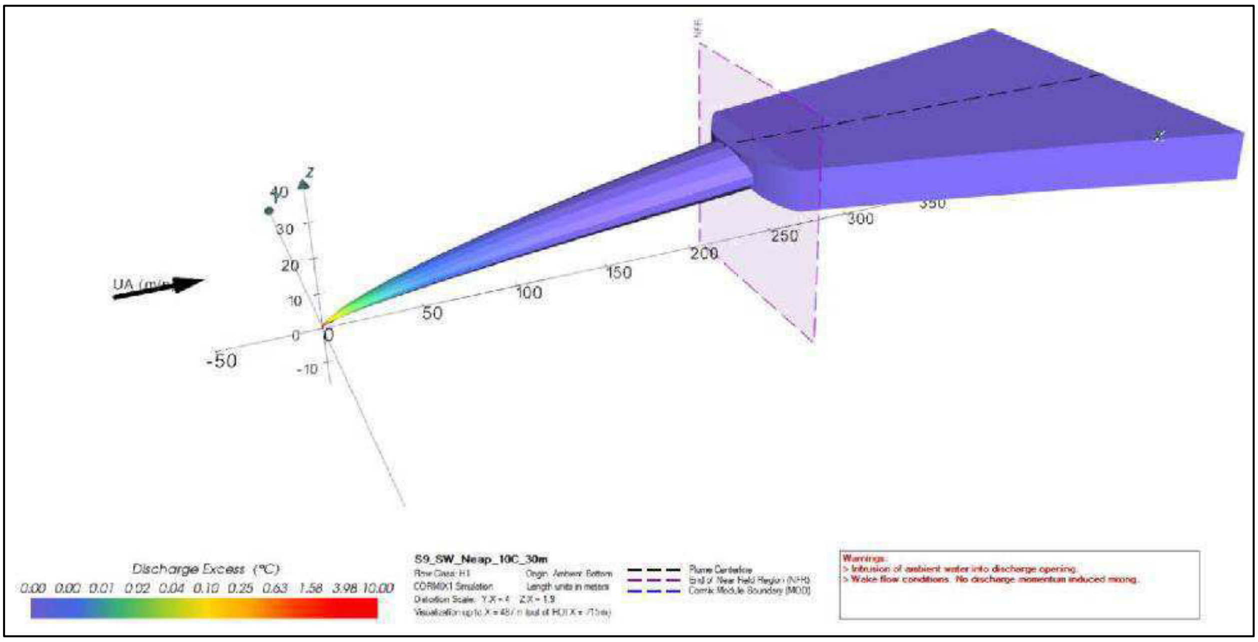

Figure B36: SW_N_09_ (Ex. Temp. = 10°C, Flow Rate=6.21 m^3/h, Depth=30m)

ANNEX C

Heat Dissipation in Far Field (MIKE 21 HD)

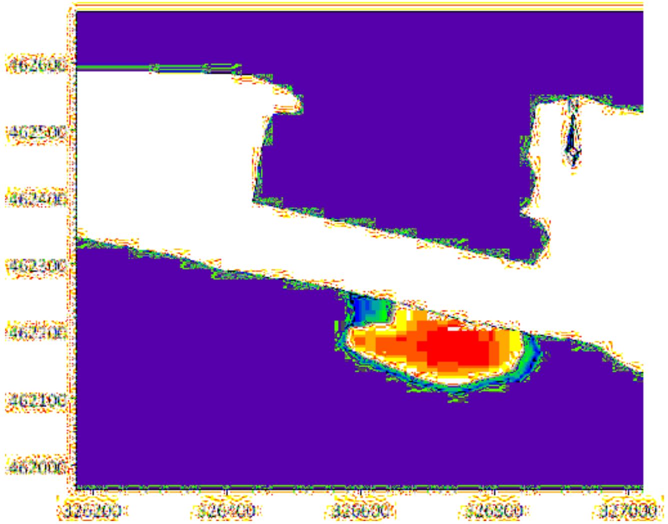

Figure C.01: NE_S_01_Eastward Flow

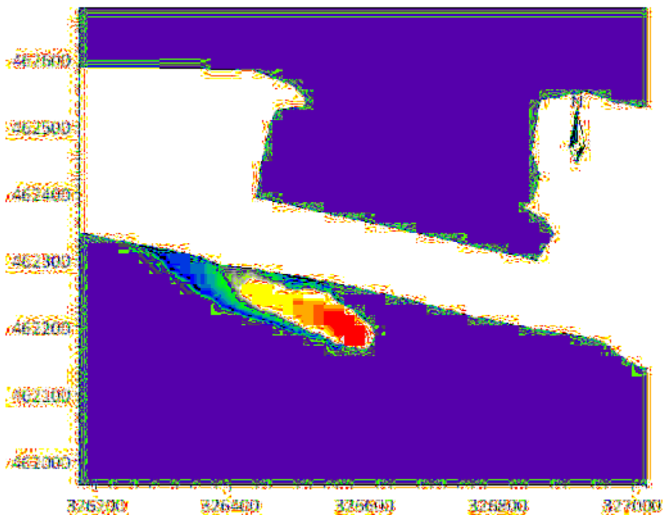

Figure C.02: NE_S_01_Westward Flow

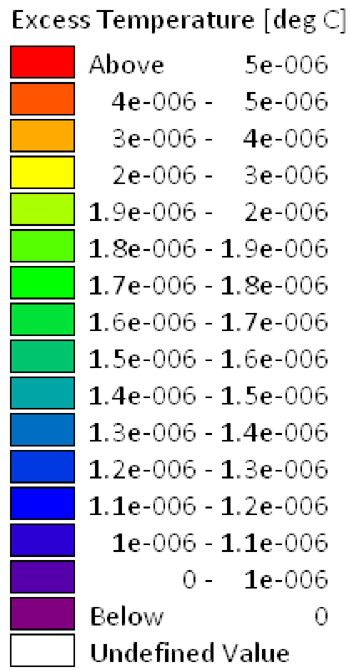

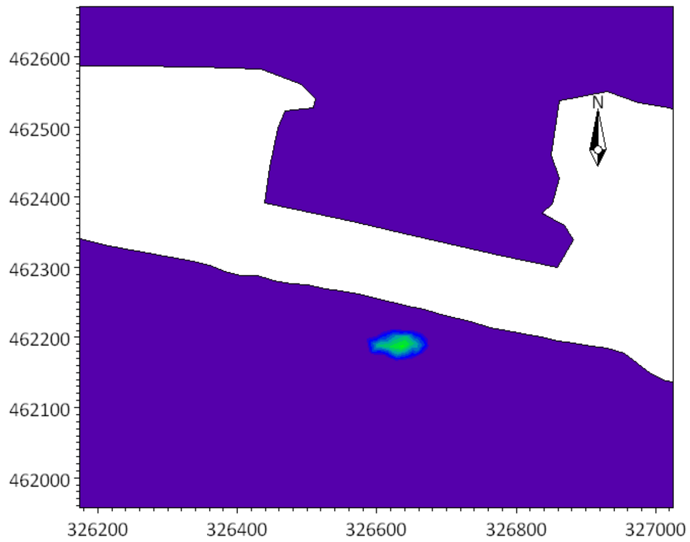

Figure C.03: NE_S_02_Eastward Flow

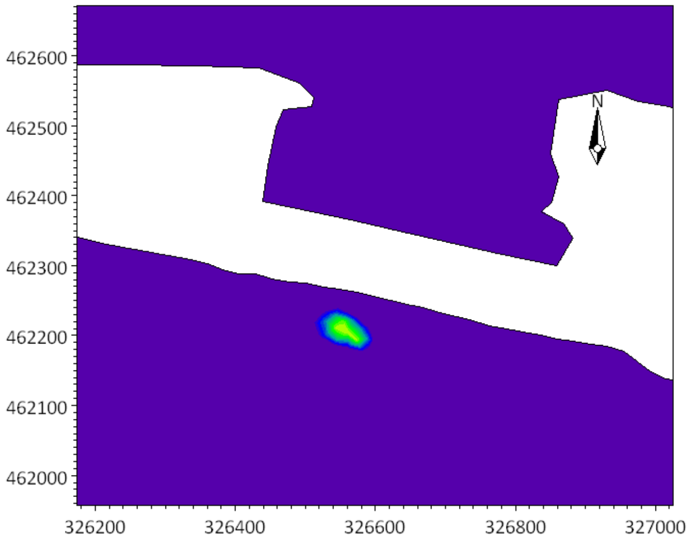

Figure C.04: NE_S_02_Westward Flow

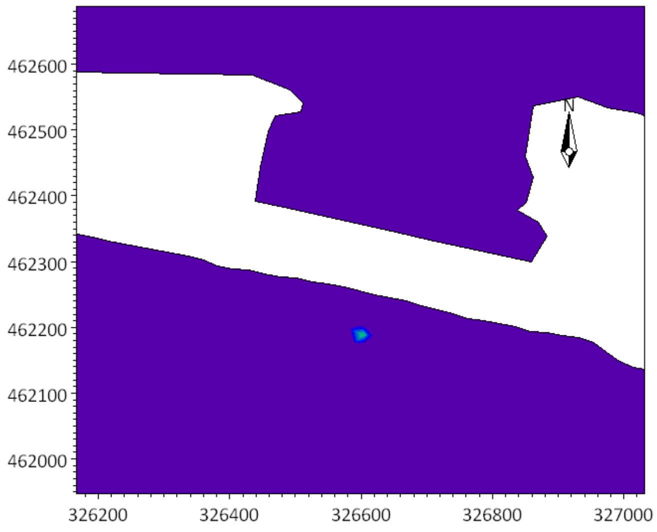

Figure C.05: NE_S_03_Eastward Flow

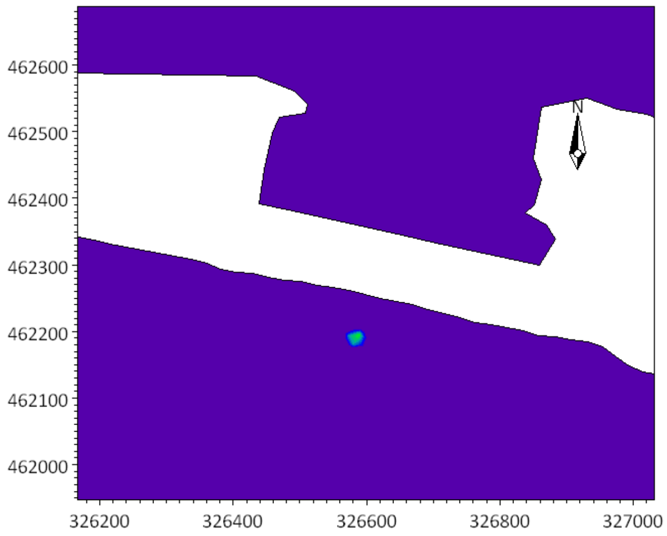

Figure C.06: NE_S_03_Westward Flow

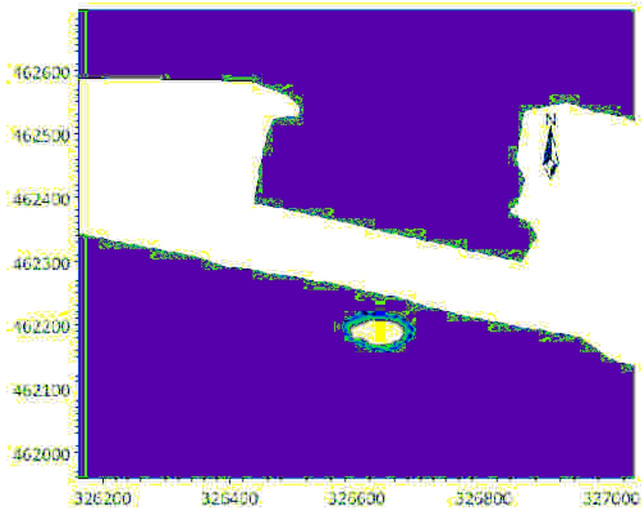

Figure C.07: NE_S_04_Eastward Flow

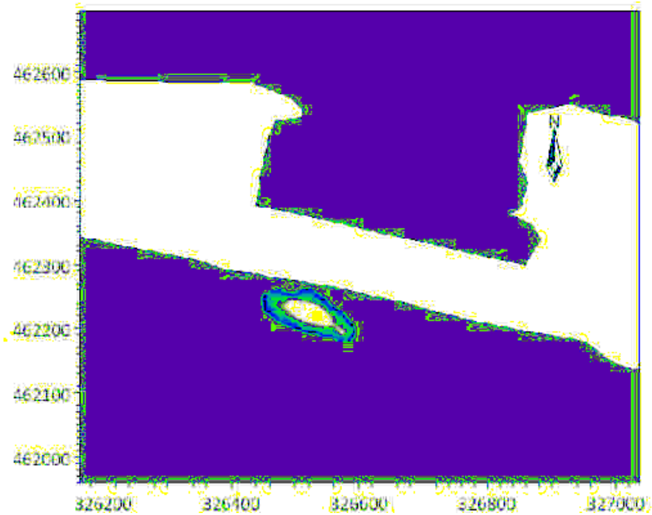

Figure C.08: NE_S_04_Westward Flow

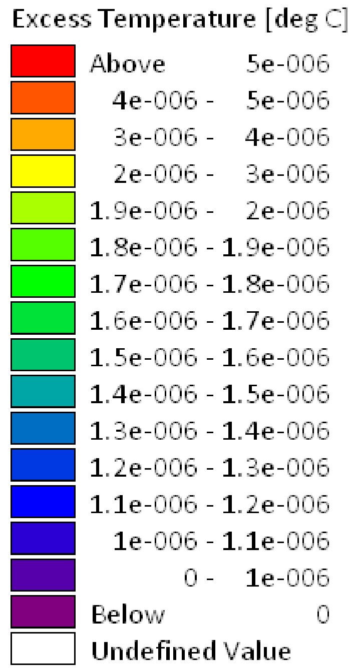

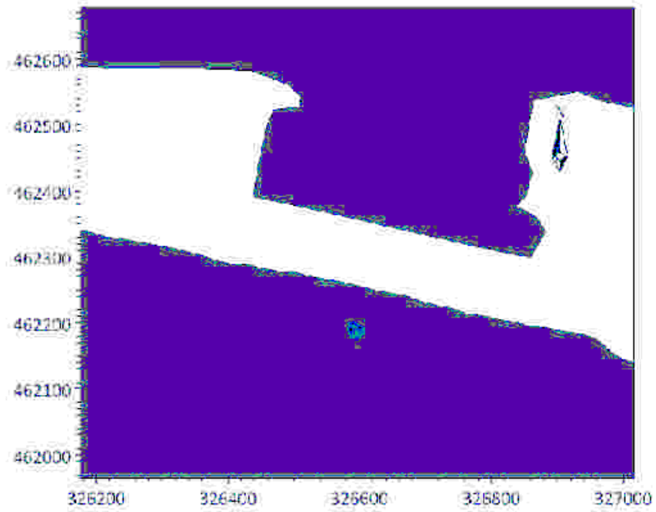

Figure C.09: NE_S_05_Eastward Flow

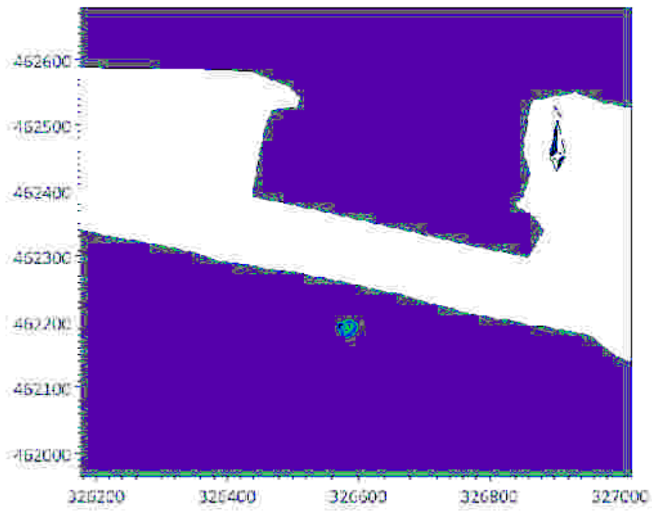

Figure C.10: NE_S_05_Westward Flow

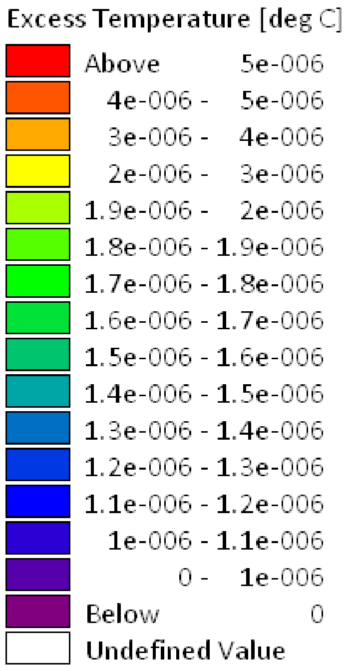

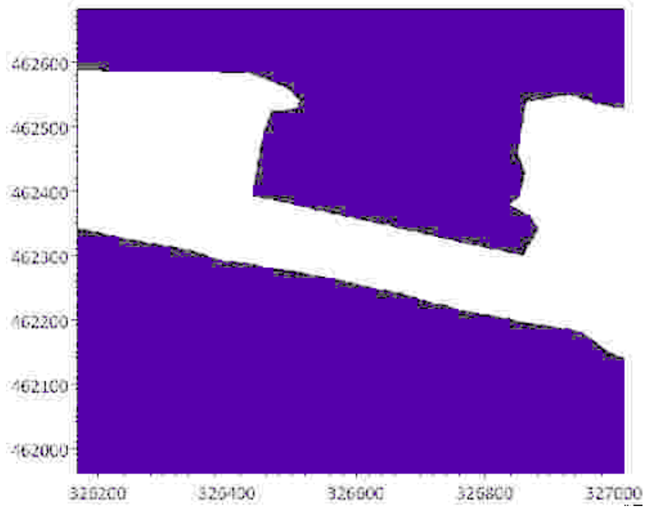

Figure C.11: NE_S_06_Eastward Flow

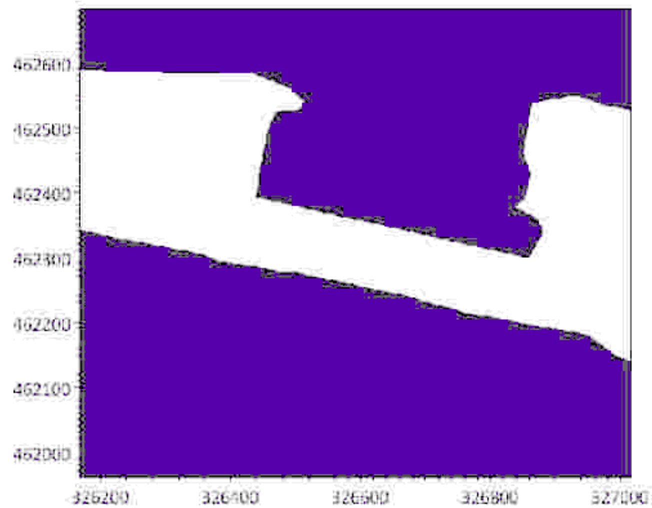

Figure C.12: NE_S_06_Westward Flow

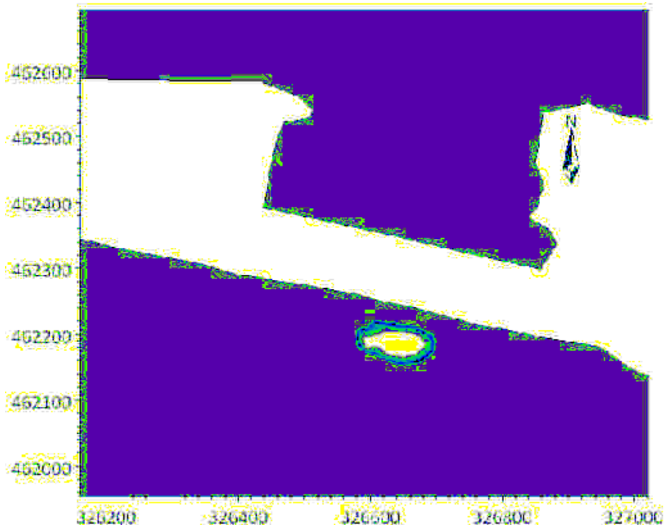

Figure C.13: NE_S_07_Eastward Flow

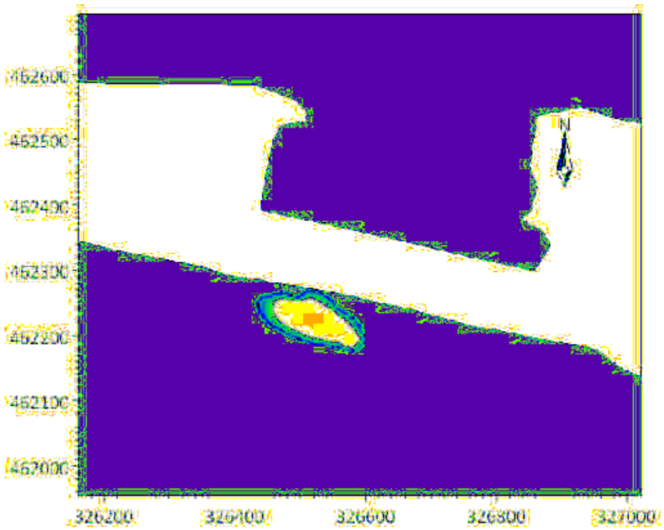

Figure C.14: NE_S_07_Westward Flow

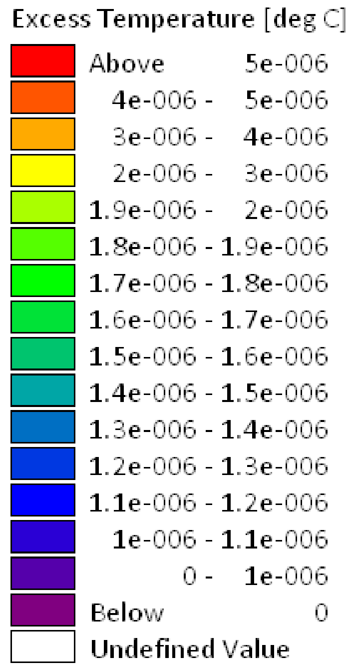

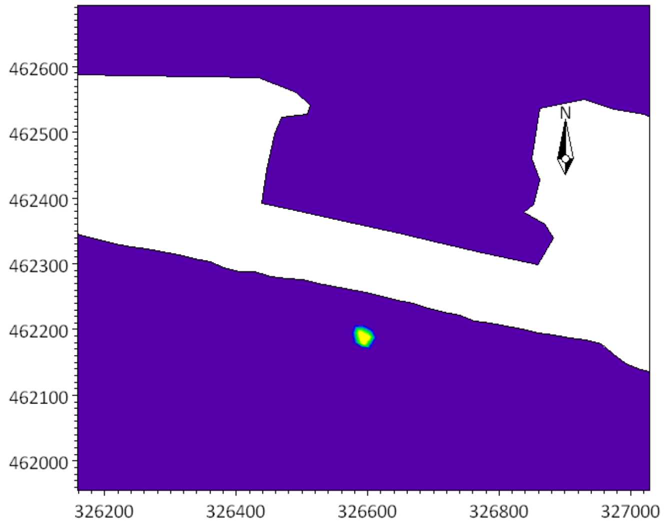

Figure C.15: NE_S_08_Eastward Flow

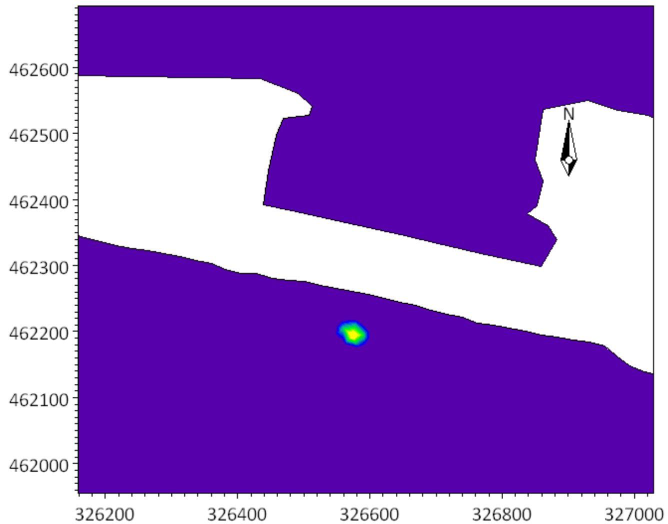

Figure C.16: NE_S_08_Westward Flow

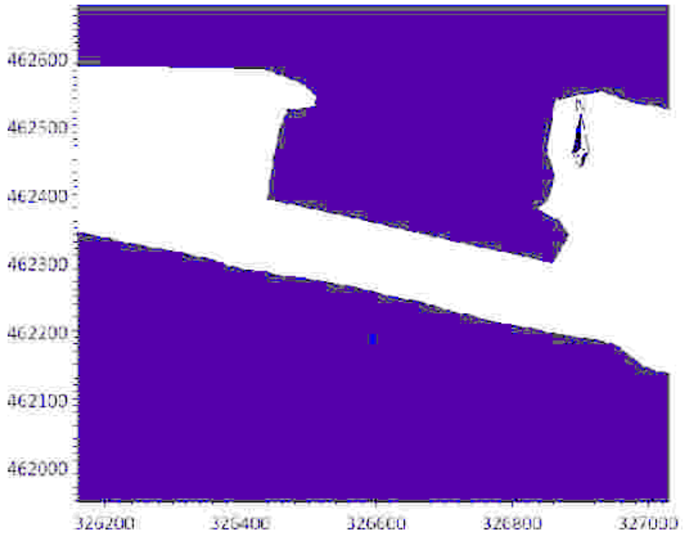

Figure C.17: NE_S_09_Eastward Flow

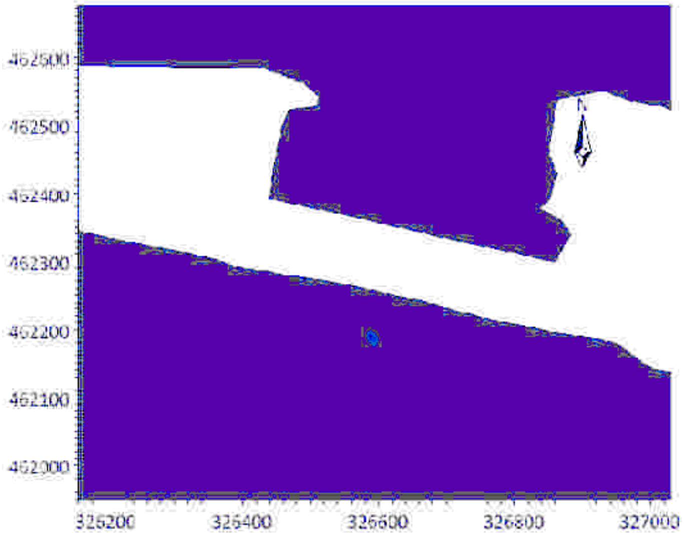

Figure C.18: NE_S_09_Westward Flow

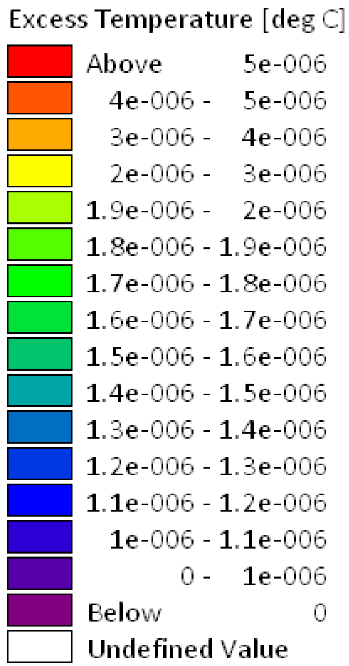

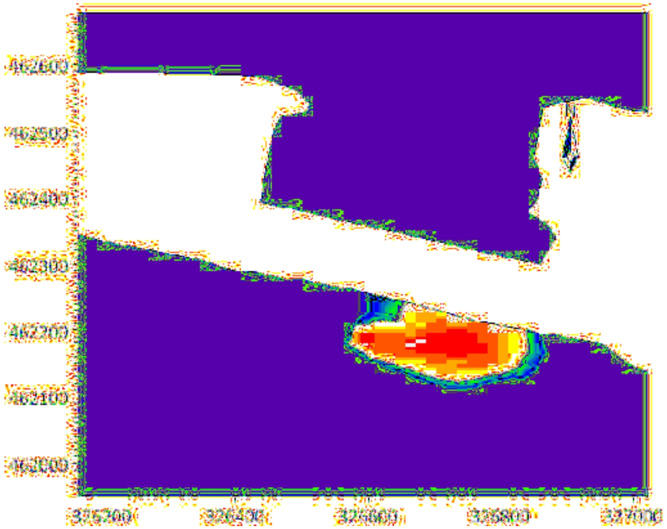

Figure C.19: NE_N_01_Eastward Flow

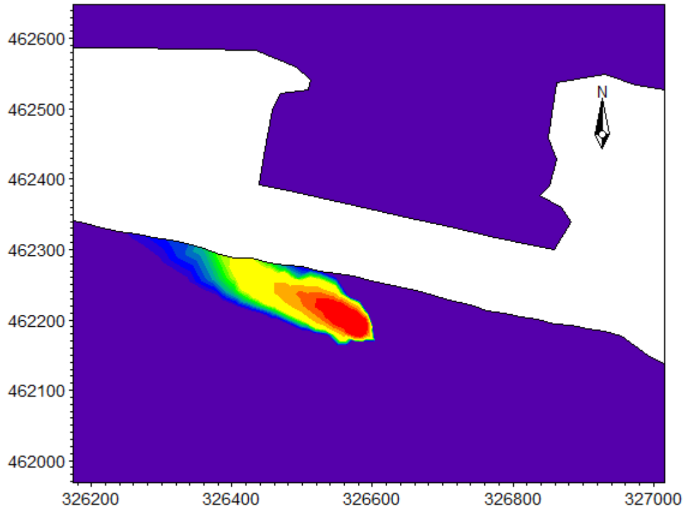

Figure C.20: NE_N_01_Westward Flow

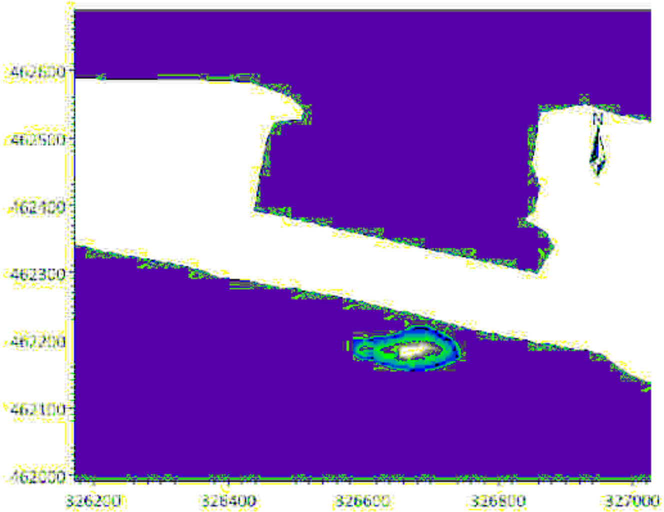

Figure C.21: NE_N_02_Eastward Flow

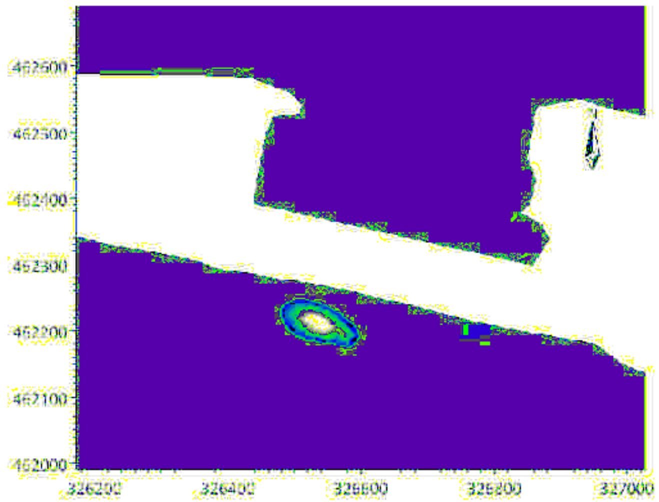

Figure C.22: SW_N_02_Westward Flow

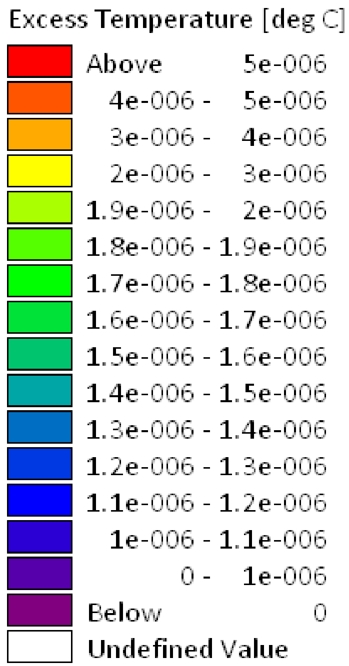

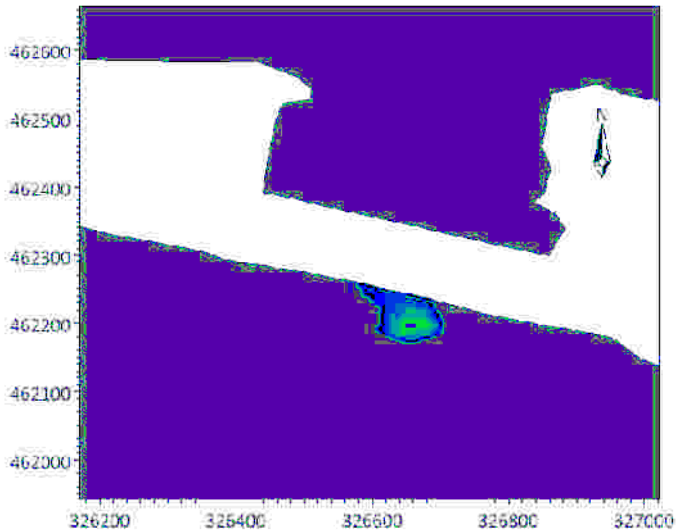

Figure C.23: NE_N_03_Eastward Flow

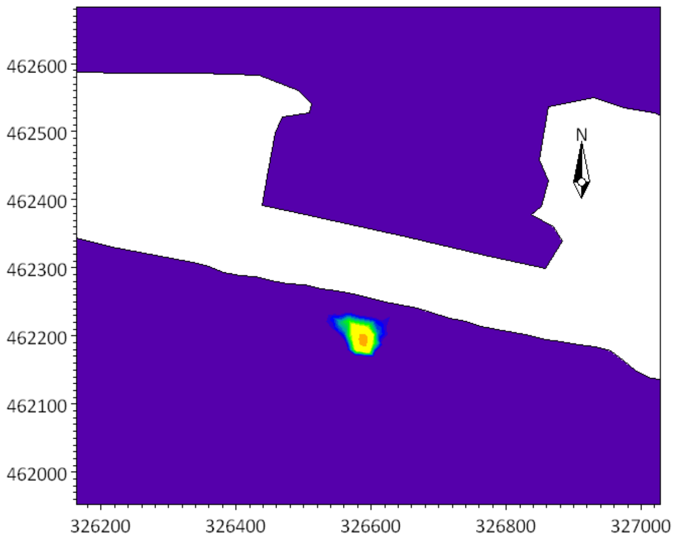

Figure C.24: NE_N_03_Westward Flow

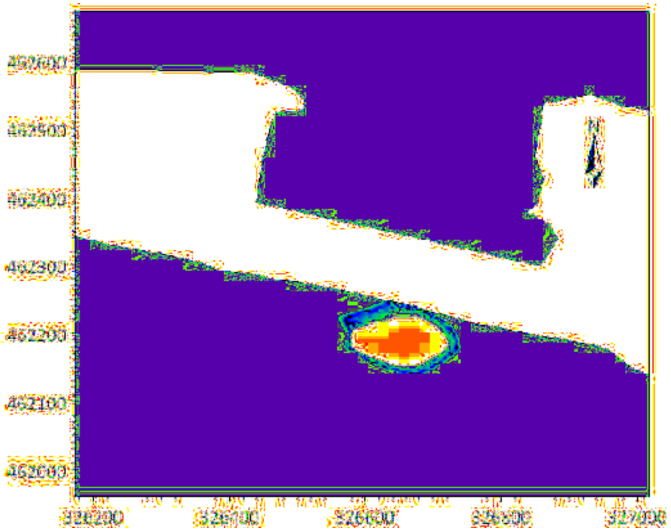

Figure C.25: NE_N_04_Eastward Flow

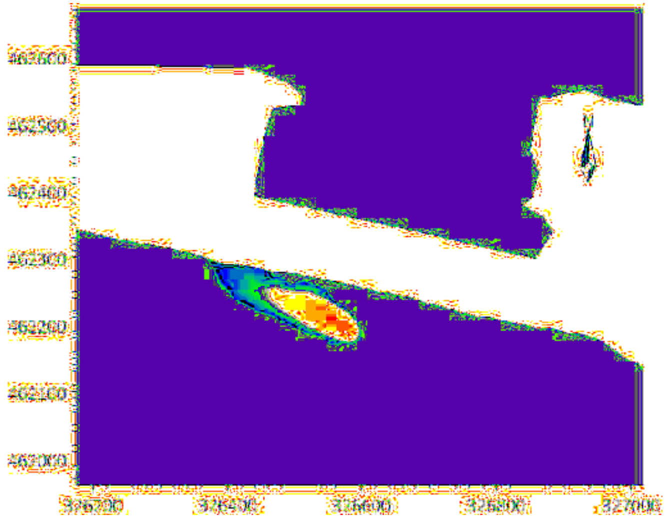

Figure C.26: SW_N_04_Westward Flow

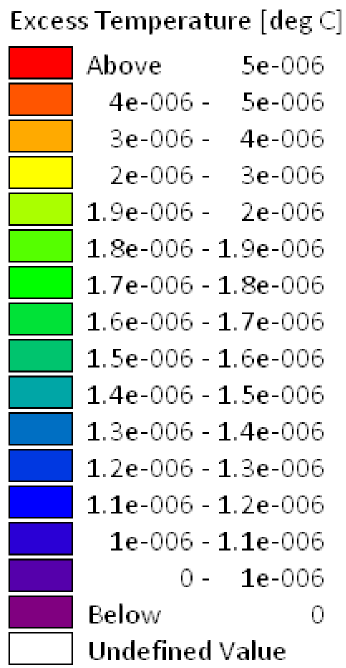

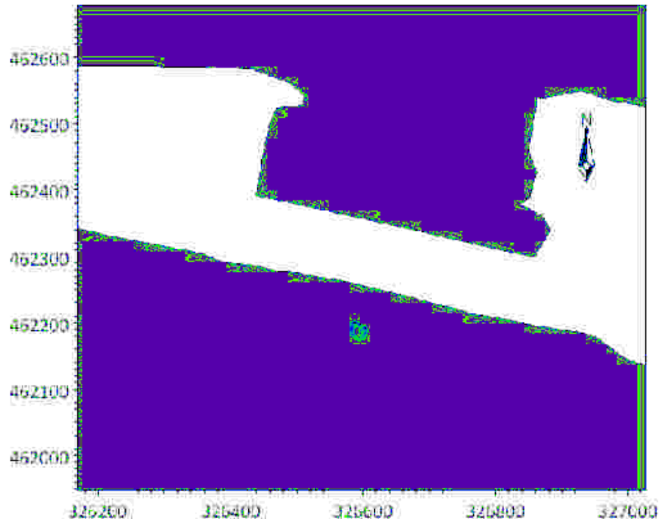

Figure C.27: NE_N_05_Eastward Flow

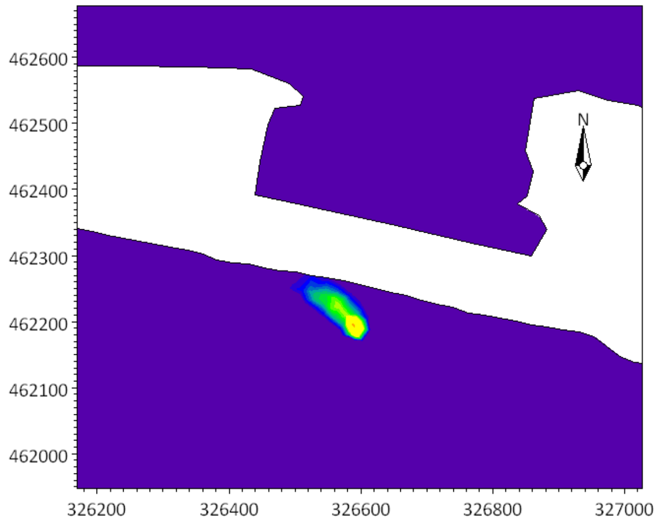

Figure C.28: NE_N_05_Westward Flow

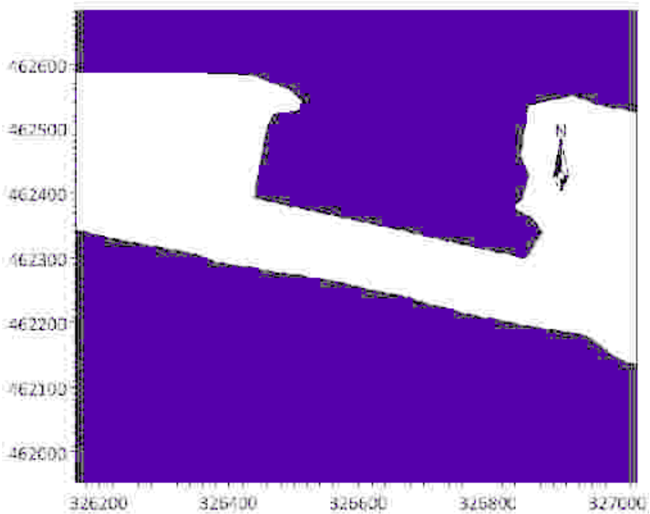

Figure C.29: NE_N_06_Eastward Flow

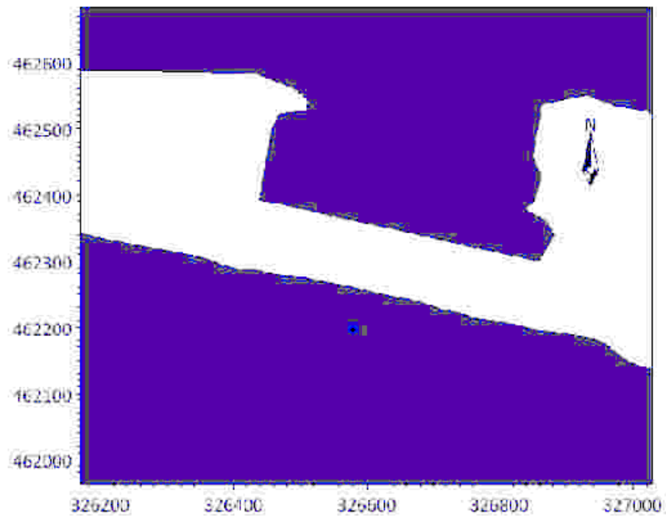

Figure C.30: NE_N_06_Westward Flow

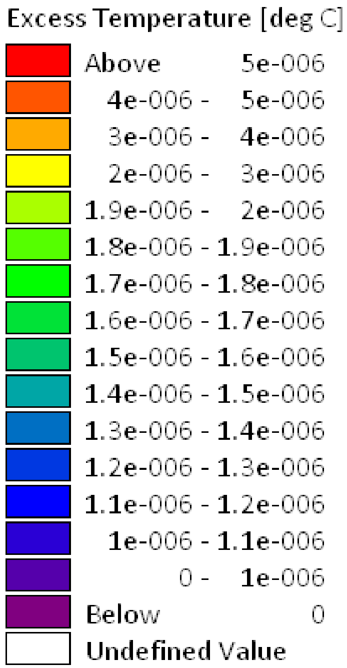

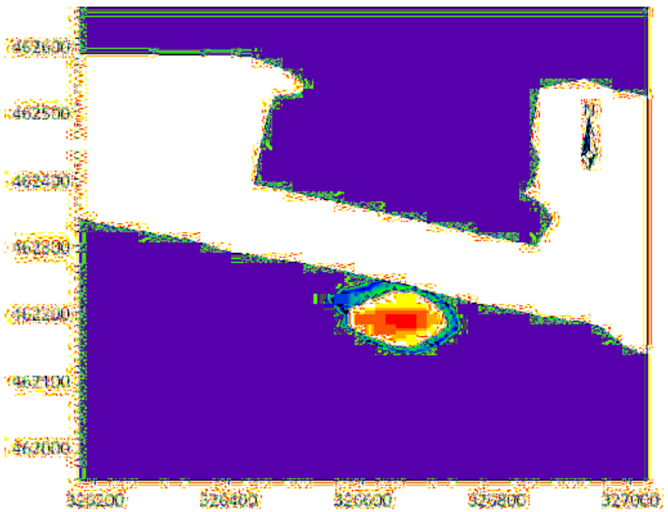

Figure C.31: NE_N_07_Eastward Flow

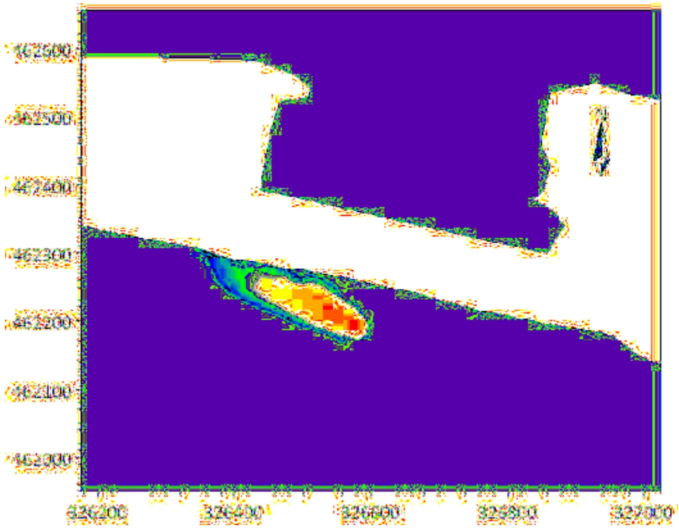

Figure C.32: NE_N_07_Westward Flow

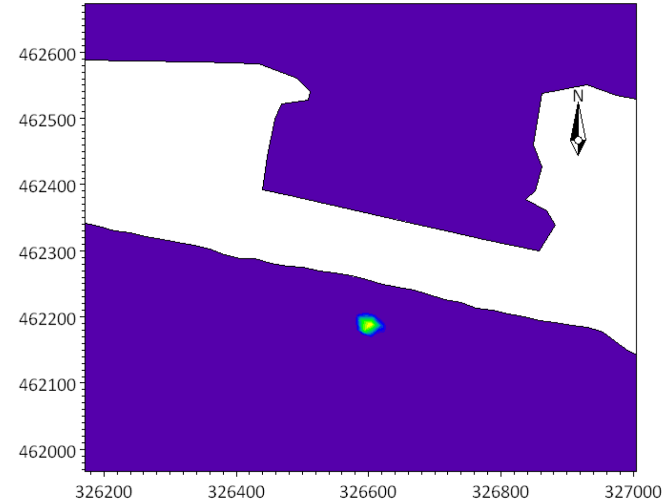

Figure C.33: NE_N_08_Eastward Flow

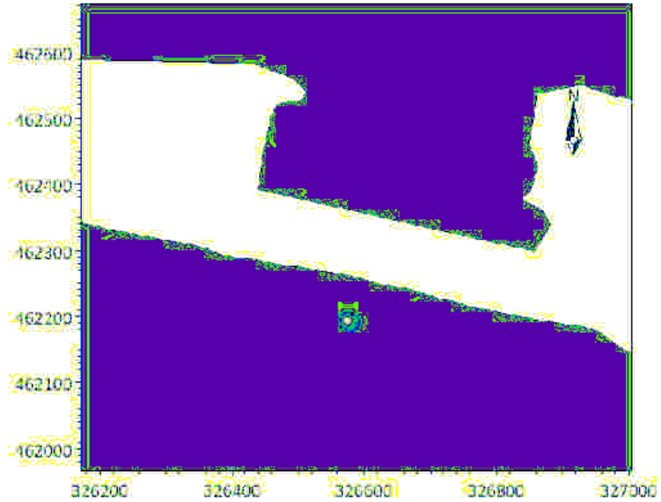

Figure C.34: NE_N_08_Westward Flow

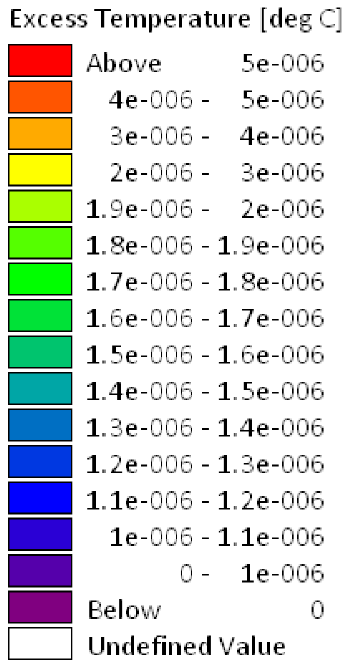

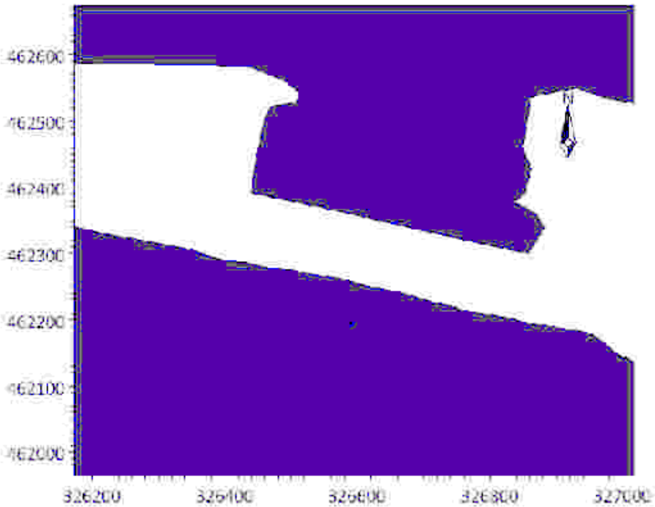

Figure C.35: NE_N_09_Eastward Flow

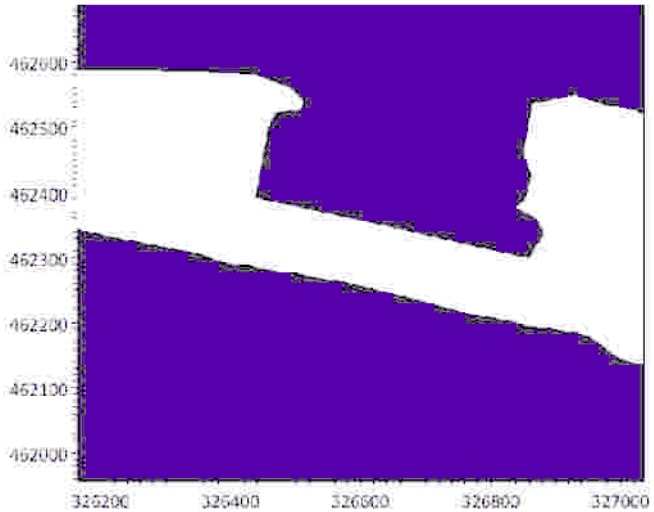

Figure C.36: NE_N_09_Westward Flow

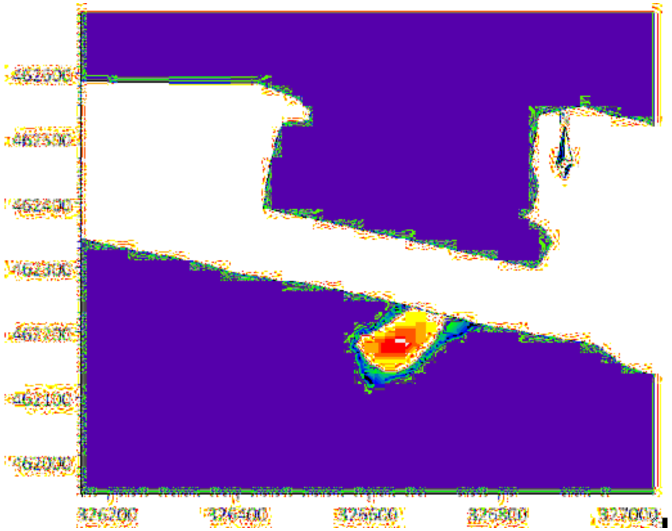

Figure C.37: SW_S_01_Eastward Flow

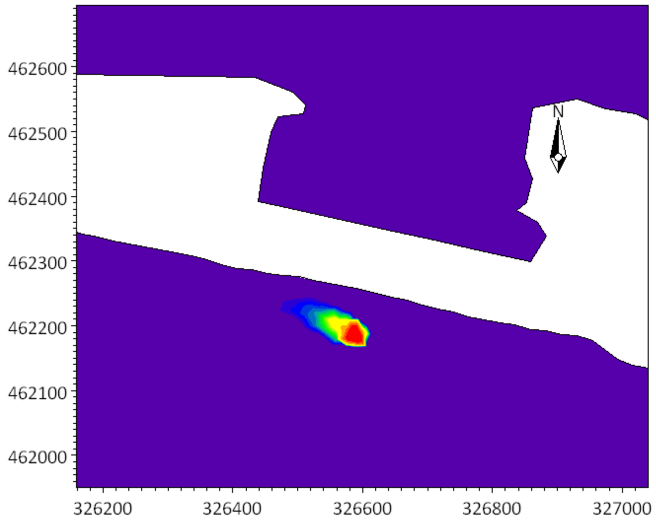

Figure C.38: SW_S_01_Westward Flow

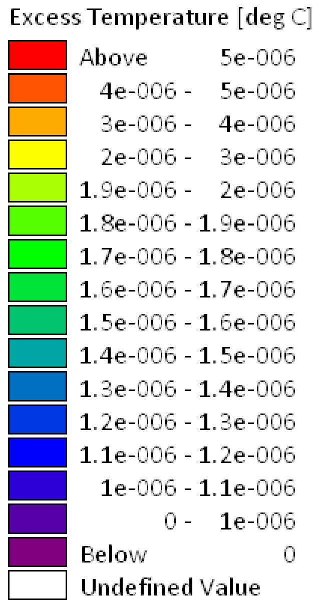

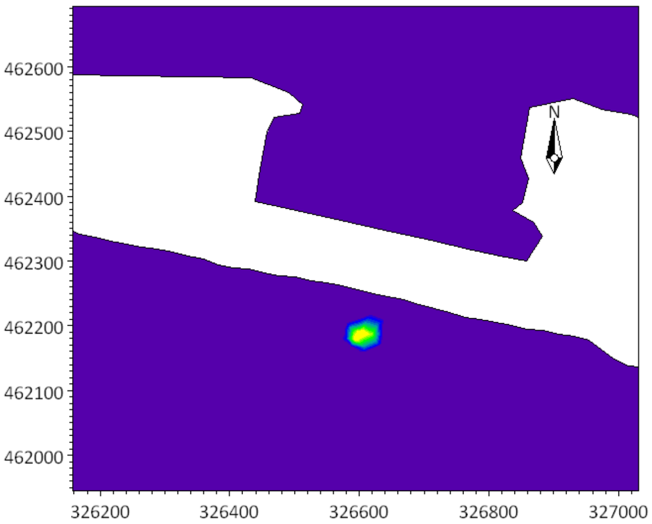

Figure C.39: SW_S_02_Eastward Flow

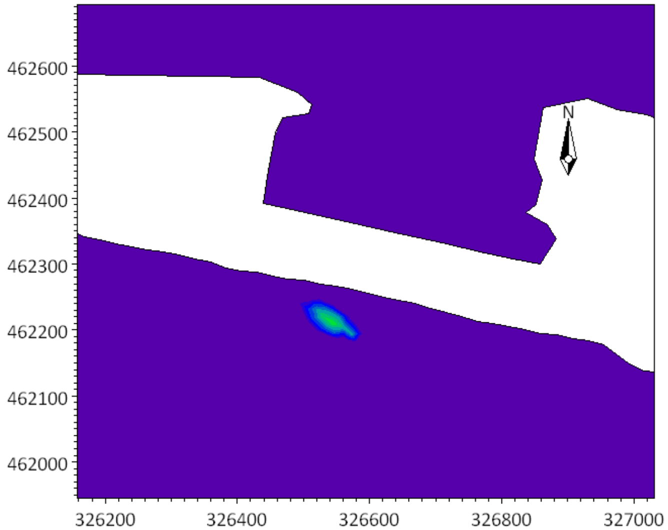

Figure C.40: SW_S_02_Westward Flow

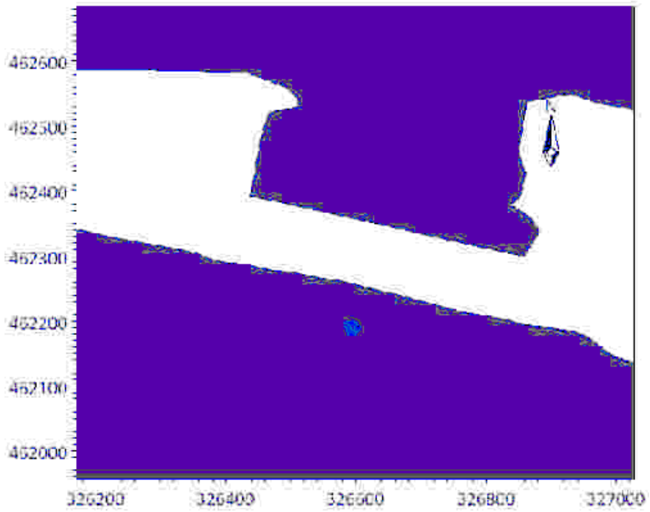

Figure C.41: SW_S_03_Eastward Flow

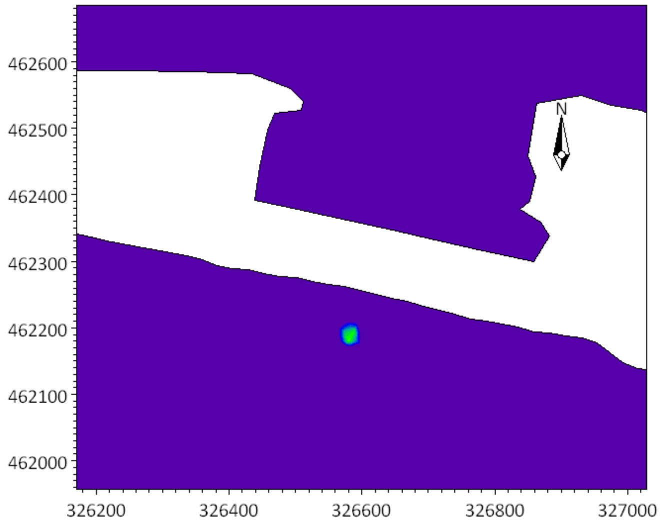

Figure C.42: SW_S_03_Westward Flow

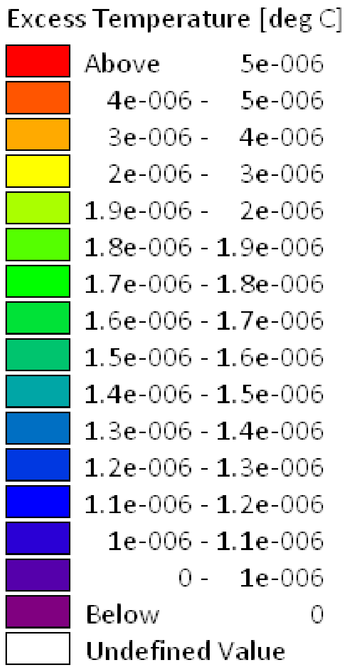

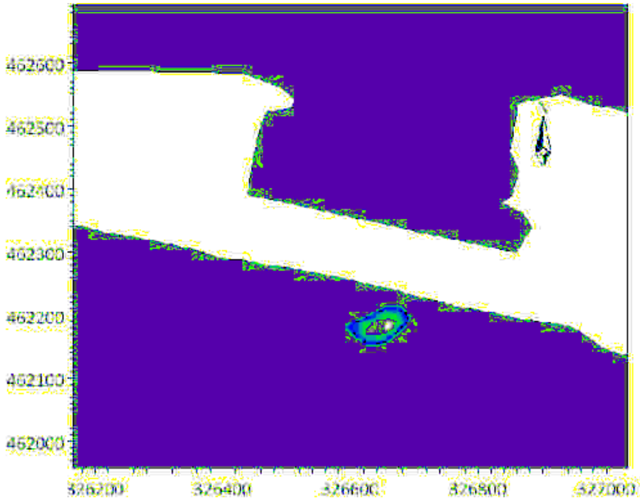

Figure C.43: SW_S_04_Eastward Flow

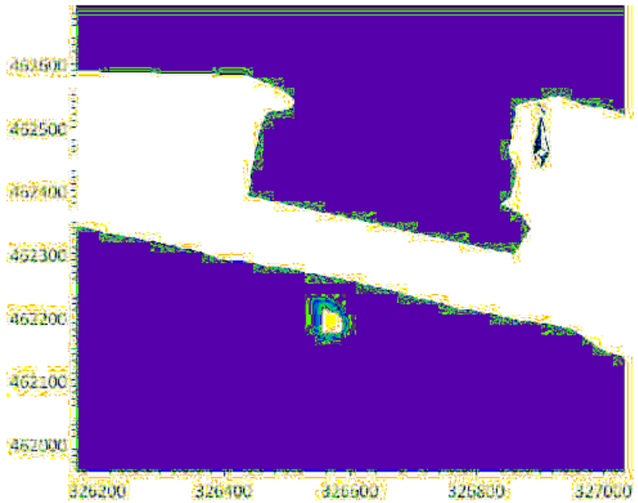

Figure C.44: SW_S_04_Westward Flow

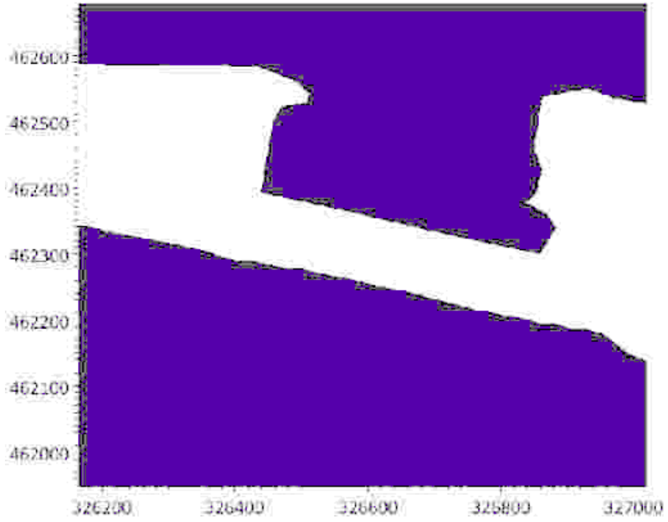

Figure C.45: SW_S_05_Eastward Flow

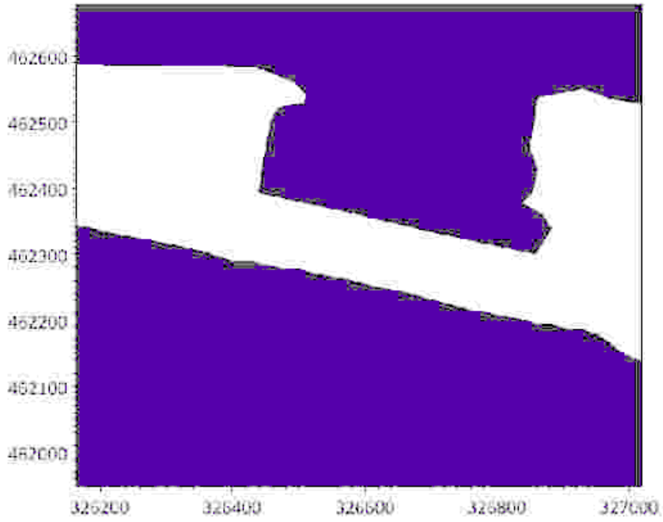

Figure C.46: SW_S_05_Westward Flow

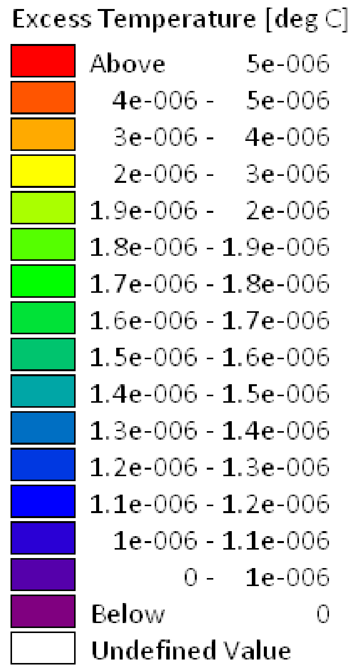

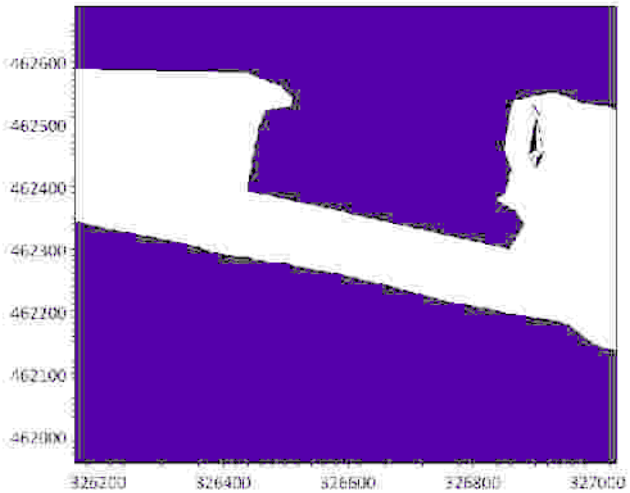

Figure C.47: SW_S_06_Eastward Flow

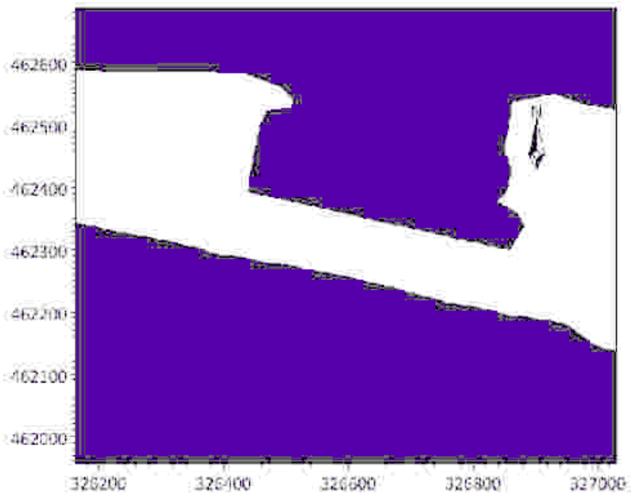

Figure C.48: SW_S_06_Westward Flow

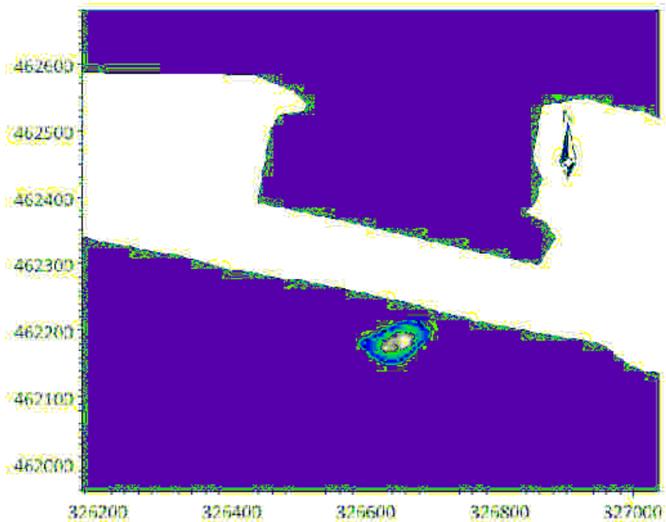

Figure C.49: SW_S_07_Eastward Flow

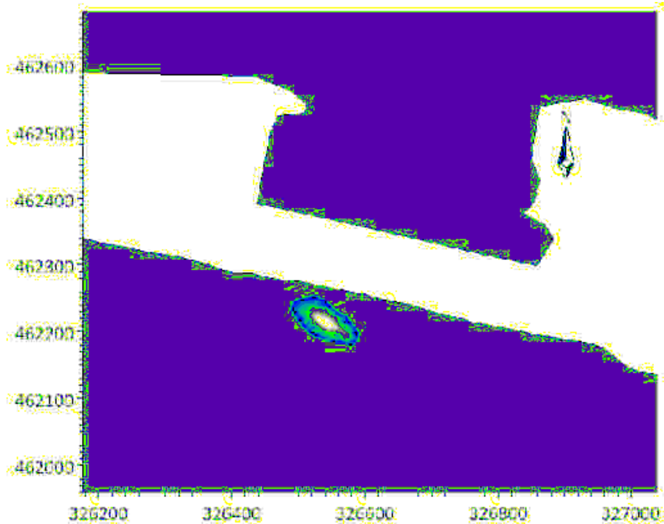

Figure C.50: SW_S_07_Westward Flow

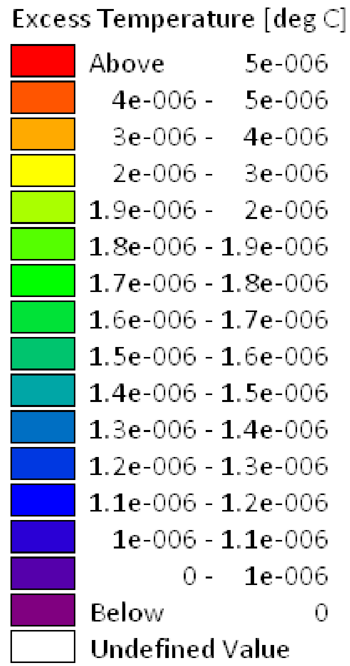

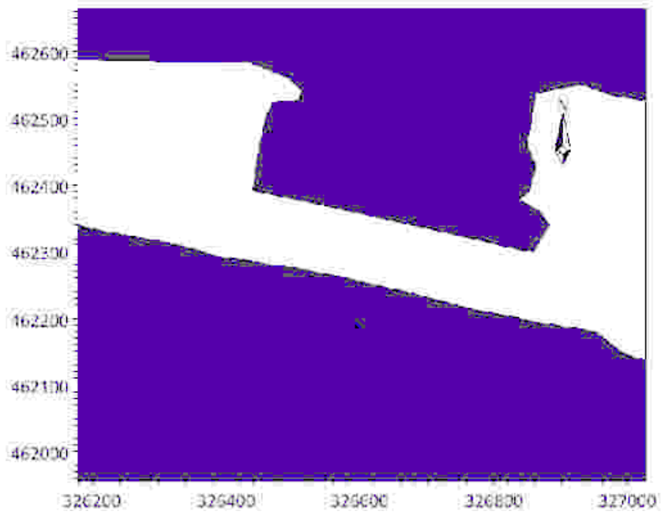

Figure C.51: SW_S_08_Eastward Flow

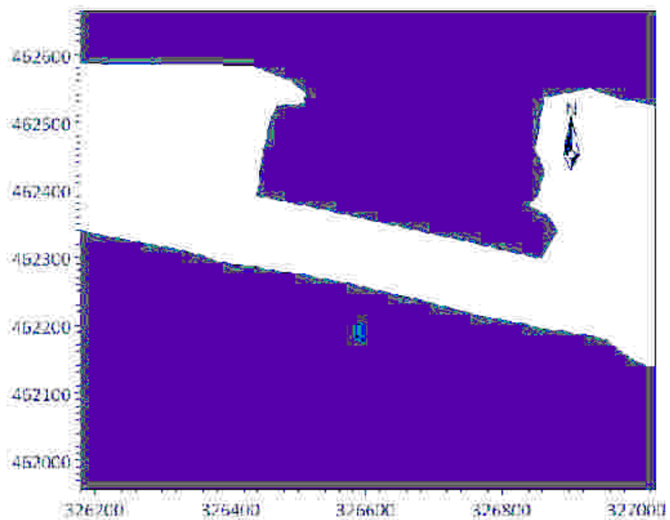

Figure C.52: SW_S_08_Westward Flow

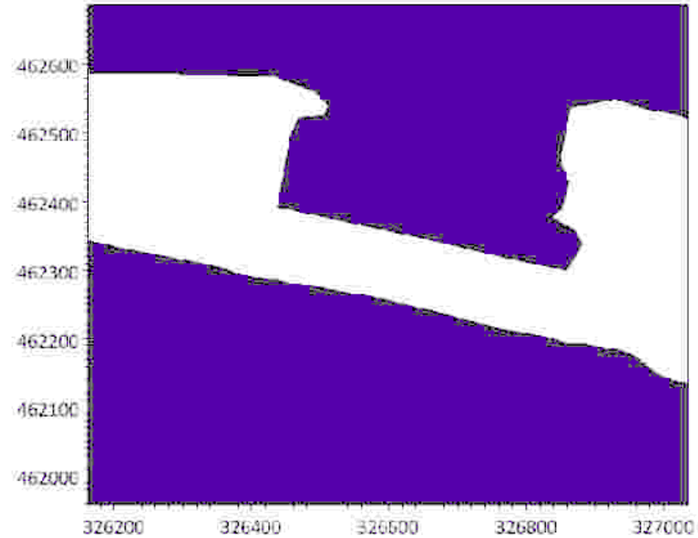

Figure C.53: SW_S_09_Eastward Flow

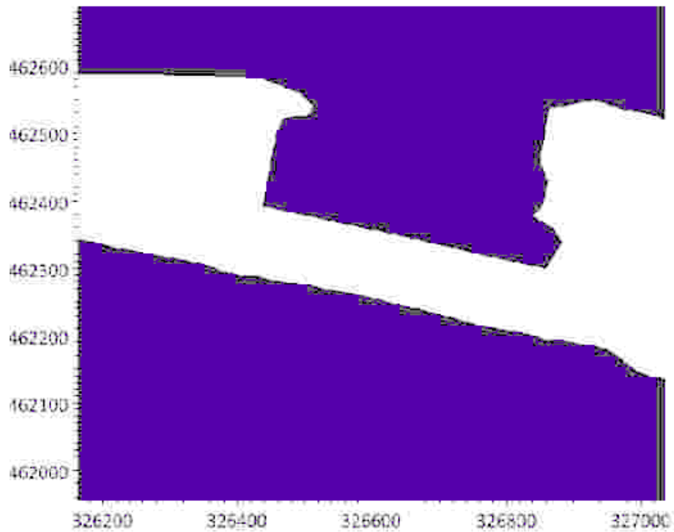

Figure C.54: SW_S_09_Westward Flow

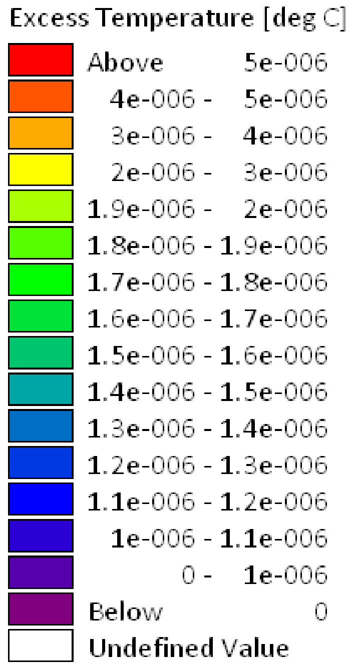

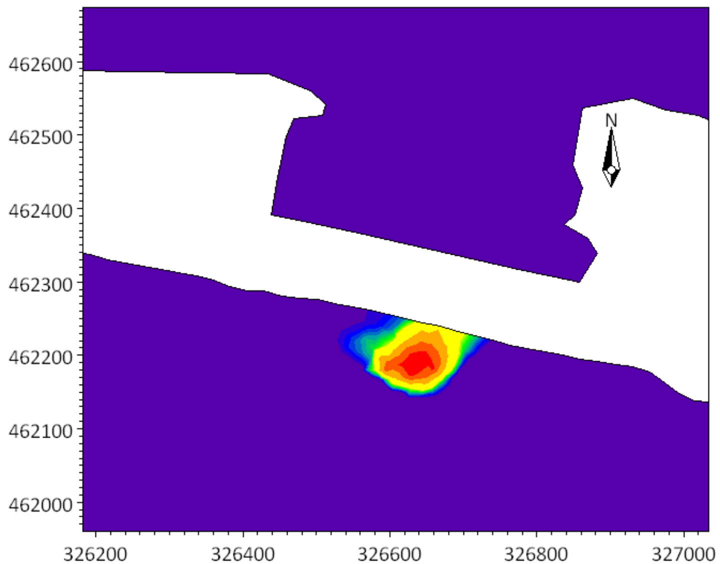

Figure C.55: SW_N_01_Eastward Flow

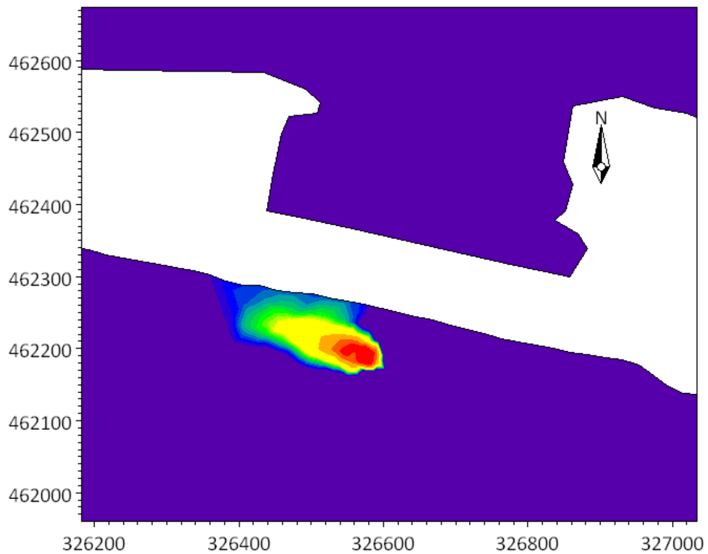

Figure C.56: SW_N_01_Westward Flow

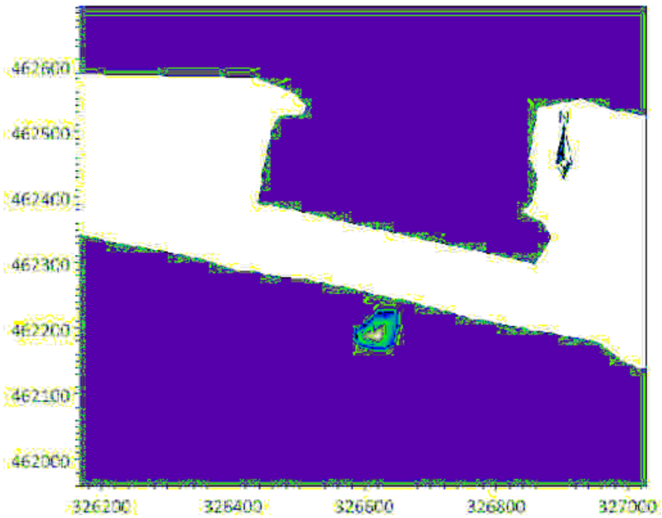

Figure C.57: SW_N_02_Eastward Flow

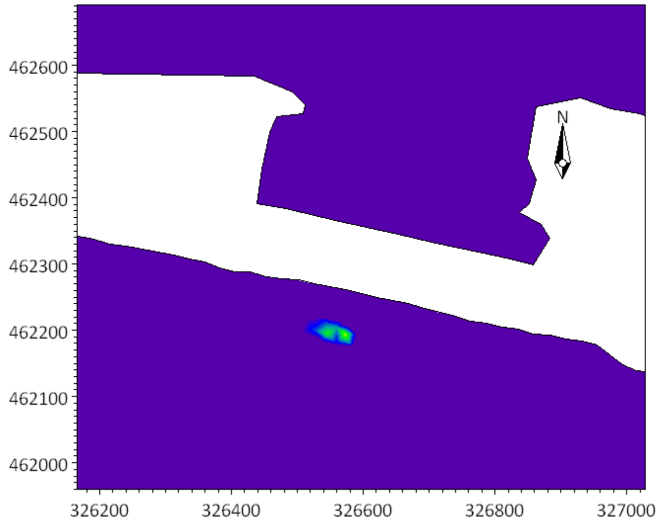

Figure C.58: SW_N_02_Westward Flow

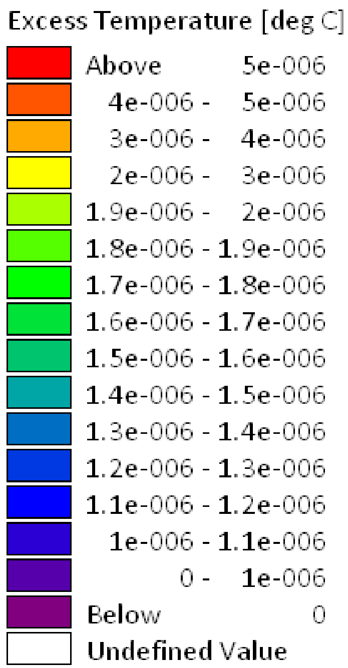

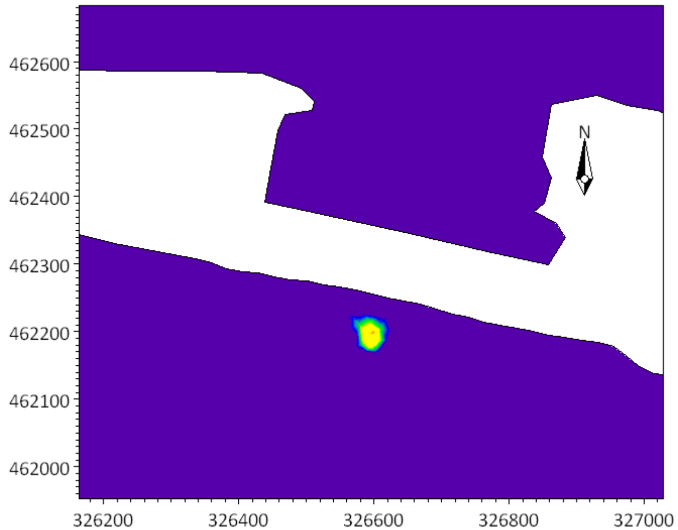

Figure C.59: SW_N_03_Eastward Flow

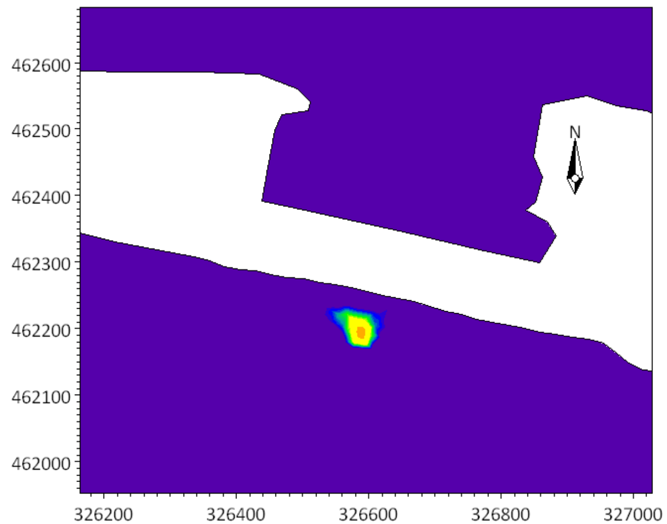

Figure C.60: SW_N_03_Westward Flow

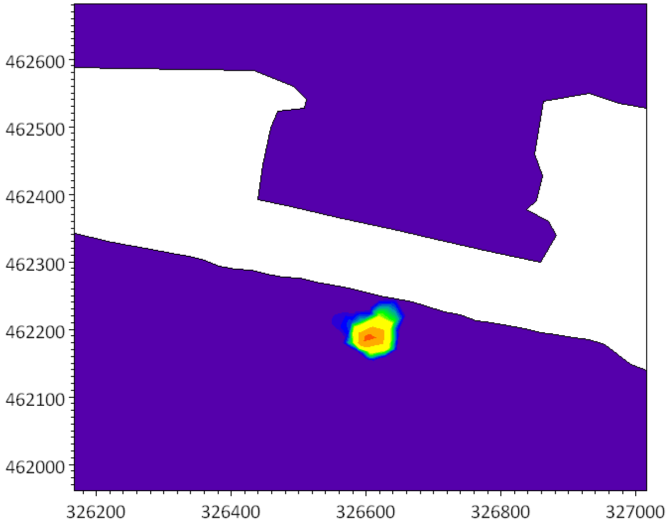

Figure C.61: SW_N_04_Eastward Flow

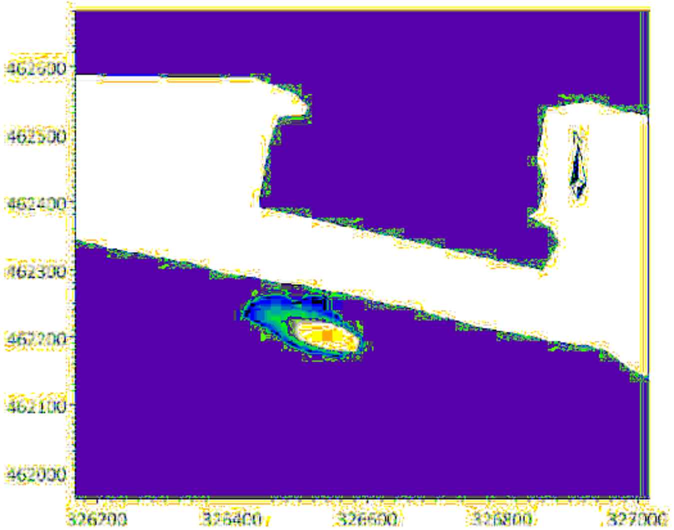

Figure C.62: SW_N_04_Westward Flow

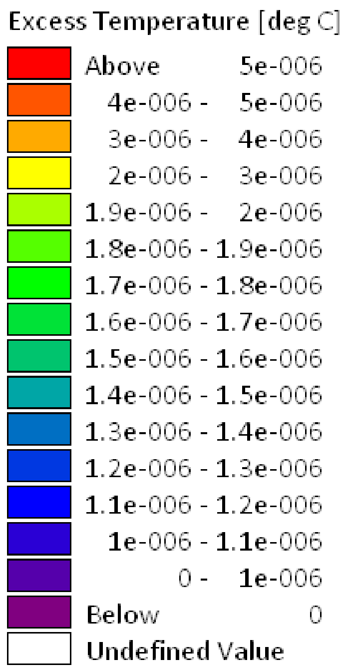

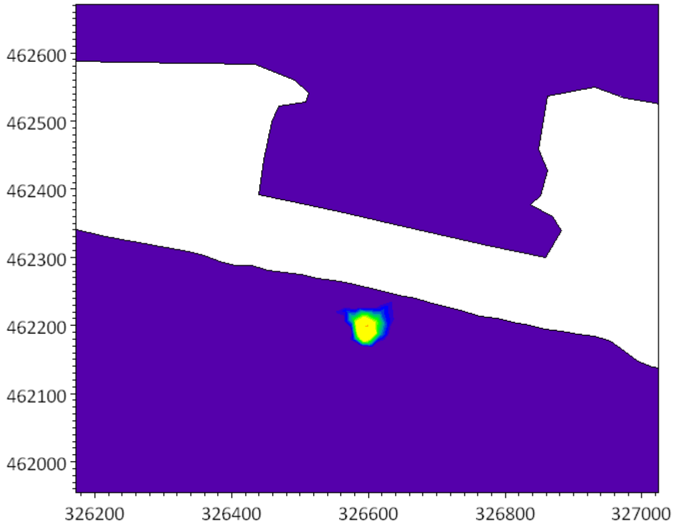

Figure C.63: SW_N_05_Eastward Flow

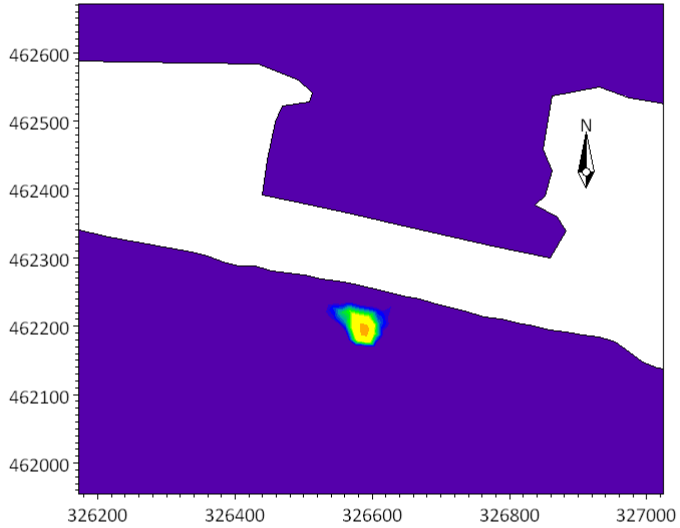

Figure C.64: SW_N_05_Westward Flow

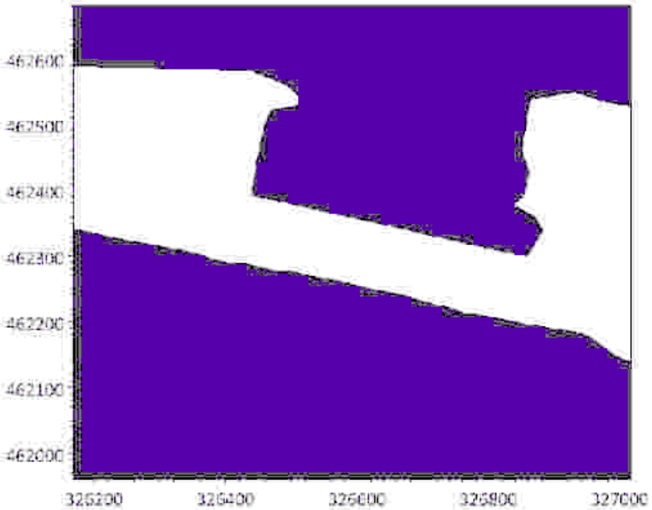

Figure C.65: SW_N_06_Eastward Flow

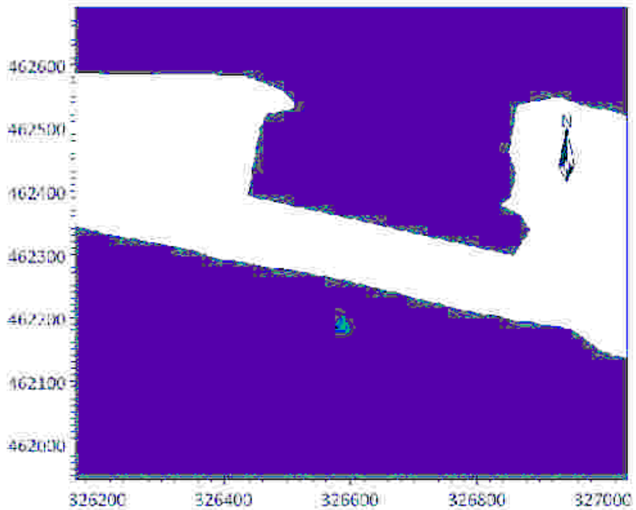

Figure C.66: SW_N_06_Westward Flow

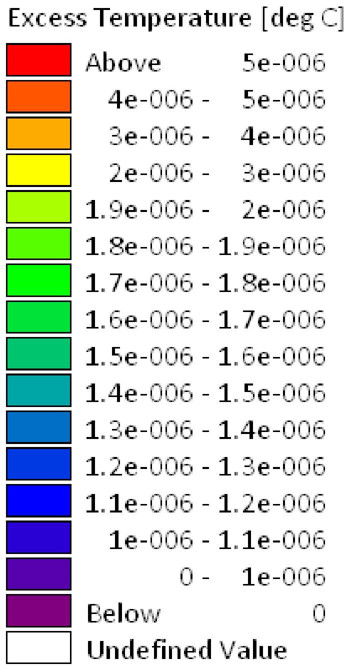

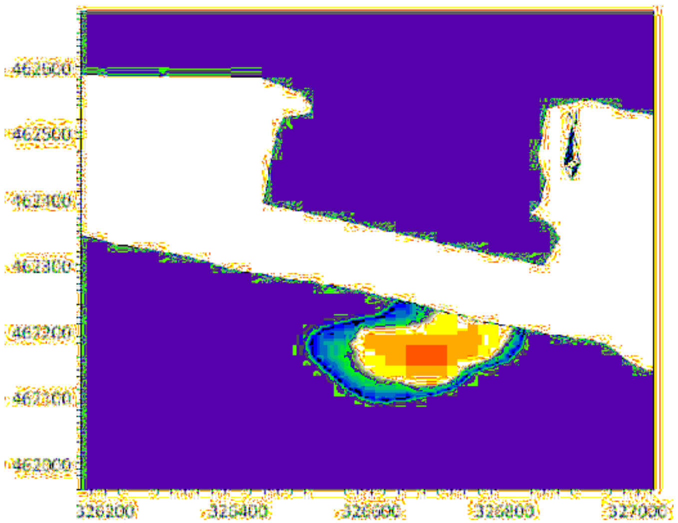

Figure C.67: SW_N_07_Eastward Flow

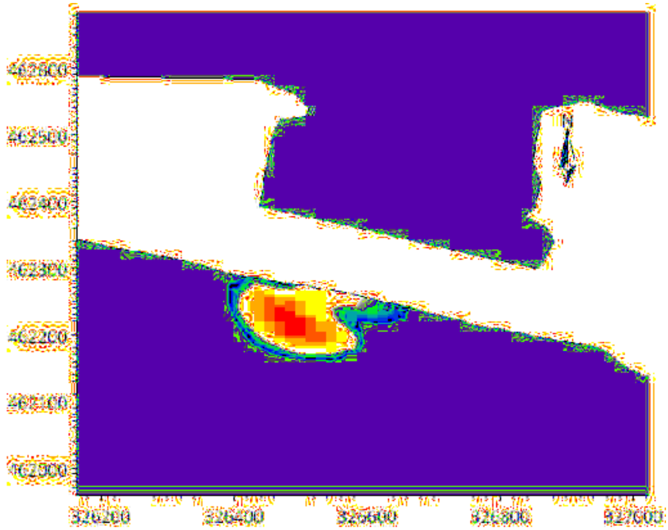

Figure C.68: SW_N_07_Westward Flow

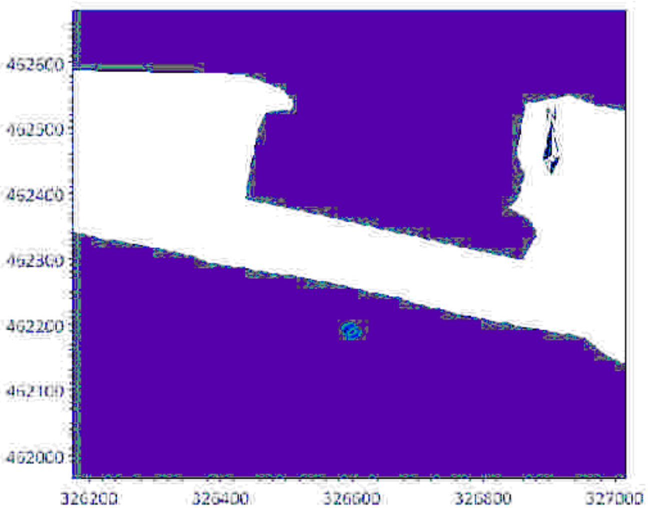

Figure C.69: SW_N_08_Eastward Flow

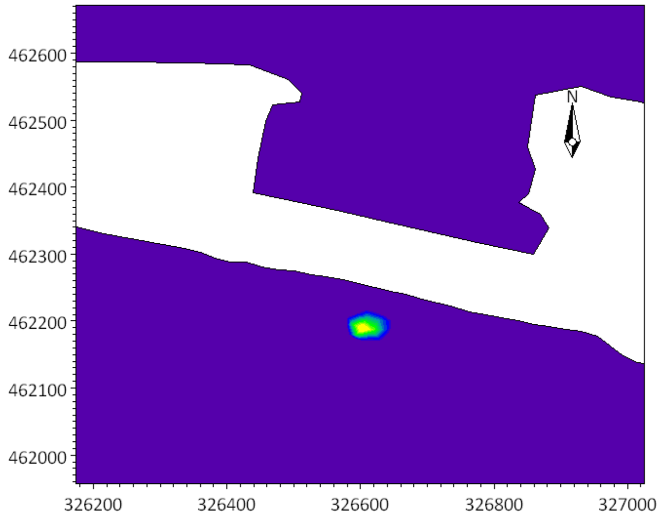

Figure C.70: SW_N_08_Westward Flow

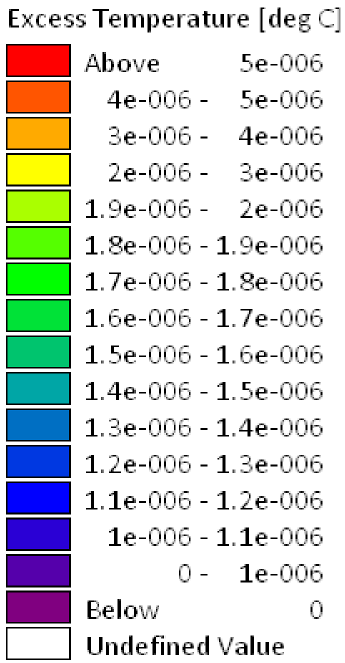

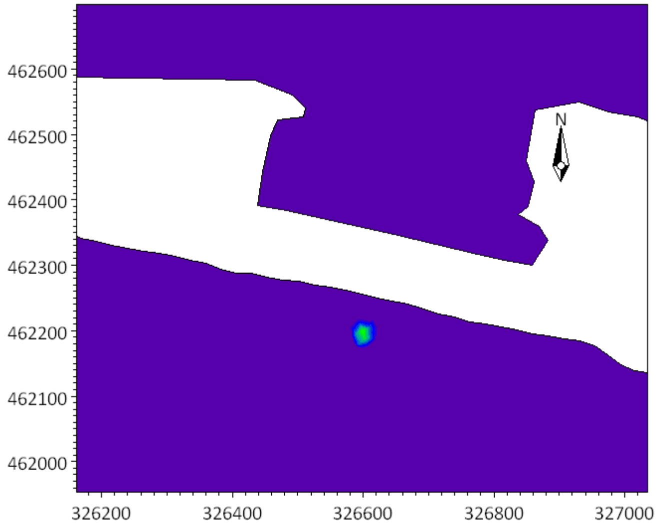

Figure C.71: SW_N_09_Eastward Flow

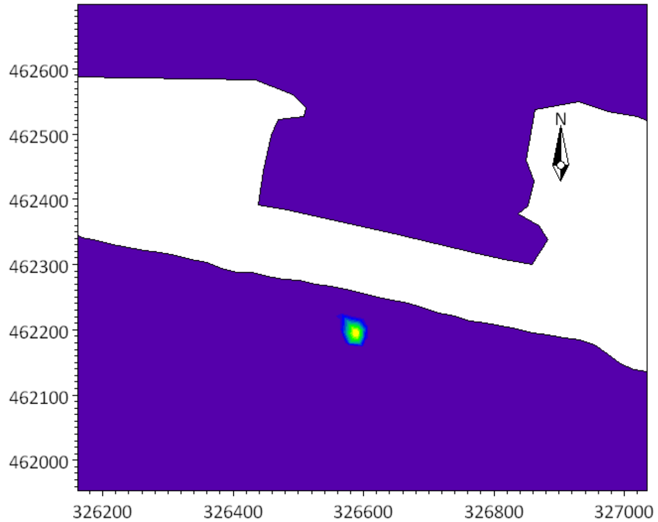

Figure C.72: SW_N_09_Westward Flow